AN INTENSIVE STUDY OF THE CURRENTS AND GENERAL HYDROLOGY OF AN ANOMALOUS UPWELLING AREA OFF SOUTH WEST AFRICA.

A thesis presented to the University of Cape Town for the degree of Master of Science.

By

Alan John Boyd.

Cape Town, 7th April 1981.

ABSTRACT

The currents, winds and hydrology of a coastal site of approximately 120 square miles off South West Africa were studied intensively for two weeks during June/July 1978. Currents were measured by means of drogues tracked by RADAR from a central station at 45m of water depth. Classical inertial motion was observed at several depths during a calm period implying a short relaxation time for pressure gradient forces and the existence of different velocity layers within the water column. Diurnal seabreezes and landbreezes controlled the currents at 2 and 5m depth with a response time of a few hours but the deeper currents were not directly affected by wind. Average surface current speeds were between 0,2 and 0,3 kts. Sustained southerly winds caused a deepending of the upper layer and were accompanied by slower currents. Selected data recorded during the diurnal wind regime yielded the relationship: Surface current speed = 0,017 x Windspeed. A meandering poleward under= current with an average velocity of 0,07 kts was detected at 30m depth whilst onshore flow of similar average speed existed at 20m.

Using the results of the experimental work as a basis, the upper layer of the sea to 8m depth was modelled as a slab, which was affected by wind, friction and the coriolis force. Analytical solutions for a landbreeze/seabreeze regime produced trajectories similar to those recorded experimentally. A numerical model was also developed with the advantage that it could use real wind input and simulate inertial effects during temporary calm conditions.

Weak thermoclines dominated the hydrology of the area, but they were subject to large temporal and spatial variation in depth. At the central station, thermocline depth changes could be directly related to the wind record. Entrainment was proposed as the process responsible for the transfer of nutrients upwards across the thermocline to the surface layer. Below the thermocline oxygen values were very low and reached virtually zero near the bottom. Nitrate existed in highest concentration in an onshore moving middle layer. Lower values above the thermocline are ascribed to biological uptake and lower values near the bottom to nitrate occurring as nitrite in the anoxic conditions. The nitrate supply process was modelled.

It is concluded that the features identified in the intensive research area would in general be applicable to the larger area from just north of Cape Cross (21°45'S) to just north of Walvis Bay (23°S).

PREFACE

This study was designed to investigate the causal aspects of upwelling off South West Africa, including the measurement of currents. It was motivated by previous publications which had noted the lack of such research, and as it developed, the study was successful in identifying upwelling mechanisms. However, these mechanisms are proposed only to be valid over the limited area between Walvis Bay and Cape Cross. Therefore, work with similar objectives still needs to be undertaken in other localities off South West Africa.

The preliminary results in respect of the currents measured were presented to a meeting of the Royal Society of South Africa in September 1978 and an abstract of this lecture was published by them in June 1979. Subsequently, the data on currents were corrected for "windage on the drogues" according to the methods discussed in Chapter 2 of this thesis, and these currents are examined and related to the wind record in Chapter 3. (An introduction is given in Chapter 1). In Chapter 4, a mathematical model of surface layer movement is developed, largely in an attempt to simulate practical results. Both analytical and numerical solutions are presented and discussed. Chapter 5 follows logically and describes, with a minimum of inference, both the hydrology of the area in a traditional sense and the short term changes. Chapter 6 is a subjective appraisal of the present direction of research in the Benguela Upwelling System.

ACKNOWLEDGEMENTS

I wish to thank the Director of the Sea Fisheries Institute (Cape Town) for permission to present this thesis. All the data used (with the exception of the wind data) were collected during a single 4 week cruise on the R.S. Sardinops, and her officers and crew are thanked for helping to make the practical phase of this project a success. During this and other stages of this study the author received notable assistance from the following four staff members of the Institute, whom I thank most sincerely. John Taunton-Clark undertook the technical preparations for the cruise, helped with construction of the drogues used for the measurement of currents and participated in the cruise. Brian Kriedermann wrote the original suite of computer programs to capture and process the current data. Emmerentia Warrington and Rosalind Mackay did all the final artwork and a significant proportion of the preparatory artwork.

This study was largely motivated by the hydrological reports published by the old Marine Research Laboratory of South West Africa, during the early and middle 1960's. My supervisor, Professor G.B. Brundrit is thanked for the flexible and positive way in which he guided this motivation. The advice received from G. Nelson and J.J. Agenbag on various topics is appreciated. I. Kruger, who accompanied the author on the cruise, is thanked for his help and wished success in the task of analysing the planktonic data he collected.

L-A. Perrins typed the draft of this thesis, and A. Beukes the final copy. Their efforts are much appreciated. The academic expenses incurred in doing this study were partially supported by the Public Service Commission, and publication costs were born by the University of Cape Town : I gratefully acknowledge this assistance.

Finally I would like to thank A.I.L. Payne for improving the abstract and preface, and my parents for proof-reading the whole thesis.

TABLE OF CONTENTS

---ooo---

1. INTRODUCTION.

1.1 The objective of this study, and the Intensive Programme.

The objective of this study was to investigate the causal relationships amongst winds, currents and hydrological changes off South West Africa. This objective dictated making observations on a time scale in keeping with the most rapid changes in the phenomena themselves which in a region with a known diurnal wind variation, is of the order of hours. Such a time scale, and the fact that only a single ship was available for this research, determined that the area of intensive study had to be small. In terms of the objective it also had to be suitable for the measuring of currents.

After investigating the subject of current measurement, the author decided to use radar to track drogues from an anchored ship, and hence a shallow site (45m depth) at a distance of 6 miles off shore between Henties Bay and Cape Cross was selected as a centre for the study. (See the position of station MG1 in Figure 1.) The uniform topography of the area was welcomed as it was thought that this would tend to make the results more general, and their interpretation simpler.

Wind data were available from Walvis Bay and winds would naturally be measured on the research ship herself, but to get a better horizontal coverage of the windfield, an additional anemometer was installed at Henties Bay, about 20 miles south-east of MG1.

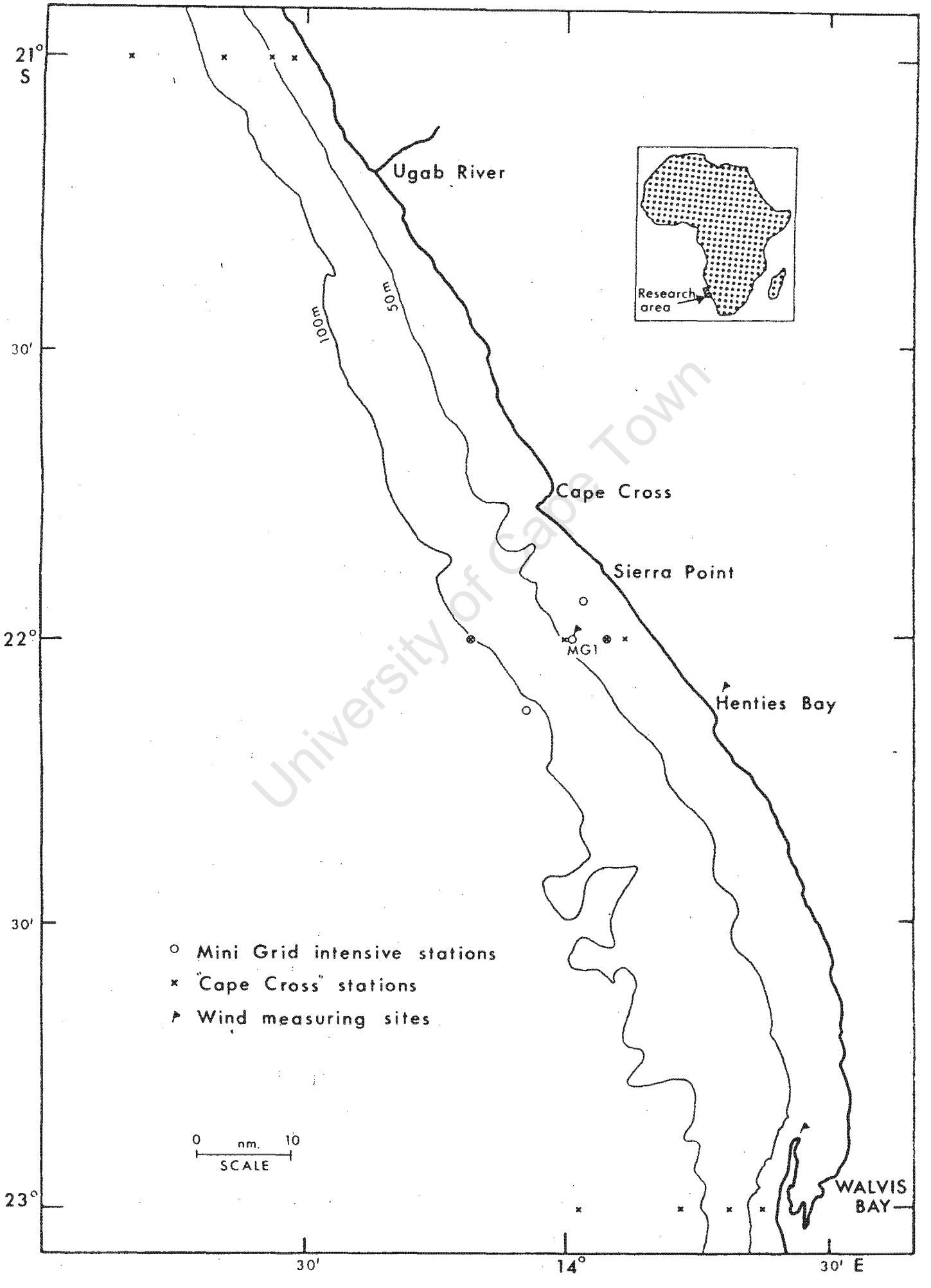

FIG. 1 THE RESEARCH AREA

Similarly in order to help interpret hydrological changes at MG1 and to assess the spatial scales of these changes, two grids were designed around that station: a large scale grid, which would be occupied before the intensive work commenced, and a smaller grid which would be occupied as part of the intensive work.

On 19 June 1978 the R.S. Sardinops anchored at MG1 and the Intensive Programme, as this research was known by then, began. The collection of data took just over two weeks, during which period both diurnal and southerly wind regimes were experienced.

1.2 Past work as a motivation.

The area between Walvis Bay and Cape Cross is one of the most thoroughly researched marine areas off South West Africa, largely because Walvis Bay was, until the mid-seventies, the centre of a thriving pelagic fishing industry. However, the oceanographic research conducted from Walvis Bay generally took the form of occupying a certain grid once a month, and whilst foreign and South African research covered a more extensive area, longer periods elapsed between successive grid occupations. In this manner the major hydrological works were restricted: Hart and Currie (1960) only occupied their grid twice, the comprehensive report on the physical nature of the Benguela Current by Stander (1964) had seasonal cruises as its basis whilst the more "intensive" works by Stander (1963) and Du Plessis (1967) relied mainly on monthly data. It is therefore hardly surprising that little note was taken of phenomena occurring on a time scale shorter than a month or the causal processes involved.

However, a few attempts were made to understand hydrological (and biological) events on a shorter time scale. Pieterse and van der Post (1967) tried to relate oceanographic conditions to the outbreak of red-tides in the area around Walvis Bay. Bang (1971) documented the effects of a single storm on the upper layers of the ocean. Stander (1963), using the small amount of short time scale data available to him, demonstrated the variability of the temperature structure in the upper layers of the ocean in the Walvis Bay vicinity, and drew attention to the inadequacy of once-a-month sampling. But of more importance as regards this study was that Stander (op. cit.) discussed the need to study the causal sequence between winds, currents, temperature and spawning (of the pilchard). Unfortunately he subsequently abandoned currents, after noting that "a clear theoretical approach to the problem did not emerge" and went on to relate wind, temperature and spawning in a more statistical manner.

The latter approach is a much more viable one, but does little to fill the gaps in our knowledge of the mechanisms and real processes going on in the ocean, particularly in coastal regions. The Intensive Programme (which formed the physical basis of this study) was designed to fill some of these gaps and inevitably at the same time it revealed many new facts about the study area.

1.3 The locale of the intensive research area.

The coastline between Walvis Bay (23°S) and Cape Cross (21°45'S) forms a west facing arc which is somewhat set back from the general lie of the coast between Lüderitz and Cape Frio; the coastline north of Cape Cross running NNW for several hundred miles to Cape Frio, whilst that to the south of Walvis Bay runs for a comparable distance directly southwards to Lüderitz. However, the 100 m and 200 m depth contours between Walvis Bay and Cape Cross are not similarly set back and hence this area has a wide shallow shelf. This shelf has in the past been held responsible for certain hydrological features, which are known to be characteristic of, or alternatively are most pronounced in ,this region.

Low oxygen conditions regularly prevail in the lower layers of the coastal waters between Walvis Bay and Cape Cross and beyond, and anoxic conditions can exist at the bottom. Hart and Currie (1960) and Stander (1964) discussed possible causes and the extent of these conditions. Extension of these conditions upwards to the surface layer has led to mortalities of pelagic fish and other organisms in the Walvis Bay region (Copenhagen, 1953; Pieterse and van der Post, 1967). Bailey (1979) attempted to quantify the processes responsible for the low oxygen of the bottom waters in the Lüderitz region (and also summarised the literature dealing with general hydrological research off the South West African coast).

A more localised feature is the high percentage occurrence of thermoclines all year round in the region between 22°30' and 21°30'S. Du Plessis (1967) attributed the prevalence (and intensity) of thermoclines in this area to the wide shallow shelf mentioned above. This shelf would also serve to limit the maximum slope of isopycnals during upwelling in contrast to areas further north and south.

Recent results of I. Kruger (presented by Agenbag, 1980) showed that an area of high phytoplankton abundance between Walvis Bay and Cape Cross occurred in winter. Agenbag (1980) attributed the absence of pelagic fish inshore in this area during winter to this phytoplankton distribution, the thermocline conditions found by Du Plessis (1967) and the low oxygen of the area.

Badenhorst and Boyd (1980) reported that pelagic eggs or larvae could on occasion suffer very little dispersion in the area, conditions they postulated to be good for initial larval survival of the anchovy.

The present study will emphasise the dominant role of thermoclines in determining the hydrology of the intensive research area and the larger area between Walvis Bay and Cape Cross. It also makes a detailed examination of factors that influence thermocline depth and the transfer of properties across thermoclines (and hence the low oxygen phenomenon). The starting point has been stated in section 1.1: the winds and the currents they cause.

2. THE INTENSIVE PROGRAMME.

2.1 Deployment of the R.S. Sardinops, equipment and methods.

The research area and various station positions are shown in Figure 1. Most time was spent at station MG1 which served as the chief drogue tracking station as well as a wind measuring station. Winds were also measured at Henties Bay and Walvis Bay. The larger scale "Cape Cross" grid was occupied once on the 15th and 16th of June, and the small scale "mini grid" was occupied seven times as part of the Intensive Programme which stretched from the 19th June to the 3rd July, 1978.

This programme consisted of drogue tracking, hydro/biological stations and wind measurement. The mini grid was worked every second day during the two week period, this taking about 10 hours. For the remaining 38 odd hours out of every 48, the research ship R.S. Sardinops anchored at station MG1 in 45 metres of water, the weather permitting. At this station drogues were released at various depths and tracked by radar for as long as possible before being retrieved. Full hydro/biological stations were worked every 12 hours and temperature profiles were obtained every 4 hours. Surface temperature was monitored continuously until the thermograph broke down towards the end of the programme.

During the 12 hourly stations at MG1, bottle samples were taken at "the surface" (actually at about 2m depth) and at additional depths of 5, 10, 20, 30 and 40 metres. These samples were analysed for salinity, dissolved oxygen (by the Winkler method), nitrate, silicate, phosphate and diatoms. In addition a bathythermograph (BT) and N50V plankton net were sent down to 40 metres.

At stations MG2 and MG5 the 40m depth sample was omitted and deeper samples were taken at 50m and 75m. Midway between all the outer intensive stations, a BT dip was done. The positions and depths of these stations and dip sites are shown in Figure 2. This figure also displays the results of a "hydrographic survey" of the research area done by the R.S. Sardinops.

During the programme the exact position of station MG1 was marked by an anchored buoy fitted with a flag and a radar reflector. Thus changes in the ship's position whilst at anchor could be monitored by reference to this buoy. On the anchor rope of the buoy a modified commercial temperature recorder was attached at a depth of 10m in an attempt to monitor temperature changes that may have been caused by internal waves.

Windspeed was measured on the R.S. Sardinops by an anemometer at a height of 15m above the sea, with direction estimated by the ship's officers. At Henties Bay a Lambrecht mechanical anemometer recorded cumulative wind distance and direction on an hourly basis. The instrument was mounted atop a pole at a height of 5 metres, and was

MINI GRID BATHYMETRY FIG. 2

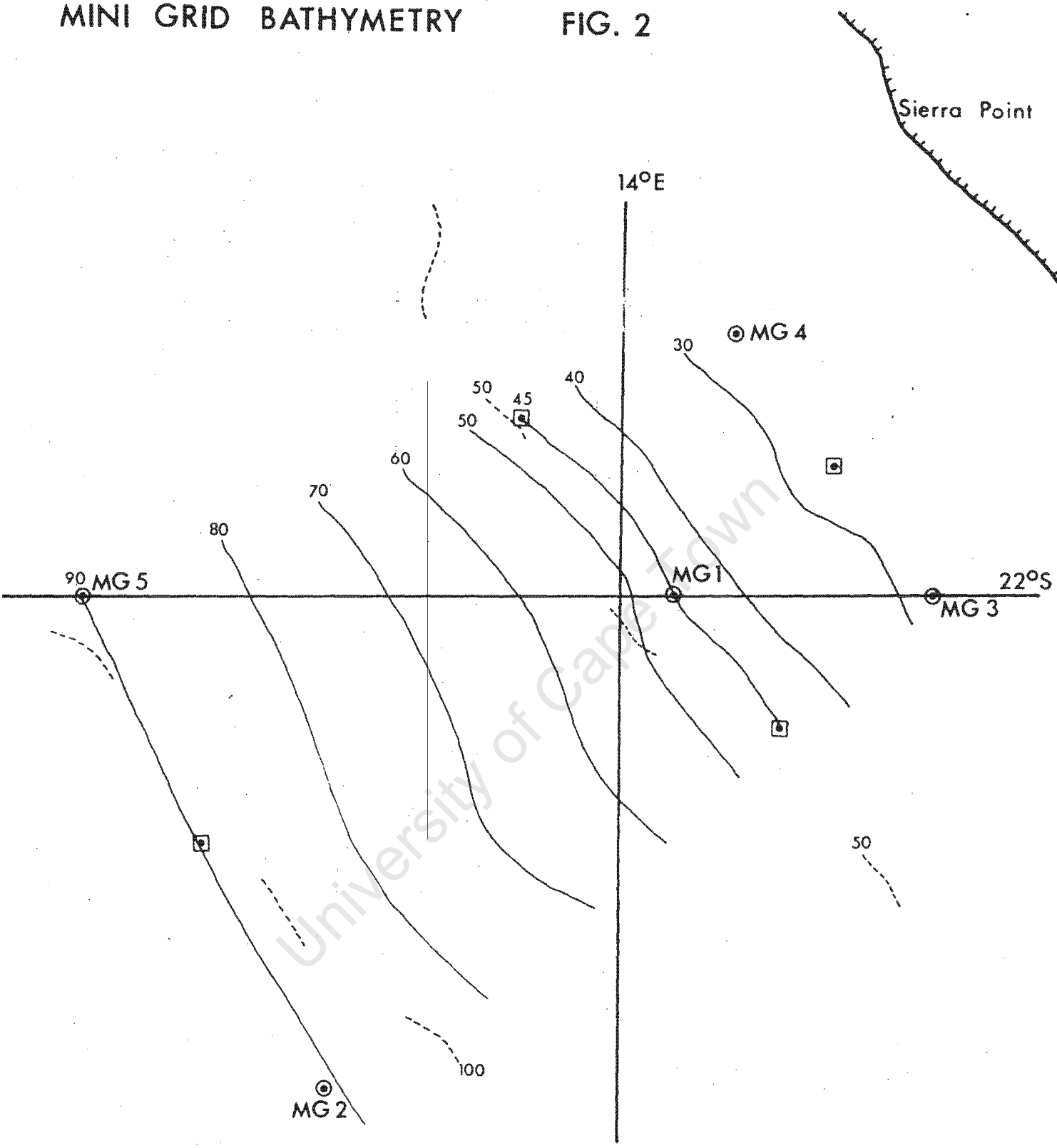

Decca chart bathymetry

Sea Fisheries Institute bathymetry (June/July 1978 survey)

Mini grid intensive stations

BT stations

0 Scale: n. mile 5

about half a kilometre from the sea. The Walvis Bay wind data came from Pelican Point lighthouse, the anemometer being positioned at a height greater than 15m.

The drogue design is shown in Figure 3. It was based on that used by Bain (pers. com.), but was substantially uprated in order to supply quantitative results. To this end three design criteria were applied. The first was that the radar reflector should be clearly visible on the ship's radar during reasonable weather conditions when the drogue was about 2 miles away from the ship. The next was that the drogue must be of sufficient size to minimize the effect of windage on the reflector. (Kirwan et al (1975) emphasized the magnitude of the errors due to the windage in drogue studies.) The third criterion was that the drogue should be able to be easily deployed, retrieved and stowed; using either a twelve foot inflatable boat or the one hundred and twenty foot R.S. Sardinops. The first and the third criteria were successfully met. However, whilst the windage on the radar reflector was reasonably well opposed by the greater size of the drogues used in this study in comparison to those used by Bain (pers. com.), windage will have to be compensated for before the drogue velocities can be regarded as current velocities. In the next section suitable correction factors will be developed using both a theoretical and practical approach. First an outline of the drogue tracking procedures and accuracy, and drogue terminology, will be given.

FIG. 3 RADAR TRACKED DROGUE

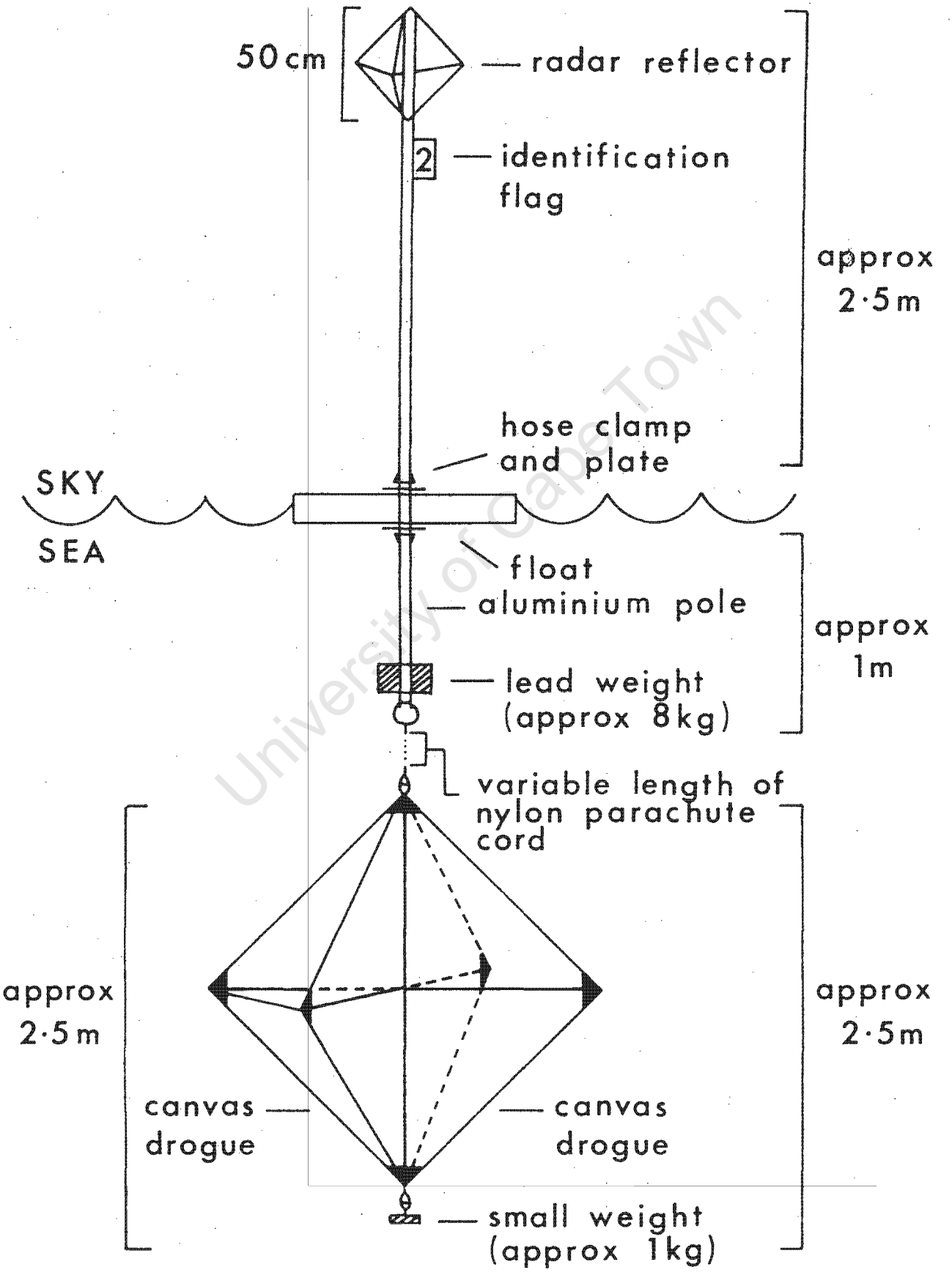

Drogue tracking was done on 14 "occasions". An "occasion" began when one or more drogues were deployed and ended when either all drogues were recovered, or some drogues were recovered and deployed again at the same depth. For example, if the 2 and 5m drogues were recovered because they had drifted too far from the R.S. Sardinops for successful tracking, and then were deployed again this would involve starting a new occasion. Other drogues that had not been recovered would be tracked as part of this new occasion from the time of the re-release of the 2 and 5m drogues. Thus a single trajectory may extend over two occasions. Complete tracking and wind data for 13 of the 14 occasions is given in Appendix A. No corrections have been made to this data.

Drogues were deployed at depths of 2, 5, 10, 20 and 30m. If conditions for tracking were favourable (i.e. winds were 15 knots or less), drogues would be deployed at all or most of these depths. Under higher windspeed conditions, generally fewer drogues would be deployed. What often happened was that a "full house" deployment would be followed by early recovery of the 2 and 5m drogues, as these drogues would be rapidly transported out of tracking range in high windspeed conditions. Hence longer and less biased sampling of the deeper currents was accomplished in comparison to the surface currents.

For 12 of the 14 occasions drogues were released from the R.S. Sardinops while she was at anchor at MG1. The positions of these drogues were obtained from the ship's radar every half hour and true bearing and distance relative to the ship were noted. The ship's

position itself was noted relative to the MG1 marker buoy. All measure= ments were made to within a degree of arc and 0,01 of a nautical mile. However, due to factors such as the impossibility of noting the positions of 5 drogues simultaneously and a certain amount of the ship's drift relative to the marker buoy for which no correction was made, true time-space accuracy is estimated to have an uncertainty of ± 0,05 n. miles about the noted value. Individual half-hourly velocity components would only have an uncertainty of about ± 0,05 knots though, as drogues were tracked in the same order. Hourly velocity components would have an uncertainty of half the above.

On two occasions a "three point drop" was made. 3 pairs of drogues, each pair consisting of a 5m drogue and a 30m drogue, were released at intervals of 2 miles along the 22 S latitude, the centre drop being done at MG1. Every two hours or so, the R.S. Sardinops would "visit" each drogue and take a DECCA fix to obtain position. This method was employed for two reasons, firstly to obtain a broader spatial picture of currents in the surface and deeper layers, and secondly to use the time constructively when rough weather prevented anchoring and/or radar tracking.

This section has outlined the methods and scope of the data collection during the Intensive Programme. The next section will describe the preliminary data processing undertaken, namely the development and application of a correction factor to compensate for windage on radar tracked drogues.

2.2 Assessment of windage on the radar tracked drogues.

During the Programme it was realised that windage on the radar reflectors was significant, inspite of the fact that the size of the drogues had been approximately doubled (in all 3 dimensions) when compared with those used by Bain (pers. com.), whilst the radar reflector had remained the same size. The effects of the wind could be clearly seen and felt during both deployment and retrieval of the drogues. It was also realised that windage was not all obscuring; drogues at 20 and 30m had on several occasions advanced, radar reflector and pole tilting backwards, into the wind. Obviously some correction factor was needed before the effect of the wind on the currents (and not just the drogues) could be discussed with confidence.

A theoretical correction factor is developed below, and it will be compared to the results of a more experimental approach.

Murray (1975) obtained an expression similar to that given below in equation 2-1 for the relative speed between the drogue and the water, i.e. the error due to windage, by assuming the drogue to be moving at a constant velocity and then balancing the force due to windage on the part above the water against the water drag on the drogue below. Murray (op. cit.) further modified the balance between these two forces by the sine of the observed maximum angle made by the line connecting the drogue to the surface float pole. This feature is not

incorporated in equation 2-1 for the reason that in practice the vertical component of the windage force would cause kiting and thus a net movement of the drogue in the direction of the wind which would not otherwise be allowed for. Also if this feature were incorporated, the angle should be a function of windspeed. Equation 2-1 expresses a straight balance between the forces on the tetrahedral reflector and drogue.

$$Uo = \left(\frac{Cr \; \rho \, air}{Cd \; \rho \, water} \right)^{1/2} \frac{Lr}{Ld} \cdot W \text{ (windspeed)} \qquad (2\text{-}1)$$

where: Uo = the relative speed between the drogue and the water

Lr = length dimension of the tetrahedral reflector (0,38m)

Ld = length dimension of the tetrahedral drogue (1,70m)

W = windspeed

ρ air = $1{,}25 \times 10^{-3}$ gm/cm^3

ρ water = 1,00 gm/cm^3

Cd and Cr are drag coefficients for the water and the air on the tetrahedral drogue and reflector respectively. The ratio of Cr to Cd will be taken as 1,5 on account of the fact that whilst the drogue is biplanar, the tetrahedral reflector also has a third plane. This gives it a surface area of 1,5 x its shadow area which will feel the wind in real conditions: i.e. when the wind causes the pole supporting the reflector to aquire a slight tilt.

From (2-1) we obtain:

$$Uo = 0{,}0097 \times \text{Windspeed} \qquad (2\text{-}2)$$

To allow for the fact that wind was measured at fifteen metres above the sea whilst the radar reflectors were at most 2m above the sea, the factor of 0,0097 in equation 2-2 will be reduced, according to a logarithmic wind profile with scales of:

W (15)m = 10 m/s

Zo (roughness length) $= 10^{-3}$m

K (Von Karmans constant) = 0,4

This gives U^* (friction velocity) = 0,416 m/s and thus

$$W(z) = \frac{U^*}{K} \ln\left(\frac{z}{zo}\right) \qquad \text{then gives :} \qquad (2\text{-}3)$$

$$W(2) = 7{,}9 \text{ m/s i.e. } W(2) = 0{,}79 \times W(15) \qquad (2\text{-}4)$$

The error due to windage can now be expressed in a form suitable for the correction of drogue tracks:

$Uo = \beta \times$ Windspeed (at 15m) (in any units for speeds)

where $\beta = 0{,}0076$ (2-5)

This result agrees well with two estimates of windage obtained from a more practical approach which is described below.

Two occasions (4 and 6) were selected in which an easterly wind was blowing whilst a drogue below the thermocline was almost stationary. As the wind decreased in speed the drogue accelerated into the wind (Figure 4). Hourly components of wind and current speed in the

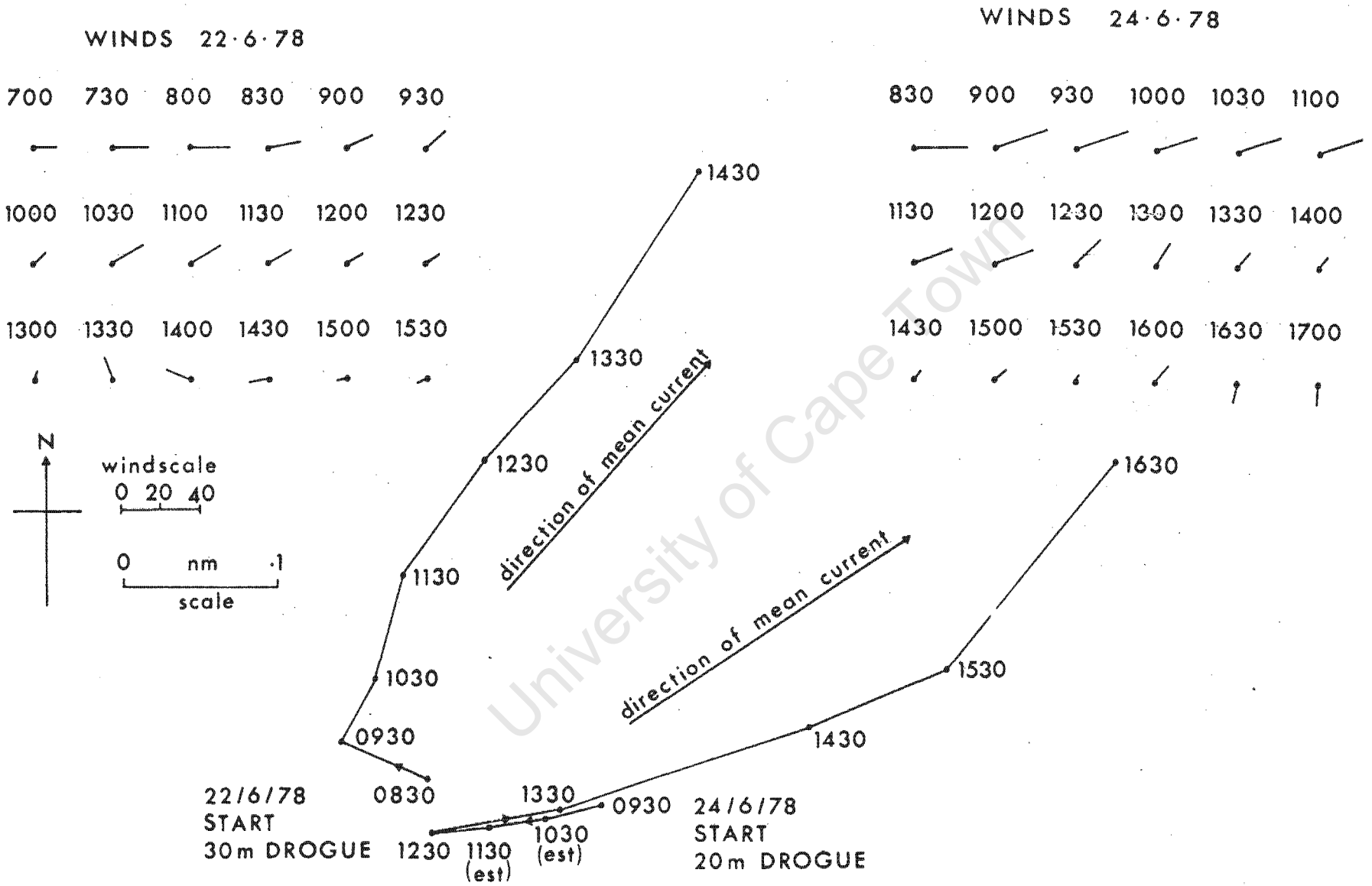

FIG. 4 OCCASIONS USED FOR EXPERIMENTAL WINDAGE ESTIMATIONS

direction of the "mean current", i.e. that obtained during the period with the lowest windspeed, were correlated separately for the two occasions. Assuming the currents to have been constant over the periods of measurement (see section 3.2), two estimates of the effect of windage on the drogues were obtained.

The drogue tracks plotted in Figure 4 have not been corrected for windage. The wind (x) and current (y) velocity components for the two occasions are shown with their two appropriate regression lines in Figure 5(a). These components were obtained graphically from the original enlarged version of Figure 4 and are tabulated below in Table 1.

Table 1: Wind and current components used for windage calculations

Time	Occasion 4, 22/6/78		Occasion 6, 24/6/78	
	Current (kts)	Wind (kts)	Current (kts)	Wind (kts)
08h30 - 09h30	-0,02	-14		
09h30 - 10h30	0,06	-15	-0,03	-27
10h30 - 11h30	0,06	-17	-0,03	-23
11h30 - 12h30	0,09	-8	-0,03	-20
12h30 - 13h30	0,09	-4	0,08	-12
13h30 - 14h30	0,14	+4	0,16	-7
14h30 - 15h30			0,09	-7
15h30 - 16h30			0,16	0

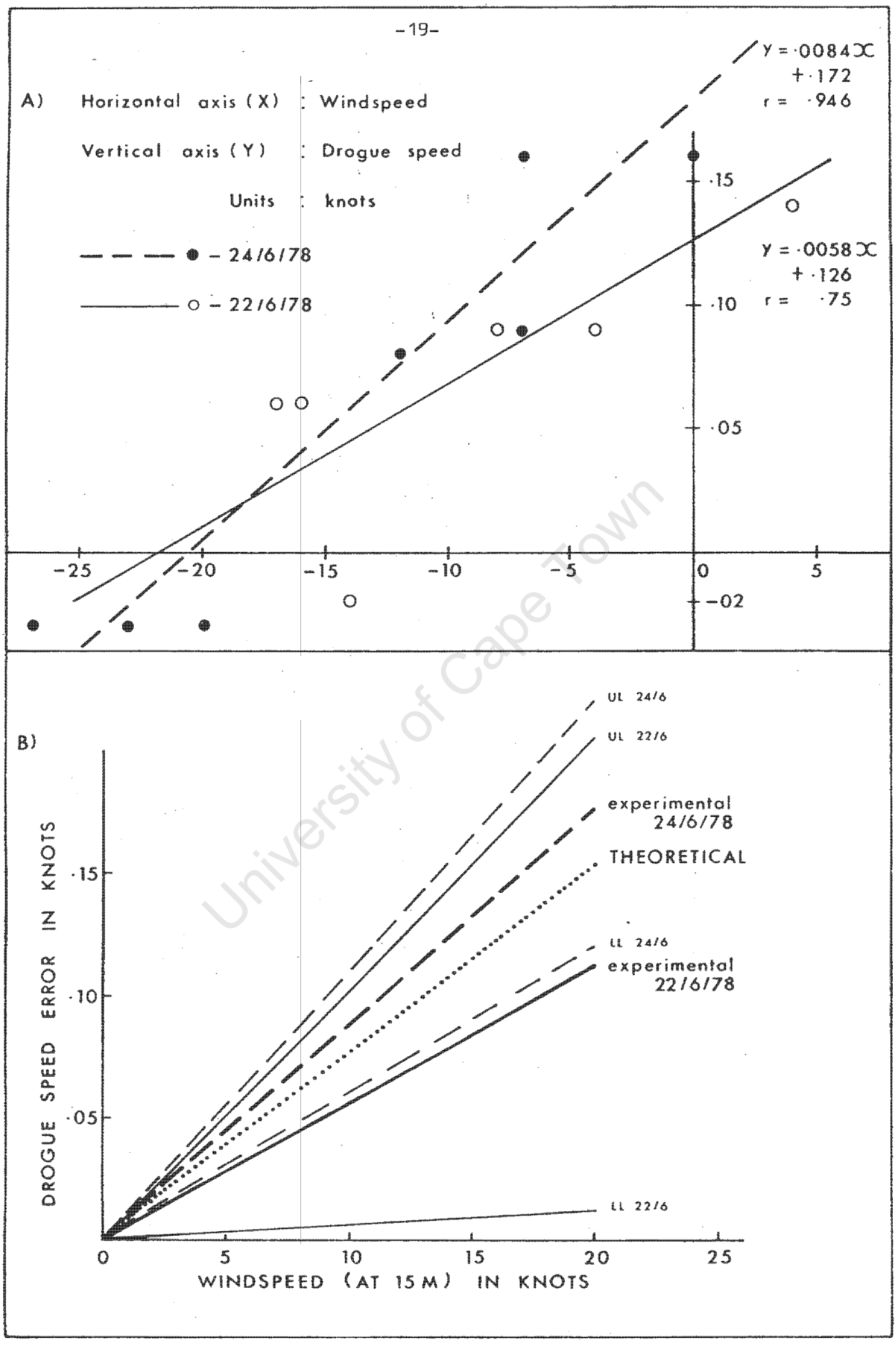

FIG. 5 ESTIMATES OF WINDAGE ON THE DROGUES

Figure 5(b) displays the theoretical and experimental estimates of drogue velocity error due to windage. The theoretical estimate only considers windage on the radar reflector, whilst the experimental estimate takes into account all manner of windage on the part of the drogue above the water and wind-induced surface drift on the float. Both relate this error to the wind at 15m height. The theoretical estimate will be used to correct all drogue tracks that appear in this thesis but the agreement between it and the two experimental estimates is heartening. The broad separation between the upper and lower 90% confidence interval limits for the practical estimates is not quite so heartening, nevertheless they are shown in Figure 5(b) and below in Table 2.

Table 2: Error/correction factors for windage on radar tracked drogues

	Occasion 4	Occasion 6	Theoretical
90% confidence interval limits for windage error, β	0,0103	0,0110	- (upper)
	0,0012	0,0058	- (lower)
β	0,0058	0,0084	0,0076

On account of these broad confidence intervals it is of importance to assess the potential error due to windage in hourly current velocity components, after correction factors have been applied. Let us consider the following hypothetical case:

(a) the "true" correction factor β is 0,0110 (the upper limit of the highest value in Table 2)

(b) a true current of 0,20kts exists in the direction of a wind of 10kts, and a drogue is in this current.

The drogue will under the above assumptions, be radar speed trapped at 0,31kts. The theoretical method will correct this to 0,23kts, a difference of less than 20% from the true value for the hourly velocity component.

Furthermore the mean wind velocity obtained from all the drogue tracking occasions over the two week programme was only 1,6kts in a northerly direction (see Figure 11). Thus if β were incorrect by a factor of 0,003, as in the case considered above, mean current speeds would be out by a factor of 0,0048 of a knot, which is negligible in any terms.

It is thus contended that:

1) Any discrepancy between current velocity and corrected drogue velocity due to an error in the estimation of windage, will be less than 0,03kts during winds of 10-15 knots. This is of the same magnitude as the uncertainty in the hourly velocity components caused by the tracking limitations mentioned in the previous section.

2) Average currents will not be noticeably affected at all by a possible error in the windage correction formula. Indeed a sampling bias will be seen to a more serious problem and this is discussed in sections 3.4 and 3.6.

It is felt that the subject of windage has been taken far enough for the purposes of this thesis. In the following chapters "corrected drogues tracks" will be considered to accurately portray water movement, although, even with spot-on corrections, this would only be true in calm conditions.

3. RESULTS OF THE DROGUE TRACKING EXPERIMENT.

3.1 Inertial Currents.

Before the influence of wind on currents is discussed, the nature and space dependence of the velocity of the currents prevailing in calm conditions will be examined. Windage corrections were minimal or zero for all drogues and thus the drogue paths can be considered true "water parcel" trajectories, with the exception of those interfered with by thermocline depth changes.

A calm period for a full 24 hours on 1 and 2 July, 1978, provided an opportunity to observe classical inertial motion at depths of 2, 5, 10 and 30m. The drogue tracks are shown in Figure 6 and have circles imposed on them for analysis. It is from these circles that the radii and periods are gleaned. The drogue at 20 metres did not inscribe an arc of a circle, but the thermocline can be seen to be located between 15 and 20 metres and thus the 20m drogue track would not reflect the movement of any one water parcel. In fact two very incomplete circular tracks seem apparent.

For the 2, 5, 10 and 30 metre drogues, the periods are in agreement with those expected theoretically in this latitude (32 hours at 22°S) and the radii measured are also reasonably in agreement with radii expected from the formula:

The occurrence of inertial motion is in itself important in that it carries the implication that residual pressure gradient forces were negligible during this period. However, a calm period from 00h00 to 08h00 on 27 June did not produce classical inertial motion in the surface layers (although the direction of velocity changes was anticlockwise) showing a relaxation time for pressure gradient forces is needed even following diurnal winds.

These features are consistent with the fact that this study was done in an area with a wide shallow shelf, which would only allow limited pressure gradients to establish, whatever the wind history. In regions where the shelf is narrower and steeper the residual pressure gradient forces could be more dominant due to the sloping of isopycnals being able to establish on a larger vertical scale.

3.2 Horizontal space dependence of current velocity.

On two occasions the spatial nature of currents was investigated and the data from one of these, that of 30 June 1978, is presented here in Figure 7. Three pairs of 5 and 30m drogues were released at three locations 2 miles apart along the 22°S latitude line and tracked, initially by DECCA and afterwards by radar.

FIG. 7 THREE-POINT DEPLOYMENT ON 30/6/78 AT 22°S

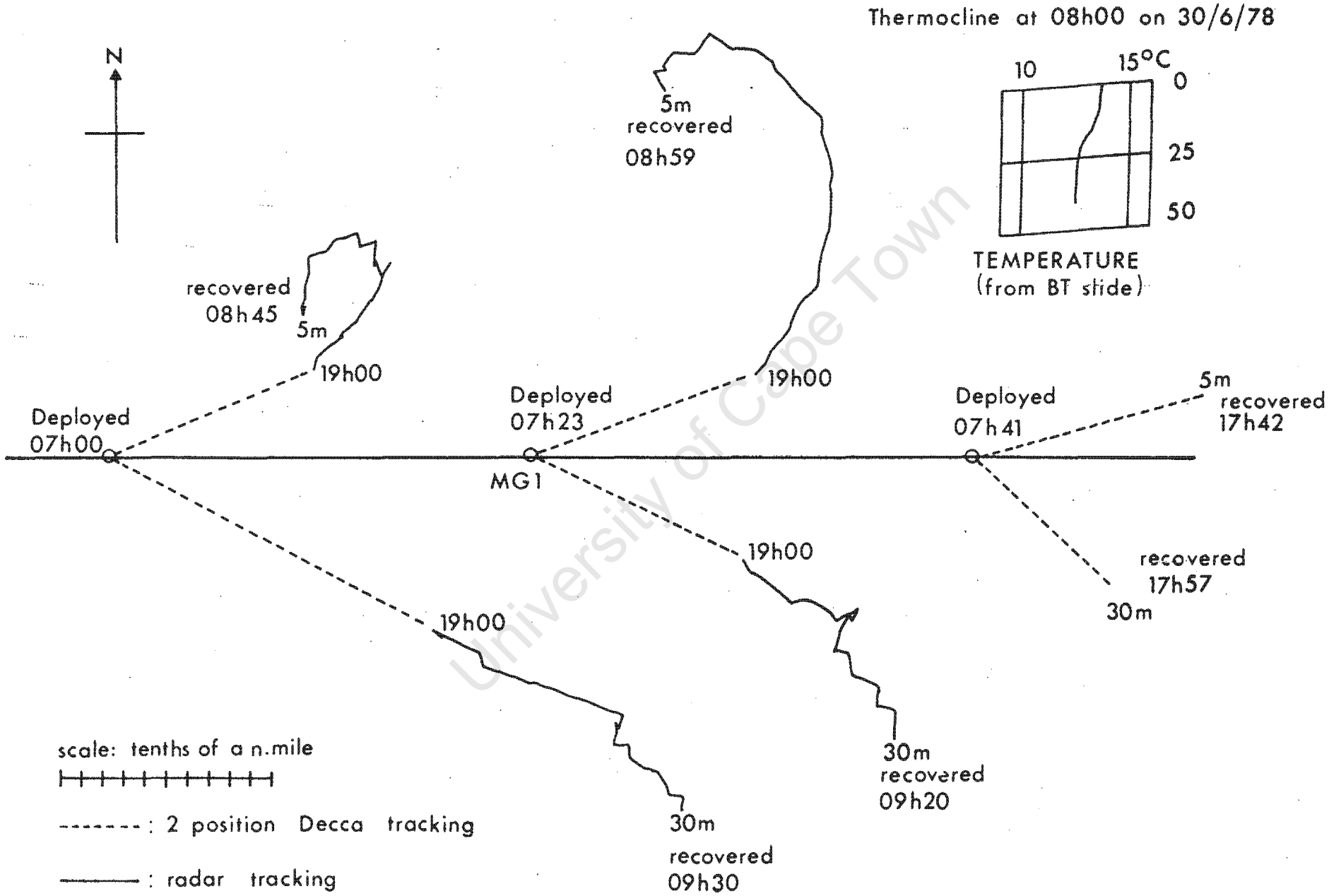

The tracks at 30m show a "counter" current flowing "southwards" along the coast, a feature that has been noted by Stander (1964) and others. The spatial velocity distribution of this current was very uniform on this occasion, although the slower and slightly more southward directed track of the furthest inshore drogue may have been influenced by the bottom topography. To this author's knowledge this is only the second time that this subsurface counter current has been measured directly off SWA, although it has often been inferred. Kuderskiy (1964, not seen in the original) was reported by Moroshin, Bubnov and Bulatov (1970) to have made "instrumental" observations of this current.

The presence of a thermocline between 10 and 20m (Figure 7) implies that apart from continuity considerations, the 5 and 30m currents would be largely unrelated. The surface currents (at 5m) show up what appears to be anticlockwise eddy formation in the surface layer. In this type of flow, as opposed to uniform longshore flow, obviously spatial differences in current velocity must occur because of the boundary imposed by the coast. The two longer 5m trajectories also show apparent frictional retardation of potential inertial motion, although this would have been abetted slightly by the light anticlockwise winds. It is noted here that so dominant was the role of the coriolis force in the research area in affecting both wind and current that not once during the entire two week experiment was clockwise rotation observed in the surface layer.

The results of this 3-point drop have shown the spatial coherence of current direction over a limited area. This feature will be made use of later when components of current velocity will be treated as if they were measured at the ship's anchor site.

3.3 Wind influence on currents and an example of diurnal variation

Two different wind regimes occurred during the R.S. Sardinops two week stay at MG1. During the first week winds consisted predominantly of land and sea breezes, while the second week was endowed with southerly winds and misty calms (Figure 8). Features of the calm occasions have been discussed already.

The southerly winds were accompanied by a fair swell which made both anchoring and radar tracking difficult or impossible, so drogue tracking was attempted by other means. Figure 9 shows velocity vectors for about 6 hours resulting from the first three point drop experiment on the 28th of June. The vectors were calculated by noting the difference between deployment and later positions of the drogues on the ship's DECCA system. Surprisingly low velocities were found at both 5 and 30m. The only explanation for this is that much energy appears to have been expended in deepening the upper mixed layer during the southerly wind period (Figure 8). Certainly this layer was well mixed (see the BT trace in Figure 9) and very little energy went into currents.

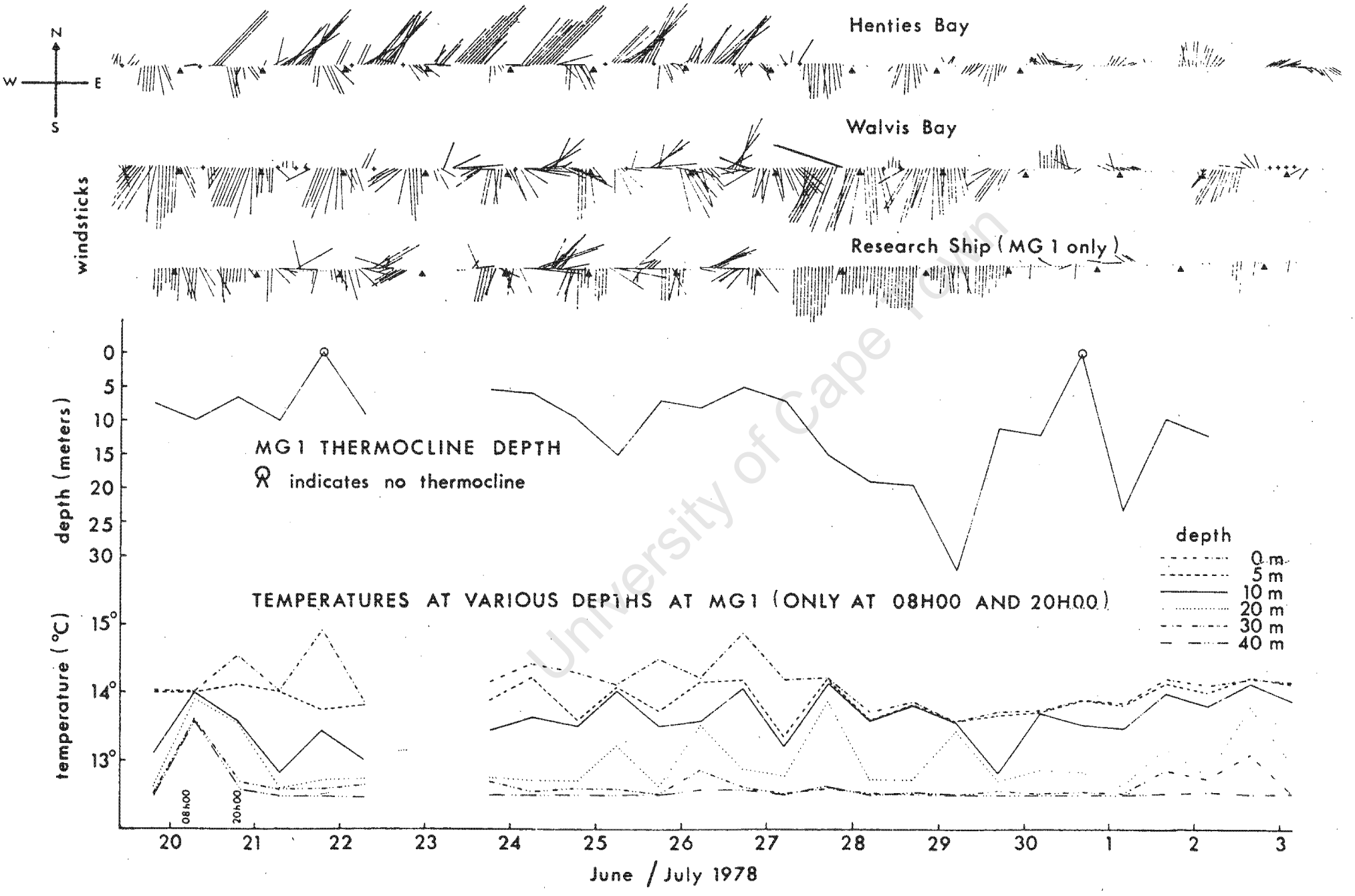

FIG. 8 TIME SERIES OF WINDS, THERMOCLINE DEPTH AND TEMPERATURES AT MG1

FIG. 9 THREE-POINT DEPLOYMENT ON 28/6/78 AT 22°S

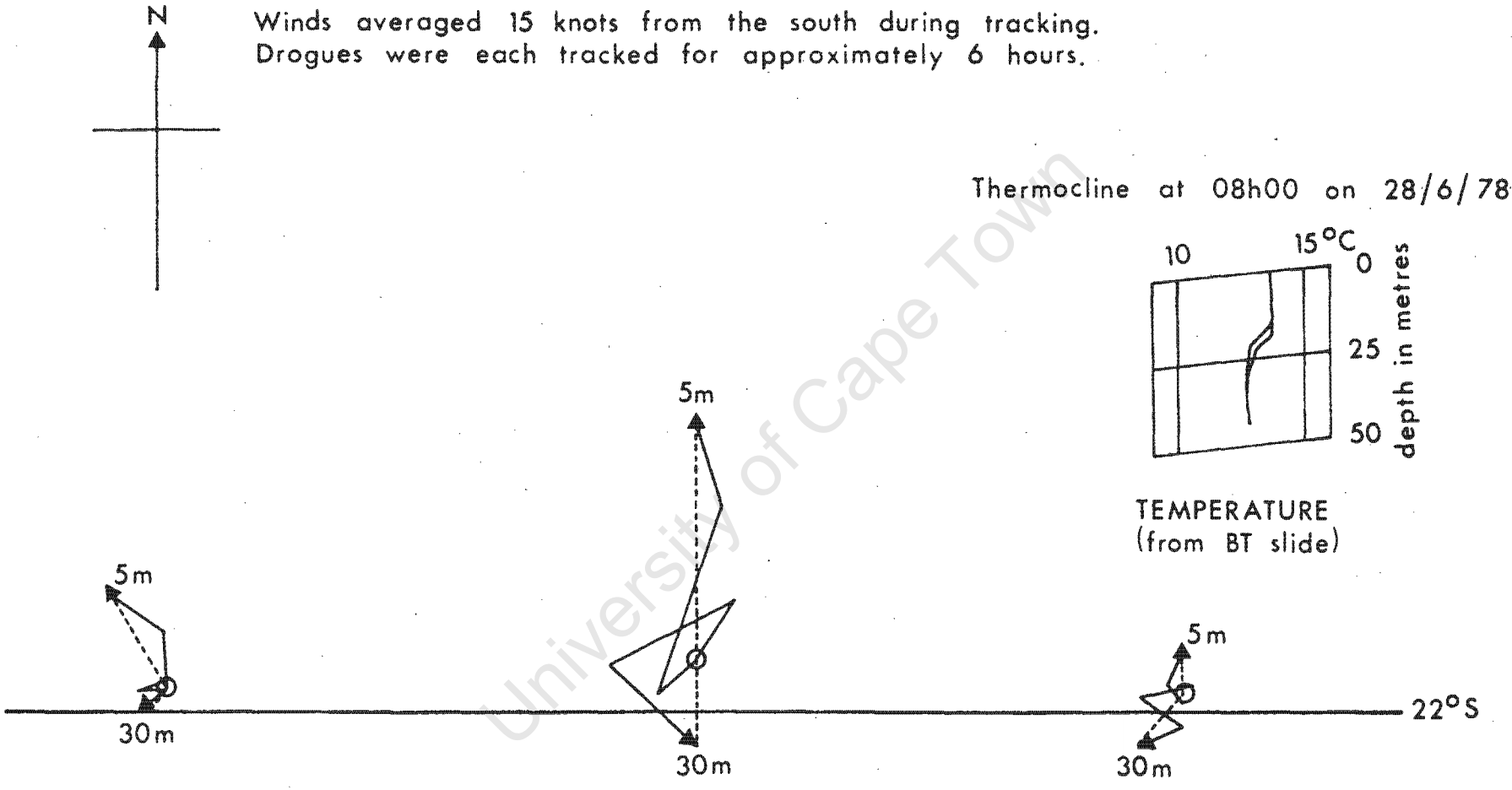

On 22, 24 and 26 June, 1978, drogues were released in typical landbreeze/seabreeze conditions (Figure 10). The best current record was obtained on 26 June and it will be described to show the response of the surface currents to the diurnal winds. Other occasions showed similar features but did not have the continuity of current measurement.

At 08h00 on 26/6/78 a rather diffuse thermocline existed between about 8 and 20m (Figure 13). At 20h00 however, two sharp thermoclines at 5 and 10m were present above the previous thermocline (Figure 13). Thus reasonably independent movements would be expected at the different depths. (This aspect is examined in detail for the 26/6/78 in section 9, hence the unfortunate jump in figure numbers.)

As can be seen in Figure 10, the landbreeze started at 06h00 and increased in velocity to reach a maximum of between 15 and 20 knots from 08h00 to 12h00. The direction was mainly 060 to 070. Five drogues at depths of 2, 5, 10, 20 and 30m were deployed between 07h00 and 08h00. The surface (2 and 5 metre) drogues immediately set off in the direction of the wind (this was obviously more marked before the windage corrections were applied) and then moved in a mean direction of 210 to 220 degrees from 08h00 till 12h00, which is about 30° to the left of the wind.

At 13h00 the wind dropped but it picked up again at 16h30 as a seabreeze from 260° before swinging around gradually to reach southerly at 21h00. The wind died at 24h00.

FIG. 10 OCCASIONS 8 AND 9 26/27 JUNE 1978
DROGUE TRACKS HAVE BEEN CORRECTED FOR WINDAGE

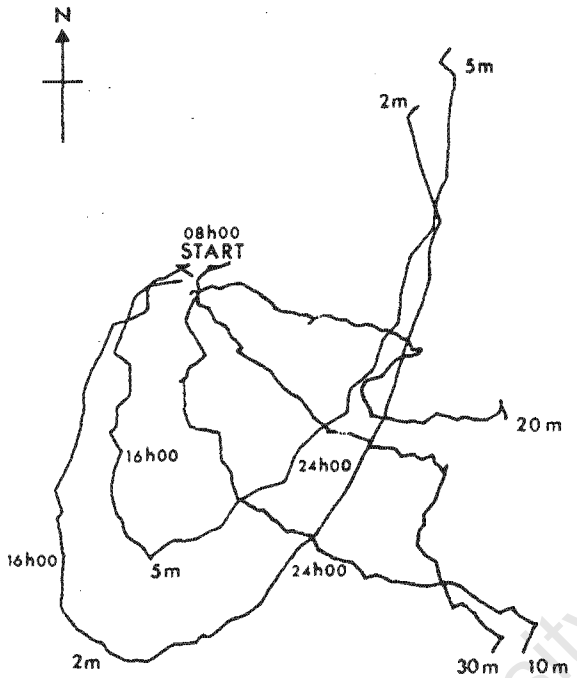

All drogue tracks end at 08h00

Mean speeds (knots)

2 m drogue = ·24

5 m drogue = ·22

10 m drogue = ·14

20 m drogue = ·11

30 m drogue = ·14

scale: tenths of a n.mile

windscale: 20 kts

WINDS FOR THE PERIOD 04h00 26th TO 08h30 27th JUNE 1978

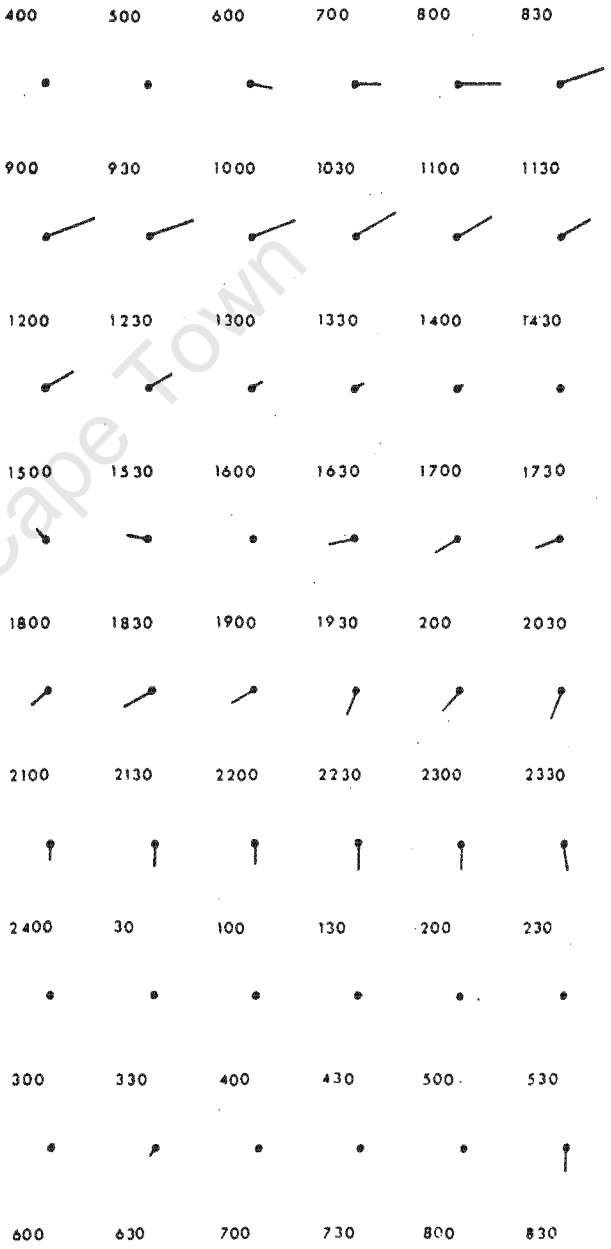

Two more surface drogues were deployed at 16h00 and the others retrieved. At 16h30, as the seabreeze started, they were heading in a southerly direction. By 20h00 their direction had swung to 090 under the influence of the seabreeze and at 24h00 the surface drogues were heading 030, now however 30° to the right of the wind.

The calm conditions from 24h00 to 08h00 the next morning saw the surface drogues swing slightly more to the left, but inertial circles were not described, as mentioned in section 3.1. During the whole diurnal cycle, the currents at 10, 20 and 30m moved in sluggish meandering manner to the southeast, "down" the coast.

Diurnal winds have been shown to be able to control the surface currents. At 08h00 on 26/6/78 the surface current was westerly, at 20h00 easterly. Thus a new time scale of 24 hours can be added to the inertial time scale of 32 hours. Ignoring pressure gradient forces, this means that during temporary calm conditions, inertial current rotation will lag behind diurnal rotation of the imaginary wind (using a complex number analogy). When the wind picks up again this lag becomes noticeable. On the other hand, in a steady state, say after 3 hours of uniform wind, the surface currents will lead the wind by about 30°. This variable phase of lag and lead will cause problems in the next section in which current and wind components are correlated.

3.4 Correlations between winds and currents above the thermocline.

An intial objective of the drogue tracking experiment was to ascertain quantitatively the response of surface currents to wind on a short time scale, by means of correlation. Several major problems were encountered and these are as follows:

Firstly the current record is far from continuous which precluded a spectral analysis of the vectors.

Secondly the longer periods of tracking, in particular those of the 2 and 5m drogues, were done in calm or low windspeed conditions. Thus viewed as a whole the data set of velocity vectors is biased. (In order to keep accuracy as high as possible only velocity vectors from radar tracking occasions were used.)

Thirdly one is forced to assume a time lag between the wind and current vectors, as currents take time to respond to the wind and, as mentioned in the previous section, wind-changes.

Nevertheless, a determined effort to relate current response at depths of 2 and 5 metres to the wind produced results which at least underscore the fact that the surface layer did respond to, and in general direction of, the wind forcing.

A time lag of 2 hours was used. The choice of this lag was decided upon after examining currents and wind trajectories pictorially.

It was noted that the current velocity seemed to correlate best with the wind velocity recorded between 1 and 3 hours previously. Had the winds been more steady in velocity a longer lag would have been no doubt better, but the "steady" occasions were few and far between and these will be discussed in section 3.8.

Another decision was to use only current speed components for correlation with their appropriate wind components if the latter had a wind speed greater than 3 knots. The component axes into which vectors were broken were primarily north-south (Y) and east-west (X). X currents were only correlated against X winds and Y currents only against Y winds. Other axis directions were also tried, including an angle between wind and current axes as a function of lag. However in view of the above-mentioned problems, particularly bias, this approach only complicated the matter.

All correlations were linear, in the line with Ekman's (1905) infinite ocean steady state equations which result in the following relationship (at 22°S):

Surface current speed = 0,021 x Windspeed (any units) (3-2)

(The eddy viscosity value used was 4,3 x Windspeed^2 and the windstress τ was taken as 2,6 x 10^{-3} x density of air x Windspeed^2, Neumann and Pierson, 1966, pp 209, 210).

Although the conditions for using the above-mentioned Ekman equation were blatantly not met, his formula has acquired a generality of application through use, particularly as regards surface current speeds.

Table 4 below displays the results of correlations using half hourly wind and current components. The X axis was taken as being positive eastwards and the Y axis as positive northwards.

Table 4: Current-wind correlations

Current depth and direction	2mY	5mY	2mX	5mX
Correlation coefficient (r)	0,60	0,65	0,73	0,45
Slope	0,015	0,015	0,012	0,007
Number of points	44	46	31	47

Of interest in the correlations is the correlation coefficient, the slope and the intercept (not shown). The square of the correlation coefficient is indicative of how much of the variance of the current components is attributable to the corresponding wind components' variance, and the slope allows an estimate to be made of wind-caused current components from wind velocity components. If there was a residual pressure gradient current this would be apparent in a significant departure from zero for the intercept. The intercept values are not given however, because after analysing them it was realised that they reflected the sampling bias more than any residual current.

The values of the slope for the 2m X and Y currents are comparable to the "slope" of 0,021 given in equation 3-2. In addition a small allowance can be made for the fact that the Ekman equations predict a surface current at angle to the wind. In the corresponding time dependent solution of Ekman's equations this angle is about 18° after two hours by which time the surface current speed is very close to its steady state speed. In a later section current speed will be related directly to windspeed without analysing components, and a "slope" of 0,017 will be obtained.

The degree of current variance which can be attributed to wind along the same axes (r^2), is on average just under half. Smoothing and averaging of current and wind vectors raised both the slopes and the r^2 values, the latter to just over half on average. However the number of components available for correlation declined to an extent that reduced the "statistical significance" of the results.

Wind-current component correlations will not be taken further in this study. However, it has been shown that the wind has prompt and "significant" influence on the surface layer movement. It is mentioned here that statistical significance can not actually be given when a biased sample is used. However, if one considers the sample to a random one of "low to moderate wind speed events", then the positive correlation between wind components and the 2m current components would be significant at the 0,1 per cent level.

In the next section the relationships between current at various depths will be examined, and it will be seen that evidence exists for a separate current structure in the surface and lower layers.

3.5 Correlations amongst current components.

A current component correlation matrix is presented in Table 5. It also includes wind components, but only those appropriate to current tracking occasions. It is mentioned again here, that currents at the different tracking depths were not always tracked simultaneously. Hence the vector data set for the 2m versus 5m correlations would not necessarily come from the same occasions as that for the 20m and 30m correlations. Thus the number of vector components used for each correlation differs and the appropriate numbers are also given in Table 5. All components considered in this matrix are unsmoothed hourly components. The average currents derived from these components are shown in Figure 11.

For the purpose of this study only the highest correlations in Table 5 will be discussed, although many others are "significant". All those discussed have r values above 0,75 and are as it happens, correlations between components along the same axes. Without the conditions imposed in the previous section, especially the 2 hour lag between wind and surface (2 and 5m) currents, these currents correlated poorly with wind components.

Table 5: Correlations amongst current components

		x					y					
		2m	5m	10m	20m	30m	Wind	2m	5m	10m	20m	30m
x	Wind	,27(48)	,32(56)	,23(58)	,11(69)	,02(84)	,47(94)	,06(48)	,07(57)	-,13(58)	-,21(70)	-,03(84)
	2m		,93(39)	,79(46)	-,02(46)	-,01(44	,25(48)	,17(48)	,20(39)	-,29(46)	-,48(46)	-,22(44)
	5m			,85(42)	,23(43)	,25(55)	,28(56)	,25(35)	,31(56)	-,28(42)	-,61(43)	-,34(55)
	10m				-,06(54)	-,22(53)	,16(58)	,20(46)	,22(43)	,02(58)	-,17(46)	,30(53)
	20m					,91(62)	-,16(69)	-,08(46)	,09(44)	,43(54)	,27(69)	-,31(62)
	30m						-,24(84)	-,08(46)	,01(56)	,40(53)	,23(63)	-,54(84)
y	Wind							-,10(48)	-,05(57)	,05(58)	-,03(70)	,07(84)
	2m								,93(39)	,17(46)	-,15(46)	-,23(44)
	5m									,54(43)	-,05(44)	-,23(56)
	10m										,81(54)	,28(53)
	20m											,49(63)

FIG. 11 AVERAGE CURRENT VELOCITIES

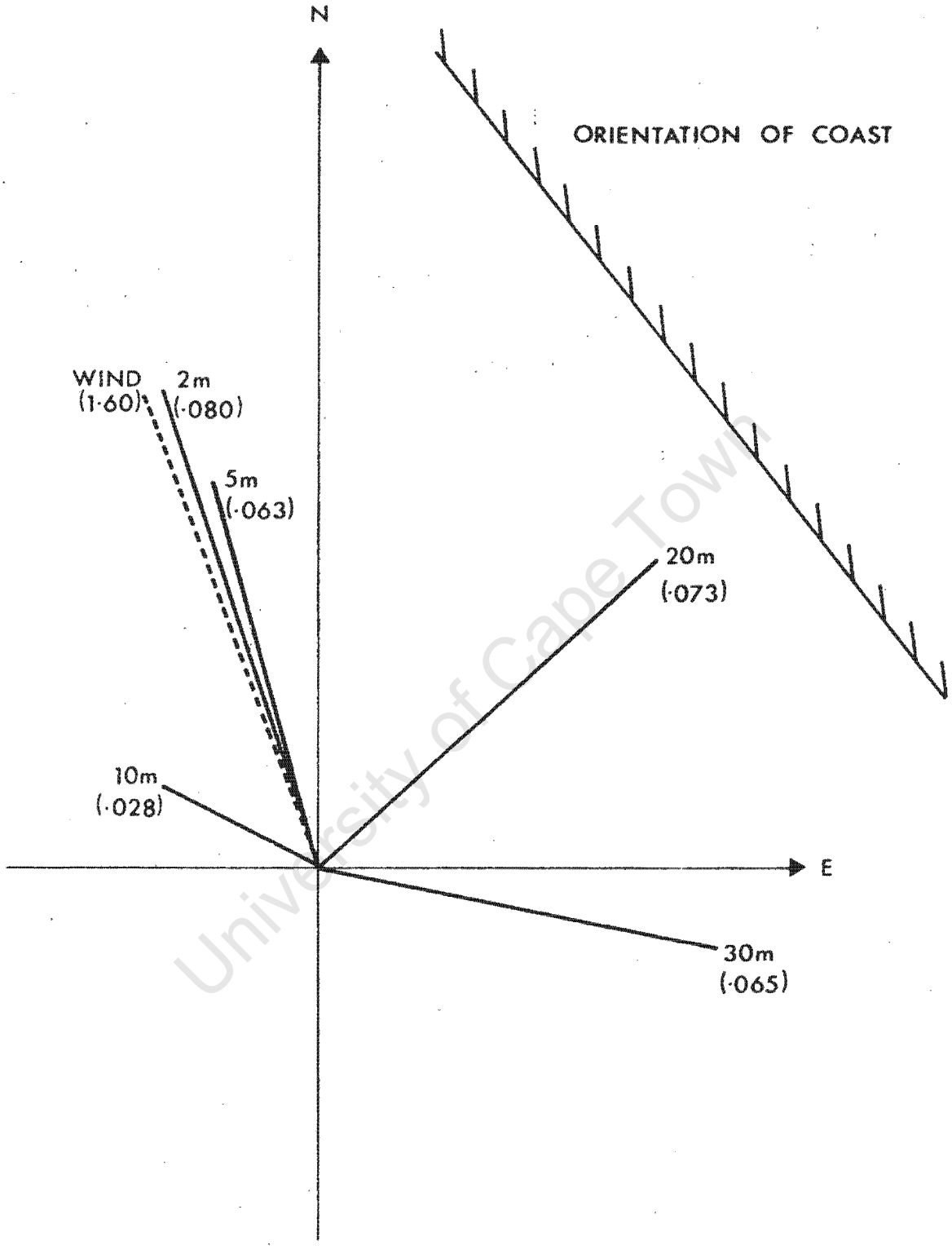

DROGUE DEPTH	2	5	10	20	30
HOURS OF TRACKING	48	56	58	69	84

3.6 Current velocities and speeds.

Examination of "average" currents over the two week period at various depths produced results (displayed in Figure 11 and Table 6) that showed net onshore transport at MG1. The average velocity at 20m was directly onshore, that at 30m had a strong "downshore" component (possibly due to topographic effects), as well as an onshore one, whilst the surface layer movement (as measured by the 2 and 5m drogues) was northwards and mainly longshore. The average 10m current velocity only had a very small offshore directed component, and could have only minimally compensated for the onshore movement at other depths. Thus for a continuity balance at the research site one must accept that more offshore directed currents must have existed in the surface layer and that these were just not adequately sampled. The significantly longer total time spent tracking the currents at 20 and 30m puts more confidence in their velocity figures.

It is, of course, not necessary to have an exact continuity balance at MG1 as it is still some 6 miles from the coast. However, it is felt that a much better balance existed than is expressed in Figure 11, in view of the bias of the current record which was discussed in section 3.4.

Table 6 summarises the extent and basic results of the current tracking done by radar.

Table 6: Current velocities and speeds.

Tracking depth (m)	2	5	10	20	30
Average velocity (kts)	0,080	0,063	0,028	0,073	0,065
Average speed (kts)	0,241	0,204	0,171	0,138	0,151
Av. velocity/speed ratio	0,33	0,31	0,16	0,53	0,41
Hours of radar tracking	48	56	58	69	84

Of special interest in Table 6 are the similarity of the velocity/speed ratios for the surface (2 and 5m) currents, the higher ratios for the lower layer (20 and 30m) and the very low ratio for 10m. These ratios can be used to support the by now oft repeated assertions that the 2 and 5m depths were both practically always in the wind controlled surface layer, the 20 and 30m currents moved more consistently (as can be seen by their higher velocity/speed ratios) with an onshore component, whilst the current at 10m depth suffered problems akin to those of a child with separated parents.

The agreement in direction between the average surface layer velocities and the average wind velocity (Figure 11) is welcome but not significant. This is because about half of the wind velocity vectors used to obtain the average were recorded during occasions when no surface tracking was done.

In the following section the emphasis will be temporarily shifted away from current vectors and current speeds will receive priority attention.

3.7 Current speed variations with depth.

Current speed profiles from all radar tracking occasions are presented in Figure 12. It must be noted that these profiles in no way infer anything about relative speeds between different depths. The mean speed and variability for the tracking depths are tabulated below in Table 7. To obtain these mean speeds hourly or half hourly vectors were not used, and occasions were not weighted according to the time the drogues were tracked. Each occasion was instead considered as sampling just one current speed per drogue. In Figure 12, the day of the month is indicated next to each profile (or point) with the occasion number in brackets.

Table 7: Current speed and variability

Tracking depth (in metres)	2	5	10	20	30
Mean speed (in knots)	0,23	0,20	0,14	0,11	0,12
Std. dev. of mean speed	0,056	0,059	0,063	0,036	0,017
Number of occasions	7	9	9	11	11

The mean speeds shown in Table 7 are similar to those of Table 6, but are somewhat lower at 10, 20 and 30m. The following points can be noted from Table 7 and seen in Figure 12.

FIG. 12 CURRENT SPEED PROFILES

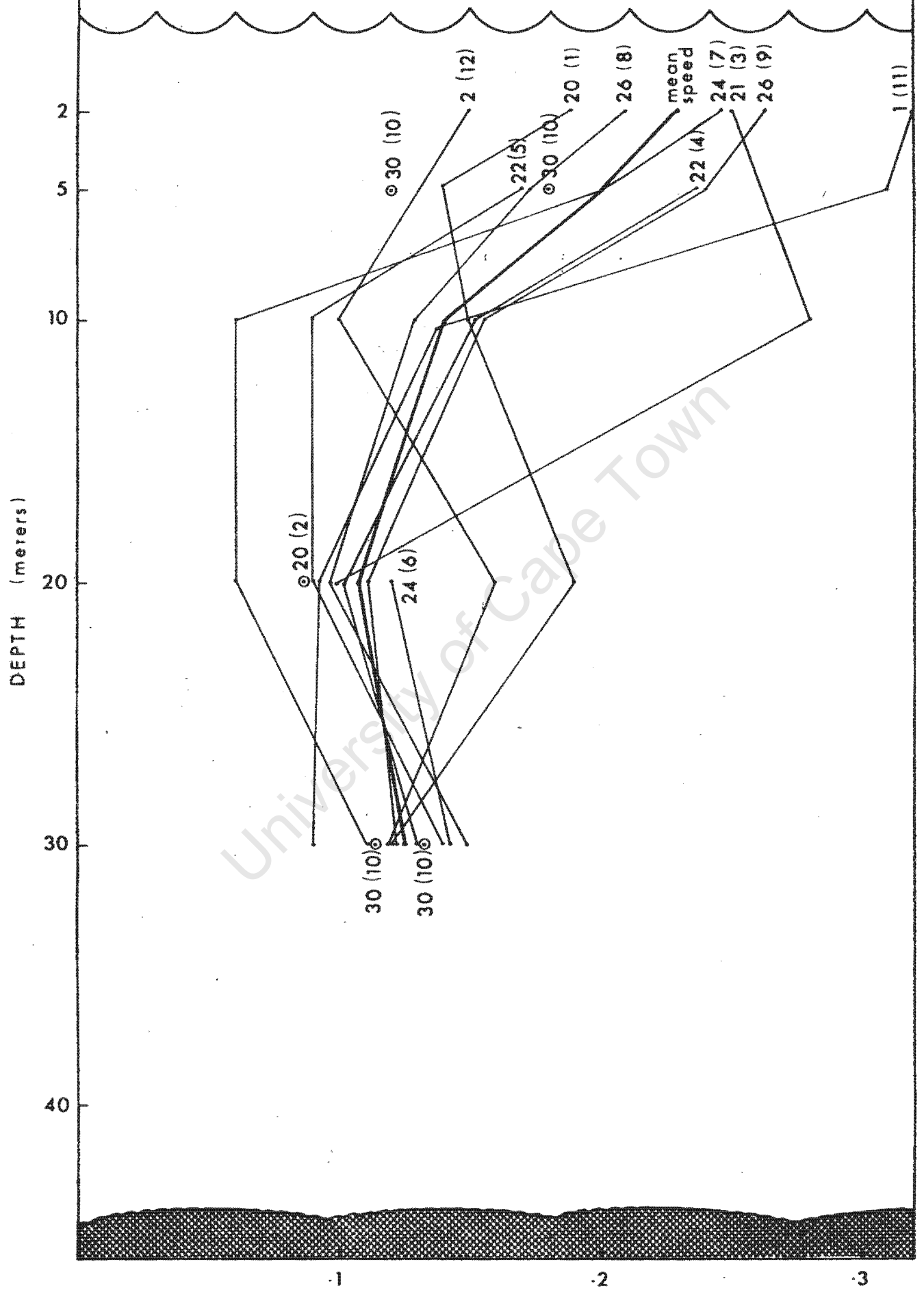

Note: This does not give relative speeds between currents at different depths during an occasion

Firstly there is very little difference as regards the speed and speed variability (i.e. std. dev.) of the 2 and 5m currents. This yet again underscores the fact that the wind driven layer extends beyond 5 metres, and that either of those tracking depths may be used to infer surface layer movement on different occasions.

Secondly the 10 and 20m currents show a notable speed decrease while the 10m current retains a high variability, emphasising again its "attachment" to both upper and lower layers on different occasions.

Thirdly the 30 metre current has a nominally higher mean speed than the 20 metre current (which can be noted from both Table 6 and Table 7), but the latter Table shows it to have an extremely low speed variability. The possibility of an "under current" continuous in time and direction is ruled out however, by the moderate value of 0,41 for its velocity/speed ratio given in Table 6. This would suggest a meandering counter current in lower layers around MG1, which is not as affected by short time-scale continuity considerations as the directly onshore 20m current.

Thus the present approach has yielded a slightly different grouping of current structure with depth. The surface layer concept and the unsteadfast nature of the 10m current have remained intact, but the 30m current has shown evidence that the lower layer is not always one, as may have been expected. It must be borne in mind though that a clue was unearthed earlier in section 3.5, where the 20 and 30m currents only correlated highly in the X (roughly onshore) direction.

This section completes the analysis of the whole current data set. In forthcoming sections particular occasions will once again be examined but on a more quantitative basis than was done previously.

3.8 Selected periods: "steady" winds and currents.

On some occasions the wind was reasonably uniform for a period of several hours and drogues were deployed at at least two of the 2, 5 and 10m depths. Four of these periods were selected, during which the wind did not change in direction by more than 10° and the windspeed was greater than 8 knots and fairly uniform for a period of at least 2 hours. Average wind vectors were calculated for this period and they are related to average current vectors for the corresponding period after a lag of two hours. The data are tabulated in Table 8 and displayed in Figure 13.

From the average data shown in Table 8, a formulation of:

$$|V(2)| = 0{,}017^{*} |\text{Windspeed}| \quad \text{------ (3-3)}$$

$^{*}(0{,}227/13{,}5) = 0{,}017$

can be obtained making no allowance for the angle between wind and current. Bearing in mind this allowance, this formulation is consistent with previous results obtained for the slope of wind-current component correlations (section 3.4 and the Ekman based relationship of $V(o) = 0{,}021$ Windspeed. The present result will be used extensively when developing the mathematical models in Chapter 4.

Table 8: "Steady" winds and currents

	Occasion 1	Occasion 4	Occasion 8	Occasion 9	Average
Wind period :	11h30-13h30	06h30-08h30	08h30-11h30	21h30-23h30	-
Velocity (kts)					
Wind	12	16	17	9	13,5
2m current	0,19	0,27 (est.)	0,22	0,27	0,227
5m current	0,13	0,22	0,14	0,24	0,183
10m current	0,13	0,13	0,12	0,08	0,115

FIG. 13 SELECTED "STEADY STATE" OCCASIONS

OCCASION 1
wind 1130 - 1330
current 1330 - 1530

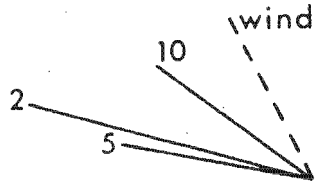

OCCASION 4
wind 0630 - 0830
current 0830 - 1030

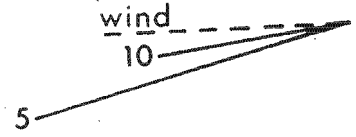

OCCASION 8
wind 0830 - 1130
current 1030 - 1330

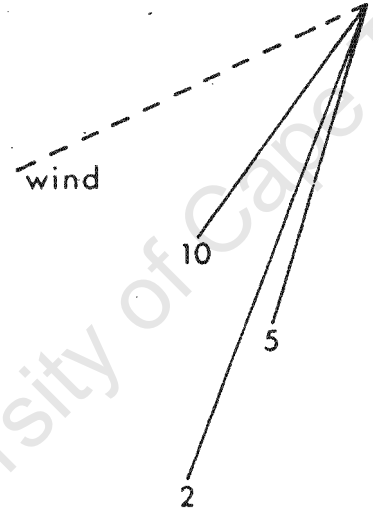

OCCASION 9
wind 2130 - 2330
current 2330 - 0130

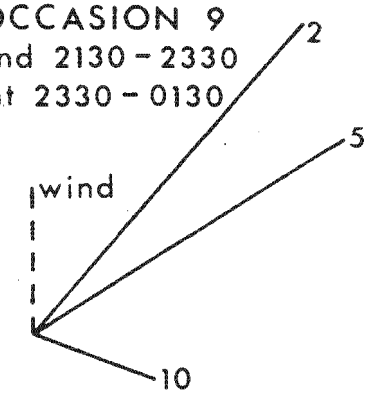

BATHYTHERMOGRAGH TRACES: TEMPERATURE (°C)
DEPTH (metres)

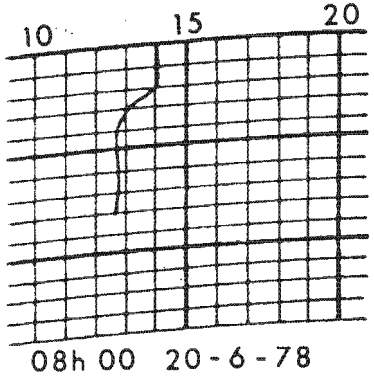

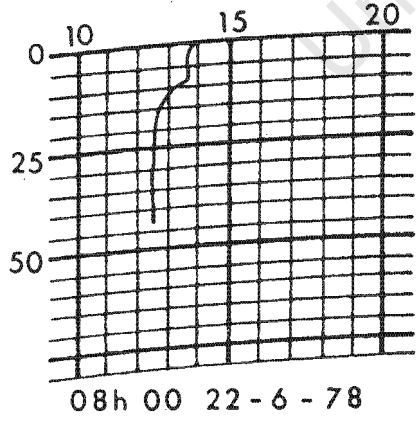

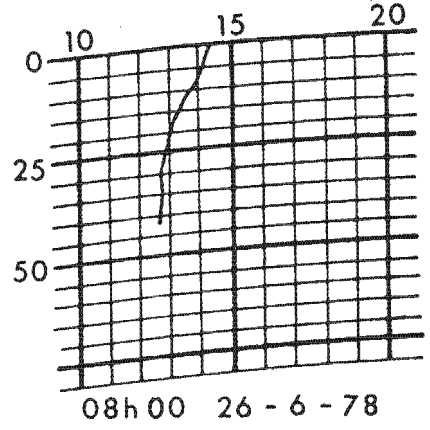

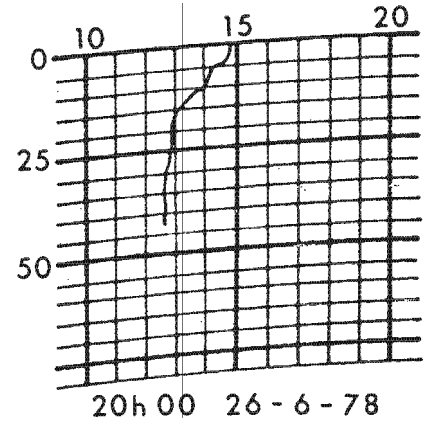

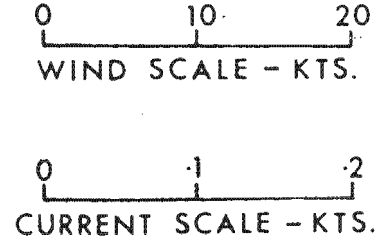

A brief description will now be given of the angular separation between the winds and currents of these four selected periods with reference to Figure 13.

In keeping with the results of previous sections, there was very little separation between the 2 and 5m drogue tracks. This can be ascribed to the balance between:

(a) the frictional and coriolis forces trying to move the 5m drogue to the left of that at 2m, and
(b) the quicker response of the 2m drogue to the leftward rotating winds.

Because these periods were chosen for their lack of wind variation, the first mentioned forces dominated except during occasion 9, when the wind had a history of such rotation before the selected period. The latter occasion also found the surface current to the right of the wind for this very reason (a previous description of occasions 8 and 9 in section 3.3 can be referred to for more details.) During the other three periods the surface current was deflected to the left of the wind.

The 10m current was on all four occasions found to the right of the surface (2 and 5m) currents. This implies that friction and the coriolis force were losing out to the response of the surface layer to the wind. The cause is stratification allowing shear flow to exist between upper and lower layers. This important aspect which

has been observable in most current data presented this far, but has not yet been discussed, will be examined in detail in the next section.

3.9 Current shear and density differences.

Current shear, that is a relative velocity between currents at different depths, is typically found most markedly over depth ranges with high density gradients. In the research area, because of the very uniform salinity distribution (see Chapter 5), this means over thermoclines. For swifter flowing currents a high density gradient is necessary for shear flow, for more sluggish currents a lower gradient can suffice. Mixing in regions of shear flow tends to reduce the density differences by a process known as entrainment, and this aspect is discussed at length in Chapter 5. In the present section, density differences and relative velocities between "layers" that occurred during occasion 8 will be examined in detail, in an attempt to provide quantitative arguments to back up the qualitative reasoning given thus far for velocity differences with depth.

The current data is given in Table 9 and the density data in Table 10.

Table 9: Relative current velocities (08h00-15h30 on 26/6/78)

Depth interval (m)	2-5	5-10	10-20	20-30
Relative velocity (cm/s)	3,6	3,1	4,8	4,0
(Relative velocity)^2	13	9,6	23	16

Table 10: Density differences x 10^5 (gm/cm^3) between depths on 26/6/78 and 27/6/78

Range:	0-5m	5-10m	10-20m	20-30m	0-30m
Time					
08h00	2	12(s)	1	13(s)	28
12h00	5(s)	4(s)	25(s)	5(s)	39
16h00	13(s)	3(?)	19(s)	12(s)	47
20h00	15	3	24	5	47
24h00	12	2	17	15	46
04h00	6	15	12	5	38
08h00	17	3	9	5	34

Note: (a) A standard salinity was used for all times and depths, as salinity was measured only at the 08h00 and 20h00 stations.

(b) (s) infers probable shear flow between layers. The period after 16h00 is not considered.

Phillips (1977) discussed the balance between stability and mixing forces and stated that for shear flow to be maintained without rapidly destroying a high density gradient the local Richardson number should not exceed 0,25 (a figure proposed by Taylor (1931)). The times, and depth ranges in which shear flow could be expected on the 26/6/78 are investigated below.

The local Richardson number $R_i = g \frac{\partial \rho}{\partial z} / \rho \left(\frac{\partial u}{\partial z}\right)^2$ (3-4)

Hence $\frac{\partial \rho}{\partial z} > 0{,}25 \frac{\rho}{g} \left(\frac{\partial u}{\partial z}\right)^2$ for shear flow (3-5)

In the present context this relationship will be written as

$$\frac{\Delta \rho}{\Delta z} > 0{,}25 \left(\frac{\Delta u}{\Delta z}\right)^2 \times 10^{-3} \qquad \text{taking } g = 10^3 \text{ cm/sec}^2 \tag{3-6}$$

In order to approximate to a local Richardson number, Δz will be taken as 100cm. All density and shear differences are then assumed to take place over this specified thermocline depth. Examination of the thermocline traces in Figure 13, particularly that for 20h00 on 26/6/78 shows that this is anything but an arbitrary assumption.

We now have the following condition for shear flow:

$$\Delta \rho \times 10^5 > 0{,}25 \ (\Delta u)^2 \tag{3-7}$$

The density differences required for shear flow in the various depth ranges on 26/6/78 are tabulated below, taking $(\Delta u)^2$ as the (relative velocity)^2 given in Table 9.

Table 11:

Depth range:	2-5m	5-10m	10-20m	20-30m
$\Delta\rho \times 10^5$ required:	3,3	2,4	5,75	4,0

Comparison of the data given in Table 11 above with that in Table 10 indicates that only in the 2-5m and 10-20m depth ranges at 08h00 would shear flow not be possible, even though the appropriate thermocline trace shows no pronounced density gradient (Figure 13). (An (s) in Table 10 indicates probable shear flow.)

Further examination of Figure 13 shows that later in the day (20h00 on 26/6/78) two distinct thermoclines are evident at about 5 and 10m depth. The current vectors at 2, 5 and 10m reflect this by having a very wide angular dispersion. The current at 10m depth is moving at right angles to that at 2m. Shear flow is definitely well developed, and in this instance the assumption of taking Δz = 100cm is well founded. However it appears that the initial density "discontinuity" which occurred above 5m according to Table 10, must have actually occurred below the 5m drogue. This is due to the fact that the surface bottle sample was actually done at about 2 m depth meaning the 5m sample was done at 7m depth. In keeping with hydrological sampling techniques no allowance was made for this, but in this instance it must be noted.

In conclusion it can be said that whilst the conditions for the existence of shear flow were commonly satisfied over more than one depth range in the water column, a small "discontinuity" appears necessary for "pronounced" shear flow.

This section closes the chapter dealing with the results of the drogue tracking experiment. Attempts will be made to model some of these results, after a brief look at the spatial distribution of winds in the Walvis Bay to Cape Cross area.

A summary of the present chapter is provided on the next 3 pages. It was designed both to separate the salient results of this chapter from the mass of methods, and to enable a reader to proceed to the modelling chapter without referring to individual sections of the present one.

3.10 A summary of the results of the drogue tracking experiment.

(The results of each section are stated under the appropriate section number.)

1.) Inertial motion was observed at different depths during a calm period with the implication that:

(a) pressure gradient forces had a relatively short relaxation time

(b) shear flow between surface and middle, and middle and lower layers must have occurred.

2.) Spatial variation in current direction, but not speed, was observed to be small at 5m. Spatial variation in velocity was small at 30m. A "poleward" undercurrent at 30m was measured.

3.) Strong southerly winds that caused vertical mixing and lowered the surface temperature were not accompanied by current velocities of any magnitude.

Diurnal winds rotated in an anticlockwise direction with the offshore landbreeze generally being the strongest. The 2 and 5m currents were basically in the direction of the wind, but the angle from wind to current was observed to change from anticlockwise to clockwise as the wind rotated through the day.

4.) Linear correlations of 2 and 5m X (i.e. easterly) currents on X wind, and 2 and 5m Y (i.e. northerly) currents on Y wind, using a current-wind time lag of 2 hours, would have been statistically significant if the wind/current data set were not biased.

5.) Correlations amongst current components yielded very high coefficients between 2 and 5m currents in both the X and Y directions ($r = 0,93$ in both cases). The 10m current correlated well with surface (2 and 5m) currents in the X direction but not in the Y direction where it is correlated better with the 20m current. The 20 and 30m currents correlated highly in the X direction (that closest to onshore) but not in the Y direction, showing that a unified "lower layer" cannot be assumed.

6.) Average currents (calculated from the whole radar tracking data set) showed mainly longshore transport in the surface layer and onshore transport at 20 and 30m depth, with a marked "downshore" component at 30m. At 10m the average velocity was low and slightly offshore. Sampling bias is thought to have led to an under-estimation of the offshore velocity of the surface layer.

7.) Current speed decreased with depth to 20 metres and then increased slightly at 30m. The 30m current had an extremely regular speed, and this together with its average velocity led to the conclusion that a meandering counter current flows "down" the coast in a south-easterly direction, the mean flow being largely unaffected by surface layer movements.

8.) Data from 4 "steady state" occasions in which total current velocity was divided by total wind velocity gave a formulation of:

"Surface" current speed = 0,017 x Windspeed

This result will be used extensively in the modelling chapter.

9.) The relative velocities between layers, and the vertical density structure showed that on a typical occasion shear flow could occur at more than one depth in the water column. Thus winds would often only directly influence the surface layer (that above 5-10m) and the mixing of water properties vertically below these depths would be severely curtailed.

3.11

A Note on the variations in the wind as measured at the Research Ship, Henties Bay and Walvis Bay during June 1978.

The winds prevailing off South West Africa have been previously discussed along two lines. Firstly, Stander (1963) and Stander and de Decker (1969) using data from Pelican Point lighthouse detailed the daily, seasonal and yearly variability of the local winds around Walvis Bay. Secondly, Hart and Currie (1960), Stander (1964), Schell (1968) and Bailey (1979) described the basic pressure systems and offshore wind regimes using ships' data.

At the present moment wind data is being collected from two anemometers along the South West African coast in addition to that at Pelican Point. They are situated at Ichaboe Island (26°S) and Henties Bay (22°S). The Henties Bay anemometer, initially installed specifically for this programme, gave data that highlighted the spatial variability of the coastal winds in both longshore and offshore directions. The wind measured at Walvis Bay, Henties Bay and the research ship during June 1978 are shown in Figures 14, 15 and 16, and are described below.

Some basic differences amongst the winds at the 3 sites are obvious, namely that the stronger winds at Walvis Bay were dominantly southerly, those at Henties Bay north-easterly, and the research ship experienced both of the above directions fairly equally (unfortunately the record is much shorter.) If a strong north-easterly was present at Henties Bay,

WIND VELOCITY AT WALVIS BAY : 78-6-1 TO 78-6-31

△ = 1200/ . = NO DATA 0 = CALM + = VARIABLE

N

The windsticks indicate the direction from which the wind was blowing

Fig. 14

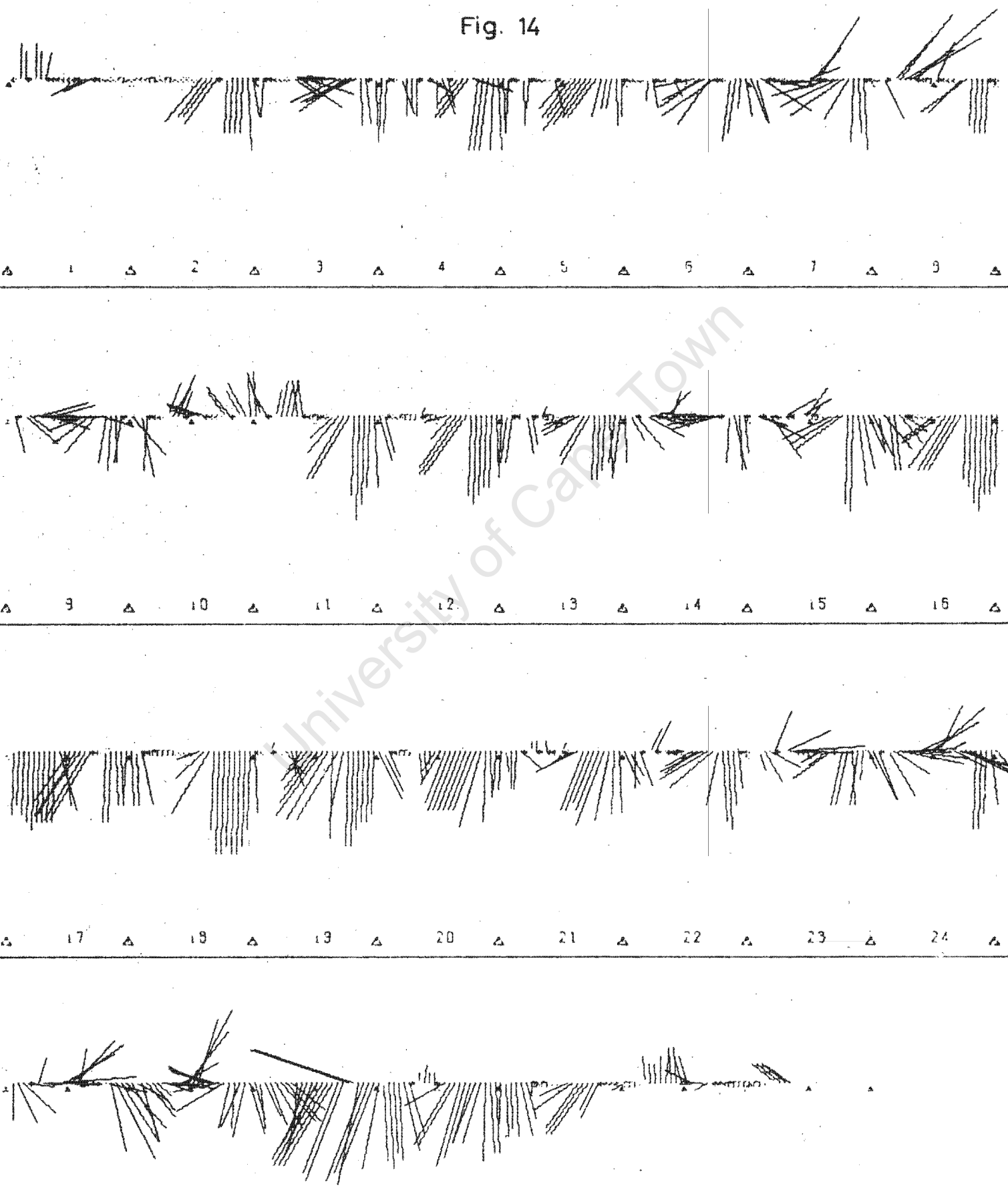

WIND VELOCITY AT HENTIES BAY : 78-5-1 TO 78-5-30

△ = 1200/ . = NO DATA 0 = CALM + = VARIABLE

N

The windsticks indicate the direction from which the wind was blowing

Fig. 15

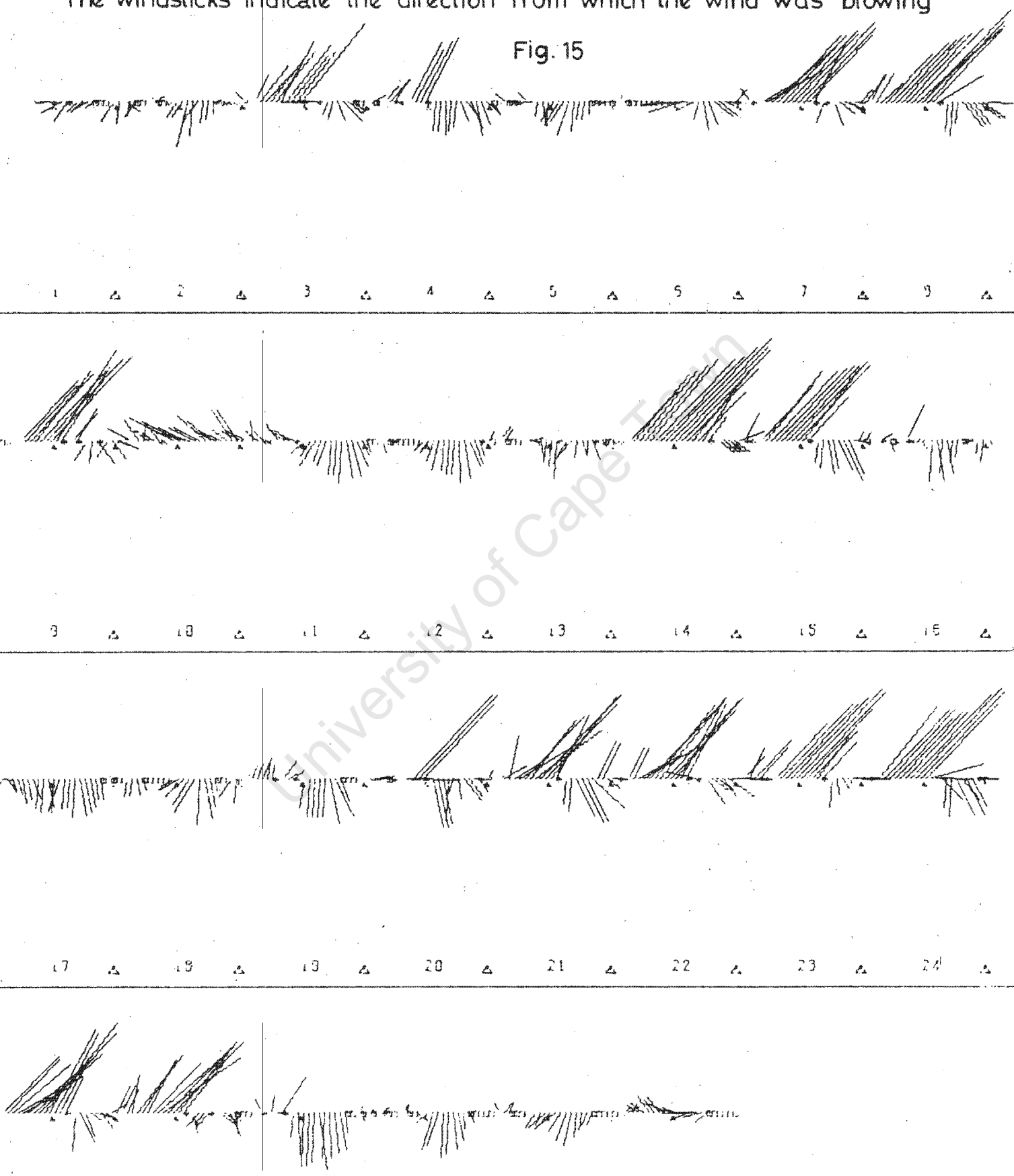

WIND VELOCITY AT RESEARCH SHIP : 78-6-19 TO 78-6-30

N

△ = 1200/ . = NO DATA 0 = CALM + = VARIABLE

The windsticks indicate the direction from which the wind was blowing

Fig. 16

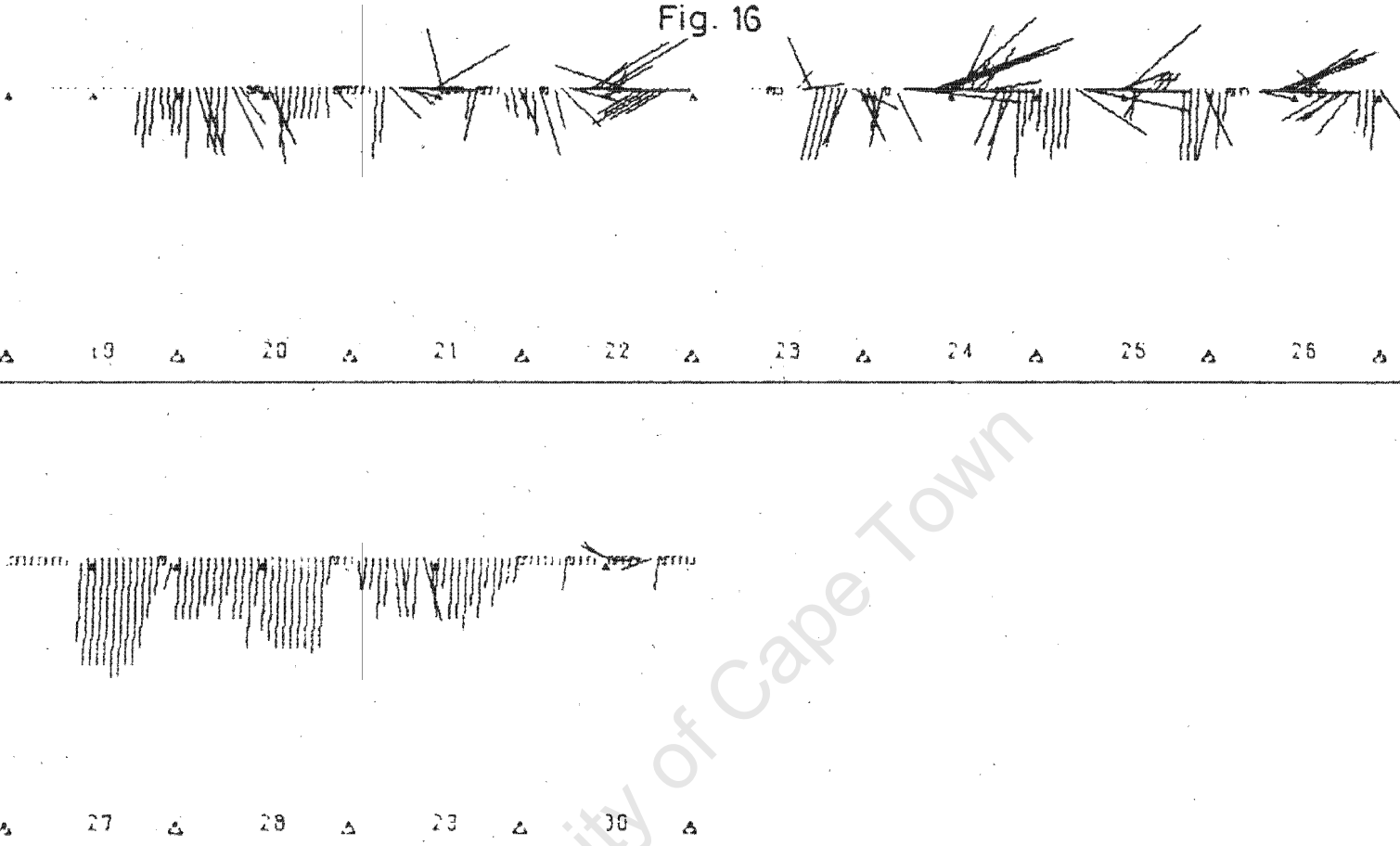

a weak wind of similar direction would probably be measured at Walvis Bay. On the other hand, if a strong southerly was recorded at Walvis Bay, a weak southerly could be expected at Henties Bay (e.g. the 11th and 12th of June 1978).

All three wind records show similarity though, in that diurnal variation is clearly discernible, albeit manifest in different ways at the three sites.

At Walvis Bay the dominant variation is that of the southerly winds, with onshore/offshore winds straddling them in time and often bordering on calms. At Henties Bay a similar pattern of southerly winds can prevail in the absence of the dominant north-easterly. Windspeeds are about half those at Walvis Bay though.

On the 12 occasions when the north-easterly did "blow" at Henties Bay in June 1978 (i.e. a minimum time duration of 8 hours and windspeeds between 20 and 35 knots), the offshore/onshore winds at Walvis Bay can be noted to be more prominent (e.g. the period from 21 to 26 June.)

The winds measured at the research ship showed less windspeed dependence on direction, and thus incorporated the characteristics of both the Walvis Bay and Henties Bay winds without their excesses.

It can also be noted that the longer timescale event of "constant" southerly winds from 27 to 29 June occurred with somewhat more uniformity in space than the shorter time scale events, i.e. the winds at the three measuring sites at least blew in the same direction, although with greatly differing speeds.

In conclusion it can be said that the average longshore windstress, the basic driving force for upwelling, was greater at Walvis Bay than at the other two sites; the Henties Bay site in particular having more offshore windstress, which because of the pulsating nature of the winds, would only generate intermittent offshore surface current pulses, with no basic longshore current. This was the case as regards currents at the research site, although, because of the greater occurrence of southerly winds and a diminution of the velocity of the easterlies (and current sampling bias) a mean northward current was detected. Further offshore from the research site, the wind regime may have more resembled that at Walvis Bay, and a more regular northward current may have existed during June 1978.

4. A MODEL SHOWING SURFACE CURRENT RESPONSE TO WIND

4.1 Introduction

A simple model of the surface layer incorporating some characteristics found experimentally is presented in this chapter. The basic objective is to investigate the prediction of surface layer movement from wind data, providing a defined surface layer exists. The current is the movement of a "slab" of water extending from the surface to an assumed depth of 8 metres. The equations are of the same form as used by Pollard and Millard (1970), but here they are solved analytically as well as numerically and will be used to examine different aspects of current response to wind. Pollard and Millard (op. cit.) used their "slab" as a means of integration and not because of any physical resemblance to reality. This is not the case here, as evidence of the regular existence of a surface layer, whose movement was basically uni-directional and not directly related to the movement of the layers below because of shear flow, has been given in the previous chapter. The following features are incorporated in the model:

1.) Time dependent wind and current, the driving force being a basic longshore wind with an imposed diurnal variation including both longshore and off-shore/onshore winds in the analytical model. In the stepwise model any hourly wind input can be used.

2.) The coriolis force.

3.) Friction proportional to current velocity and acting in the opposite direction. Later, friction proportional to wind speed as well.

4.) Independent movement of a surface layer of specified depth.

The following features are amongst those omitted:

1.) Explicit depth dependence of current speed W, i.e. if the slab is 5 metres deep $W(o) = W(5)$, but if a different layer depth is chosen $W(d)$ will not be the same as above.

2.) Horizontal and vertical continuity and coastal boundaries, although for discussion an imaginary coast will be considered parallel to the y axis on the positive x side of the origin. In the experimental section no evidence of direct coastal influence on current response to wind was found, although the off-shore/onshore and longshore winds, and hence currents they caused, differed. The ostensible lack of direct coastal influence is attributed to the even bottom topography of the area under investigation.

4.2 The co-ordinate system, terms and basic equations

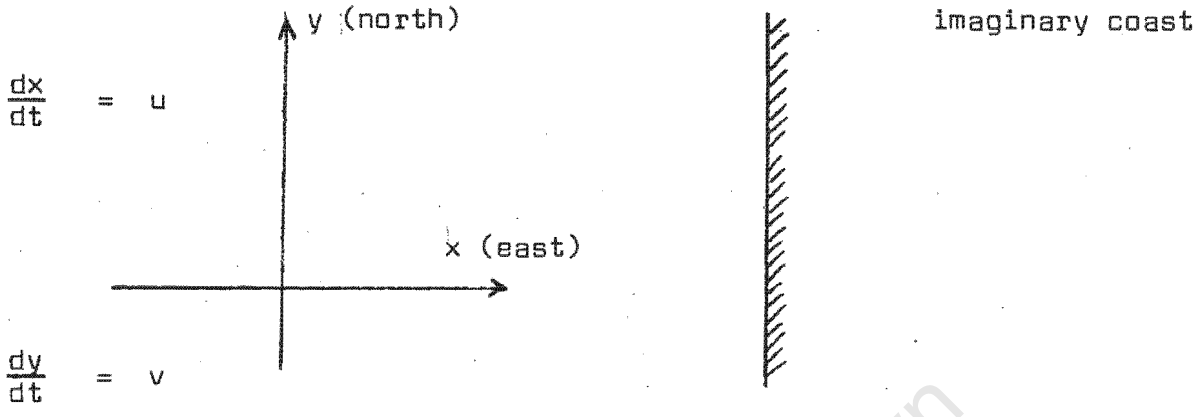

The equations are:

$$\frac{\partial u}{\partial t} + fv = Rv + Q1 \qquad (4\text{-}1)$$

$$\frac{\partial v}{\partial t} - fv = Rv + Q2 \qquad (4\text{-}2)$$

Q1 and Q2 are wind formulations in the x and y directions respectively.

R is a negative frictional coefficient having dimensions of(time)$^{-1}$.

f is the coriolis parameter and is taken as being constant and positive in the above equations.

This pair of coupled equations will firstly be solved by letting:

$W = u + iv$ and $Q = Q1 + iQ2$ where Q has a simple analytical form.

$$\frac{dW}{dt} - (R + if)W = Q \qquad (4\text{-}3)$$

$$\frac{dW}{dt} + pW = Q \text{ where } p = -(R + if) \qquad (4\text{-}4)$$

If $I \triangleq \int p\,dt$ then we have a general solution for W in the form.

$$W = \exp(-I)\left[\int Q\exp(I)\,dt\right] + C\exp(-I) \qquad (4\text{-}5)$$

4.3 A steady state solution

In order to obtain a value for R, Q was put equal to i (tc s/d) representing a case with a constant wind s in the y direction, with tc as a transfer coefficient having dimensions depth/time, and d is the depth of the mixed layer. The d dependence will be incorporated in tc from now on and this will be discussed later. A steady solution is looked for in this instance.

$$W = \exp(Rt + ift)\left\{\int istc\exp[-(Rt + ift)]\,dt\right\} + C\exp(Rt + ift)$$

$$= \frac{istc}{R^2 + f^2} + C\exp(Rt)\exp(ift) \qquad (4\text{-}6)$$

The steady state solution is:

$$V = \frac{-R s t_c}{R^2 + f^2} \qquad U = \frac{-f s t_c}{R^2 + f^2} \qquad (4\text{-}7)$$

It is apparent from (4-7) that the value of R, or the $|R/f|$ ratio, determines both the angle between the wind and the current and the speed of the current.

If there is extremely little friction ($|R/f|$ tends to zero) there is a westerly current, 90° to the left of the forcing wind. On the other hand, as $|R/f|$ increases the northerly current increases relative to the westerly component. The maximum current velocity is achieved with R = 0 and it decreases as R increases. The current velocity decreases proportionally to $\left(1/\tan^2\theta + 1\right)^{-1}$ as θ goes from 90° to the left of the wind towards 0° i.e. approaching the wind direction.

Thus to obtain a value for R one must accept a value for the angle of the current deflection from the wind direction in the steady state. In this section "standard angles" of 45° and 26 1/2° will be considered, both for convenience as they correspond to R values of -f and -2f respectively, and because they are in line with Ekman's (1905) result and various practical results reviewed by Neuman and Pierson (1966). Pollard and Millard (1970) made no such assumptions about R but used various values in attempts to get their model to reproduce experimental results.

A value is also needed for tc before numerical results can be obtained.

Since $|w| = (u^2 + v^2)^{1/2}$ it follows from (4-7) that

$$|w| = \frac{stc}{(f^2 + R^2)^{1/2}} \qquad (4\text{-}8)$$

In the experimental part of this report dealing with the 4 "steady state" occasions the relationship

$|\text{Current velocity}| = 0{,}017 \times |\text{Wind Velocity}|$ was obtained (equation 3-3)

In the terminology of the present chapter this can be written

$|w| = 0{,}017\ |s|$

Thus $\frac{tc}{(f^2 + R^2)^{1/2}}$ will be put = 0,017 (4-9)

These values of tc will be assumed to be valid for a slab of 8 metres depth i.e. the implicit d = 8 metres. This is because shear flow and stratification were noted to occur usually between 5 and 10 metres when the criteria for using the slab model in the first place were met, and because of the very high correlations between 2 and 5m current velocities and their similar speeds.

4.4 An analytical solution with diurnally varying wind input

A specific application of the analytical model was to see if the surface trajectories recorded in occasions 8 and 9 during the sea-breeze/landbreeze regime could be approximated by a model incorporating a theoretical representation of this wind.

A longshore wind with both steady and fluctuating components of magnitudes S and y' respectively, is thus considered together with a fluctuating onshore/off-shore wind of magnitude x'.

$$Q = Q1 + iQ2$$

$$Q_1 = -x' t_c \sin \omega t \equiv -X \sin \omega t \qquad (4\text{-}10)$$

$$Q_2 = S t_c + y' t_c \cos \omega t \equiv S + Y \cos \omega t$$

It can be noted that the wind is nominally structured such that:

the <u>diurnal</u> easterly component	reaches a maximum at	06h00
northerly		12h00
westerly		18h00
southerly		24h00

$\omega = 2\pi/24$ and t will be in hours giving the trigonometric functions a twenty four hour periodicity. We have:

$$W = \exp(-I)\left[\int Q \exp(I)\, dt\right] + C \exp(-I)$$

where $I = -[Rt + ift]$

We are seeking solutions for both W and $\int_0^t W dt$. Once set up the equation below was solved term by term, as the solution for each term is an independent solution to a section of the problem.

$$W = \exp(-I)\left\{\int[-X\sin\omega t + i(S + Y\cos\omega t)]\exp(I)dt\right\} + C\exp(-I)$$

$$= \exp(-I)\left\{\int X\left[\frac{\exp(-i\omega t) - \exp(i\omega t)}{2i}\right]\exp(I)dt\right\} \quad \text{(first term)}$$

$$+ \exp(-I)\left[\int S\exp(I)dt\right] \quad \text{(second term)}$$

$$+ \exp(-I)\left\{\int iY\left[\frac{\exp(i\omega t) + \exp(-i\omega t)}{2}\right]\exp(I)dt\right\} \quad \text{(third term)}$$

$$+ C\exp(-I) \quad \text{(fourth term)}$$

---------- (4-11)

These terms were integrated and the real solutions were obtained for u, v and $\int_0^t u\,dt$ and $\int_0^t v\,dt$. These solutions are presented below. They are steady state solutions and exclude the fourth term, the transient, which will be discussed separately.

$$u(t) = \left[\frac{X}{2} + \frac{Y}{2}\right]\left[\frac{(\omega - f)\cos\omega t + R\sin\omega t}{(\omega - f)^2 + R^2}\right] + \left[\frac{X}{2} - \frac{Y}{2}\right]\left[\frac{(\omega + f)\cos\omega t + R\sin\omega t}{(\omega + f)^2 + R^2}\right] - \frac{fS}{R^2 + f^2}$$

$$v(t) = \left[\frac{X}{2} + \frac{Y}{2}\right]\left[\frac{(\omega - f)\sin\omega t - R\cos\omega t}{(\omega - f)^2 + R^2}\right] + \left[\frac{X}{2} - \frac{Y}{2}\right]\left[\frac{R\cos\omega t - (\omega + f)\sin\omega t}{(\omega + f)^2 + R^2}\right] - \frac{RS}{R^2 + f^2}$$

$$x(t) = \frac{1}{\omega}\left\{\left[\frac{X}{2} + \frac{Y}{2}\right]\left[\frac{(\omega - f)\sin\omega t - R\cos\omega t}{(\omega - f)^2 + R^2}\right] + \left[\frac{X}{2} - \frac{Y}{2}\right]\left[\frac{(\omega + f)\sin\omega t - R\cos\omega t}{(\omega + f)^2 + R^2}\right]\right\} - \frac{fSt}{R^2 + f^2}$$

$$y(t) = \frac{1}{\omega}\left\{\left[\frac{X}{2} + \frac{Y}{2}\right]\left[\frac{(f - \omega)\cos\omega t - R\sin\omega t}{(\omega - f)^2 + R^2}\right] + \left[\frac{X}{2} - \frac{Y}{2}\right]\left[\frac{R\sin\omega t + (\omega + f)\cos\omega t}{(\omega + f)^2 + R^2}\right]\right\} - \frac{RSt}{R^2 + f^2}$$

---------- (4-12)

It can be noted that the above solutions for u(t) and v(t), which exclude the transient, have a 24 hour periodicity, as cosine and sine of $(2\pi/24)$ x (a multiple of 24) have identical values. Hence the net displacement changes over any 24 hour period is dependent only on the constant longshore wind s.

It can also be noted that the x', y' and s winds give independent X, Y&S terms and thus one could keep on adding wind input functions, possibly with a periodicity other than 24 hours, if this was thought necessary for a better wind description.

Before the above solutions are used for trials and simulation the transient term will be discussed.

4.5 Transient effects in the analytical model

$$\text{Transient}\left[W(t)\right] = C\exp(Rt)\exp(ift) \qquad (4\text{-}13)$$

where C is complex, but exp (Rt) reduces both the real and imaginary parts of the transient with time, depending on the value of R.

What Pollard and Millard (1970) refer to as an "e folding time" namely the time taken for the transient to be reduced to 1/e of its initial value is given by -1/R and has values of 5 and 10 hours when -R is set equal to 2f and f respectively. This is much smaller than the e folding times used by Pollard and Millard (op. cit.) theirs ranging from 2 to 20 days with 4 and 8 days being preferred.

It can also be noted that the values of 5 and 10 hours are based on angles of deflection of the slab of 26 1/2° and 45° respectively cum sole of a steady wind. Pollard and Millard (1970) have thus made the implicit assumption, by means of favouring such long "e folding times", that their slab would move close to 90° away from a given steady wind direction. This is evidence for the earlier statement that they used this representation as a convenience only: a slab being an integration over a depth similar to the Ekman depth of frictional resistance.

The formulas derived from u, v and x and y displacements were incorporated into a program, so that for each hour over a 48 hour period values of u, v, $\sqrt{u^2 + v^2}$, x, y and total distance travelled i.e. $\sum\sqrt{(u^2 + v^2)}$ were printed out, and the slab trajectory and wind were plotted on an HP plotter. This facilitated comparison with the drogue trajectories. No transient effects were included because they would have only markedly influenced the first few values of the above variables. Also transient effects can be examined better in a numerical model which can incorporate both step function analytical winds, and real wind input. Such a model is developed later in this chapter and will be used inter alia to investigate transient effects.

The values for x', y' and s wind input to the analytical model were used firstly to investigate their characteristic effects in conjunction with various frictional values, before being used for simulation. These effects in turn necessitated the study of the influence of latitude, especially manifest in the terms (w-f) and (w+f), on slab trajectories with variable winds.

4.6 Discussion of the (ω - f) and (ω + f) terms in the analytical solution

Trials with various values of R in relation to f, using two values of f appropriate to 11°S south and 22° south produced results that were initially disconcerting. At 11°S, mean current speeds due to rotational winds appeared to increase if friction assumed a greater value in relation to f. On the other hand at 22°S, greater friction caused a reduction in average current speeds (Table 11). (It must be noted that these changes in the f : R ratio were accompanied by a form of renormalisation discussed in b.) below.

The cause for these differing trends at 11°S and 22°S was thought to be mainly with the (ω - f) term and also the (ω + f) term in the equations for u(t) and v(t) given in (4-12).

The following procedures were adopted to clarify the situation:

a.) Since $$u(t) = \left[\frac{X}{2} + \frac{Y}{2}\right]\left[\frac{(\omega-f)\cos\omega t + R\sin\omega t}{R^2 + (\omega-f)^2}\right] + \left[\frac{X}{2} - \frac{Y}{2}\right]\left[\frac{(\omega+f)\cos\omega t + R\sin\omega t}{R^2 + (\omega+f)^2}\right]$$

--------- (4-14)

(ignoring transient and longshore wind effects) and v(t) has a similar form, it can be seen that by having equal x and y diurnal wind the second part of the above equation would = 0, equal but opposite x and y winds would cause the first part = 0, and an x wind input only would allow contribution from both terms.

Thus only diurnal winds were considered, and the magnitudes of the x and y components were chosen such that the characteristics of the solutions containing only (ω - f) and (ω + f) terms, and a combination, could be examined separately.

b.) Because different f values would be considered, the implicit transfer coefficients in X and Y (X = tc x', Y = tc y') were made explicit and made to change with latitude according to the Ekman relationship:

$$\text{Surface current speed} \propto (\sin \phi)^{-1/2} \qquad (4\text{-}15)$$

From the above and equation (4-9)

$$tc = 0{,}017 \left(\frac{\sin 22}{\sin \phi}\right)^{1/2} \left(R^2 + f(\phi)^2\right)^{1/2} \qquad (4\text{-}16)$$

It must be noted that at 22°S with a steady longshore wind S, $|w|$ will always equal 0,017 x$|S|$using the above equation for tc, regardless of the value of R. This means that tc is automatically renormalised to compensate for increasing friction ACCORDING THE STEADY STATE RELATIONSHIP given in equation (4-9).

However even with this renormalisation, the R : f ratio can greatly influence the mean speed of the slab during rotational winds, the amount of this influence being a function of latitude.

Table 11: Current speed as a function of the friction to coriolis ratio at 22°S

coriolis parameter (f) = 0,196 hours^{-1} x' = 20 knots y' = 0

friction (as a multiple of -f)	average current speed (knots)
0,2	0,448
0,4	0,355
0,6	0,294
0,8	0,259
1,0	0,238
1,2	0,225
1,4	0,218
1,6	0,213
1,8	0,210
2,0	0,208
2,2	0,208
2,4	0,207
2,6	0,207
2,8	0,207
3,0	0,208

c.) It had also been observed from running the model with diurnal winds and different R and f values that the phase relationship between wind maxima and current maxima was dependent on both f and R. Thus the speed had to be summed over a 24 hour period and averaged. An integral could not have been used as $\int_0^{24} W(t)\,dt = 0$ using only a diurnal wind input. Integrals over other time periods would have led to

the problem of $W(t)$ phase changes with f and R in relation to the forcing wind.

$$\text{Thus } \overline{|W|} \equiv \frac{1}{24}\sum_{i=1}^{24}\left[u^2(i) + v^2(i)\right]^{1/2} \qquad (4\text{-}17)$$

The mean speed $\overline{|w|}$ was calculated for 15 ratios of frictional to coriolis force for latitudes from 10° to 80° in 5 degree steps. The results of trials with three different wind inputs are discussed below.

Trials

1.) A wind input of x' = y' = 10 knots was used so that only the term incorporating (w - f) would remain. At 10° south $\overline{|w|}$ increased with an increasing friction to coriolis ratio. However at 15° south $\overline{|w|}$ displayed very little dependence on friction and at 20° south and at all greater latitudes $\overline{|w|}$ decreased with an increasing friction to coriolis ratio. This explains the different trends noted at 11°S and 22°S which prompted this investigation. Other facts also emerged from this trial with regard to the $\overline{|w|}$ maximum. With R = -f the highest value for $\overline{|w|}$ occurred at 20°S and with R = -2f at 15°S. When R was set equal to -0,2f (its smallest value) reached a maximum at 30°S because there the inertial and diurnal periods are the same.

These features are of importance because it is around these latitudes (15°- 30°) that classical seabreeze/landbreeze wind regimes often occur along west coast environments.

2.) A (10,-10) wind input was used in this trial so that only the (ω + f) terms would remain. Physically what such a wind input implies is that the rotating winds and the coriolis force are trying to drive the current in opposite rotational directions. The coriolis force obviously cannot dominate and so the highest average velocity was achieved when friction was greatest in relation to f. Thus there was a steady increase in $\overline{|w|}$ with increasing $|R|$ at all latitudes. This trend was most marked where f was least (10°S). $\overline{|w|}$ dependence on R and f was not pronounced though. With R = -0,2f, $\overline{|w|}$ = 0,066 at 10°S and 0,070 at 80°S, whilst with R = -3f, $\overline{|w|}$ = 0,161 at 10°S and 0,099 at 80°S. This is consistent with the fact that the (ω + f) terms have no resonances at particular f values. This type of wind forcing is not very likely to occur as the typical rotational nature of diurnal winds is dictated by the coriolis force.

3.) This trial used a 10 knot diurnal wind input in the x direction only, so both the (ω + f) and (ω - f) terms would be present. The suspected dominance of the (ω - f) terms was confirmed.

$\overline{|w|}$ increased with the $|R : f|$ ratio at 10°S, at 15° south there was very little dependence and at greater latitudes $\overline{w}$ decreased with increasing $|R : f|$, except for when $R \doteq -3f$ at 20 and 22°S. Generally very little variation in $\overline{|w|}$ occurred when $-3f \leqslant R \leqslant -2f$ regardless of latitude (Table 11). With $R = -f$, $\overline{|w|}$ reached a maximum at 20°S and with $R = 2f$, this maximum occurred at 15°S. With $|R|$ at its minimum value ($-0{,}2f$) the greatest mean current speed was observed at 30°S. These trends are basically the same as those discussed for the first trial.

Thus the $(\omega - f)$ terms dominated trends from 15° towards greater latitudes. Only at 10° did the $(\omega + f)$ terms give the same trends as the combined solution. Local effects at 22°S can now be observed from a broader perspective.

4.7 Results of running the analytical model (at 22°S)

Trial 1

A steady longshore wind produced the expected straight line trajectories with angles between wind and current dependent on R. From the printout for trial 1 the results of using a 10 knot southerly wind with three frictional formulations were checked.

1.) R was set = -f

2.) R was set = -2f but tc was renormalised to get $|W| = 0{,}017|S|$

3.) R was set = -2f but without renormalisation.

(Unless specified to the contrary tc will always be renormalised to give $|W| = 0{,}017|S|$ in future trials.)

In the first two instances speeds were obviously the same by virtue of renormalisation but 1.) had the slab moving at 45° to the wind whilst 2.) had it moving at 26 1/2° to the wind. In 3.) the direction was the same as 2.) but the current speed was reduced by 36%.

This trial both tests part of the model (and adaptions to the plotting software used for the drogues) and supplies the net rate of movement per day of the slab in relation to the strength of the steady longshore wind s for all future trials. It has been seen though, that the total distance and average speed of the slab is a function of the R : f ratio, latitude and diurnal wind strengths even after renormalisation of tc and this aspect is investigated below.

Trial 2

The model was run with a 20 knot diurnal x wind only, with R = f and -2f. The trajectories (Figure 17) appear elliptical, although they are not true ellipses. The flatter trajectory occurred with R = -2f and the angle between the "major axis" and the x axis was also less than that for the trajectory with R = -f. If the $|R : f|$ ratio

THEORETICAL MODEL TRAJECTORIES WITH DIURNAL WINDS AND DIFFERENT R:f RATIOS FIG. 17

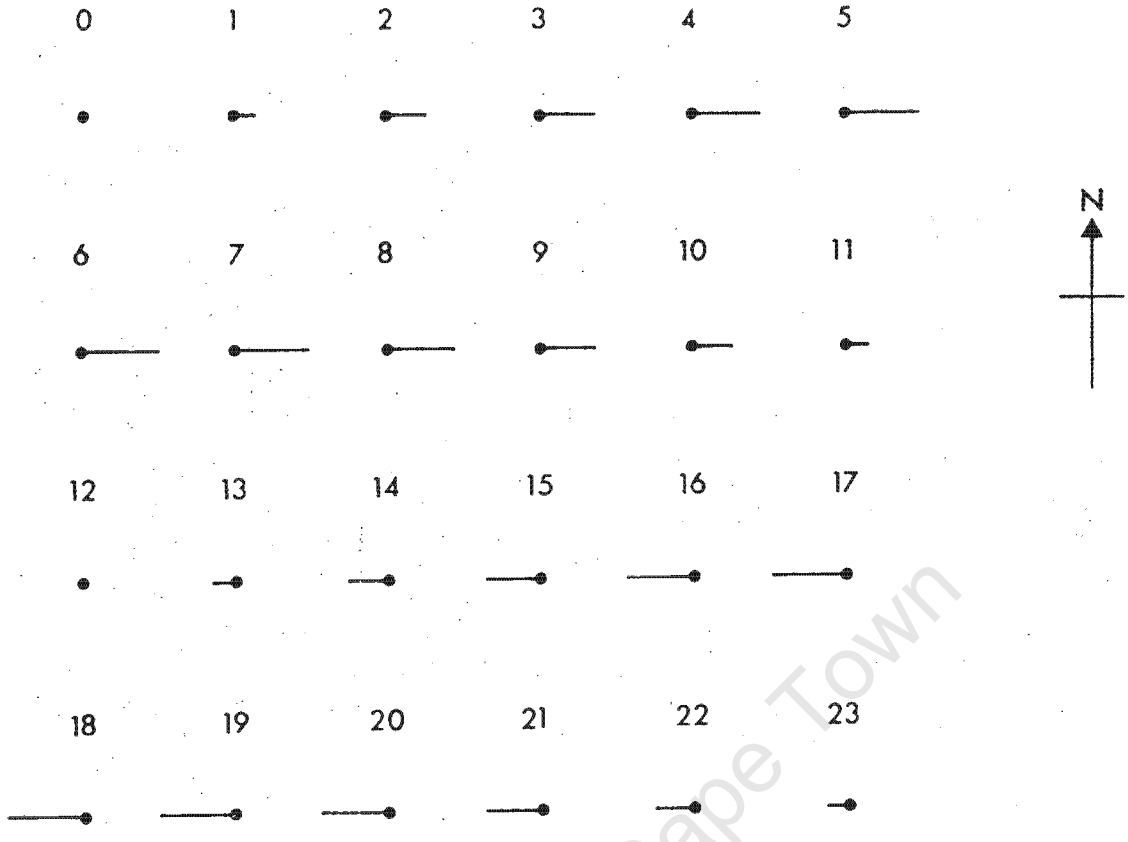

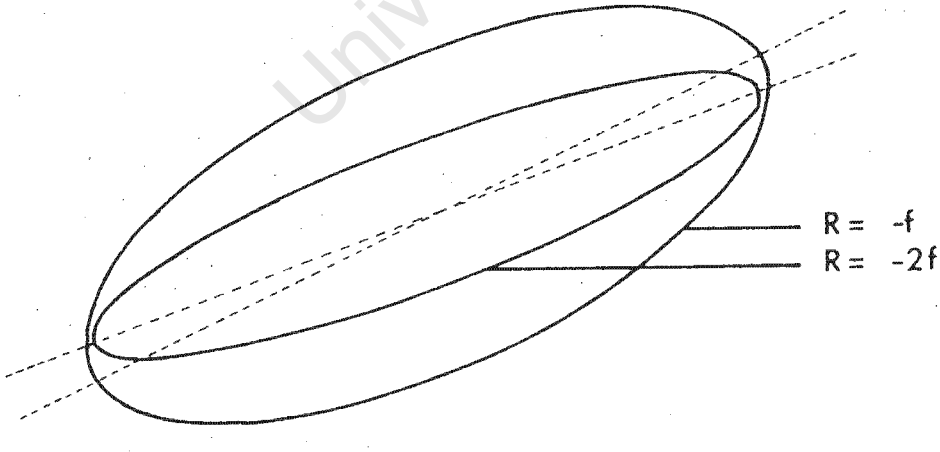

Mean speeds (knots)

slab with R=-2f : ·24

slab with R=-f : ·21

scale: tenths of a n.mile

windscale: 20 kts

reached very high values the current would merely move slowly backwards and forwards almost in the direction of the forcing wind. This can be confirmed by noting that $u(t)/v(t)$ is large for large $|R|$ if there is only an x wind input. With $|R : f|$ very small on the other hand the trajectory would become more circular.

In terms of mean speeds the trajectory with R = -2f had a value of 15% less than for the R = -f case. This aspect has been discussed simultaneously with the effects of latitudinal variation, and was shown in Table 11 for 22° south with R ranging from -0,2f to -3f.

The only other point from this trial which deserves mention is the aspect of lags between windspeed maxima and current speed maxima. In the x direction, the direction of the wind forcing, the current component maximum occurs two hours after the wind maximum with both R formulations. However the y component reaches a maximum 2 hours before its imaginary wind maximum with R =-2f, and occurs simultaneously with it with R = -f.

Runs with other wind inputs, which will not be discussed separately, confirmed the trends indicated above:

a.) That the axis of the dominant wind has greater lags between wind and current maxima than the axis with the lesser wind (or no wind).

b.) Increasing R tends to reduce those lags on both axes.

Other features shown in these runs include the following:

c.) Over a period of time of 24, 48 hours etc. the currents will be the same and the net displacement change is dictated only by the longshore wind input (R and f constant.)

d.) An increased diurnal wind and thus current component in one direction leads to increased current components in both directions.

e.) Noticeably greater (by about 15%) current speeds were obtained with $R = -f$ than for $R = -2f$ at 22°S.

f.) The effect of changing the layer depth from the implicit 8 metres assumed so far, is inversely proportional to changing the wind input. Thus if a slab of 4 metres thick was to be investigated with a real 5 knot wind, a 10 knot wind would have to be the input. This slab would have double the velocities of the 8m slab, but as the slab model in this study attempts reasonable physical realism, all further runs will use a slab of 8m. Thinner slabs may be applicable to specific areas and times such as sheltered seas and lakes in summer, and possibly the present research area in summer. However wind speeds would have to be kept low to avoid breaking down the stratification at the base of the slab.

Simulation 1

An attempt was made to produce a trajectory which bore resemblance to the 2 amd 5m drogue trajectories recorded during occasions 8 and 9. During occasion 9 the wind died at 24h00 and so the model and experimental trajectories are expected to be dissimilar after that time.

A diurnal off/onshore wind of 15 knots was chosen as a compromise between the 20 knot offshore and 10 knot onshore recorded experimentally during occasions 8 and 9. A 5 knot constant longshore wind would supply northward displacement of the correct magnitude over 24 hours. This would have to be modified by a 10 knot diurnal component in order to get the required midday northerly wind. Friction was set = -f.

The experimental trajectories along with the model trajectory and wind input are shown in Figure 18. Several features of the experimental trajectories can be related to that of the model:

1.) Both trajectories are of a distorted circular nature.

2.) Average speeds over the 24 hour period are comparable: model (0,29 knots), 2m trajectory (0,24 knots), 5m trajectory (0,22 knots).

3.) The absence of an offshore wind on 27/6/78 as had occurred on 26/6/78 is largely responsible for the experimental velocities not having come round to the west by 08h00.

FIG. 18 THEORETICAL SLAB TRAJECTORY AND EXPERIMENTAL DROGUE TRAJECTORIES

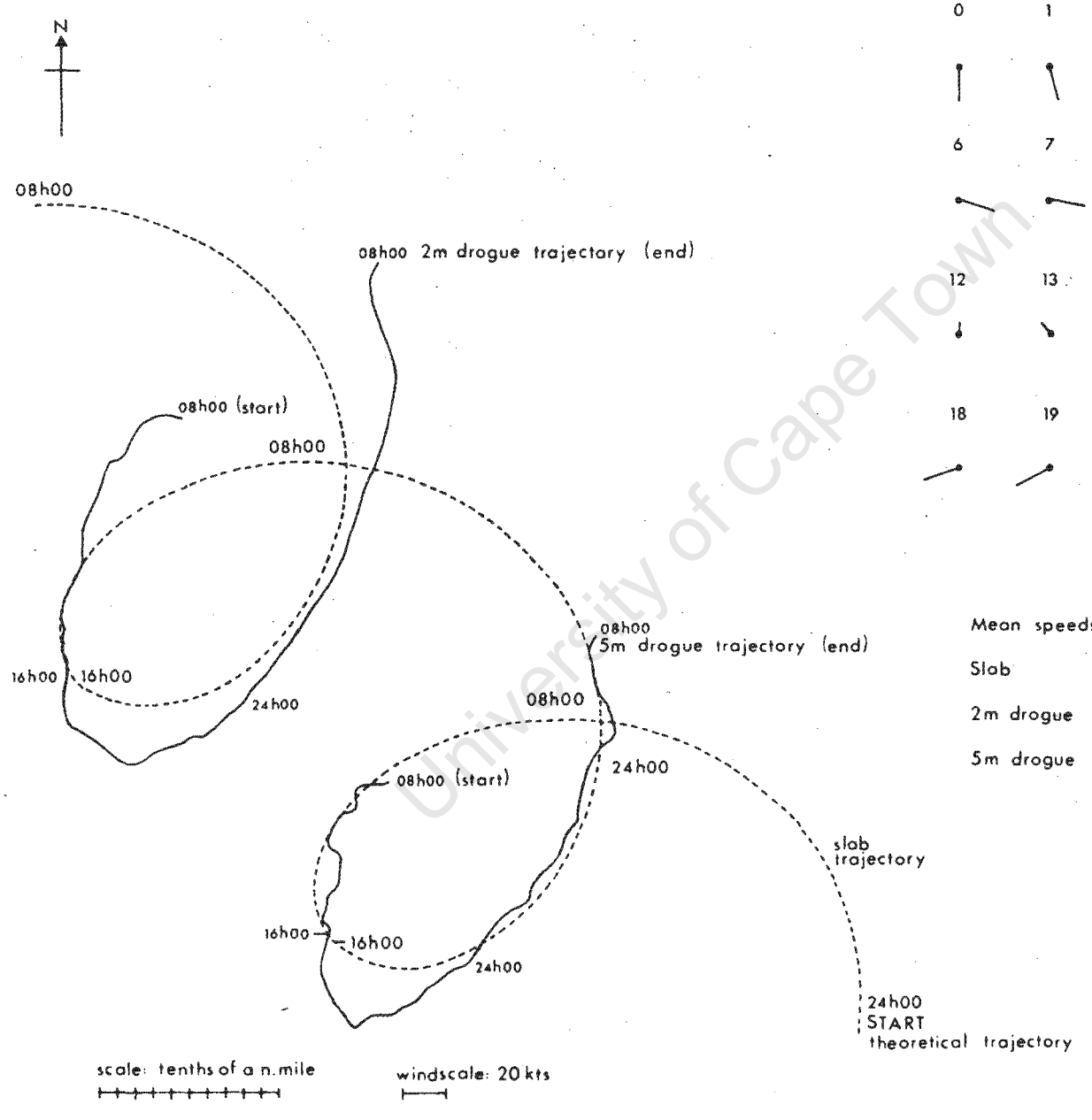

THEORETICAL WINDS

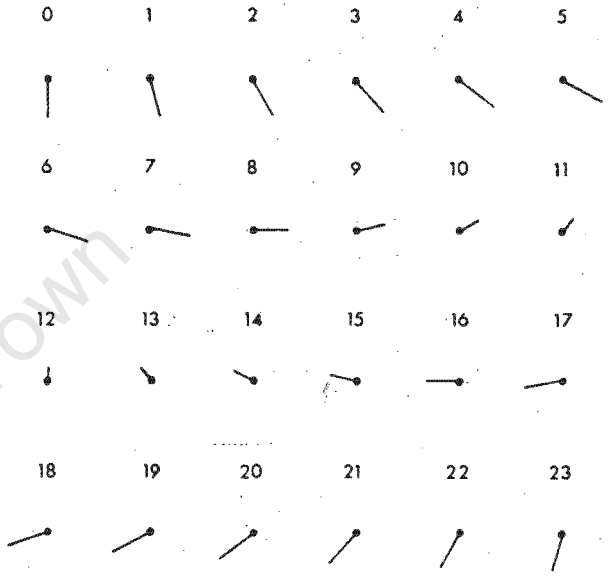

Mean speeds over 24 hours (kts)

Slab	·29
2m drogue	·24
5m drogue	·22

Overall, as regards modelling classical situations the agreement between the model and reality is heartening.

Other wind inputs within the present solution were able to simulate certain sections of the experimental trajectories better. In addition new analytical solutions could be derived, possibly incorporating functions of a different periodicity, but particularly with a constant wind component in directions other than longshore. For example a steady 5 knot easterly wind with a 10 knot diurnal component would have the effect of making the diurnal off-shore stronger than the onshore. It is felt however, that not much more would be achieved by these experiments as the data set for comparative purpose is too small.

The alternative is a step-wise model which could employ both theoretical and real winds as inputs. Two very attractive features of this model are that it will be able to simulate transient effects and inertial effects. The one bad point is that the model must be run in order to examine results; there are no terms as in an analytical solution which can be examined in order to guage their effect.

It is mentioned here that the greatly increased average current speeds due to the duirnal winds will greatly increase property exchange across the boundary between "the slab and that below" by entrainment, although there is no net daily displacement of the slab due to these winds. Thus this model does have implications associated with enhanced property transfers; these will be mentioned later.

4.8 A step-wise solution to the model and its stability

Solutions for u(t), v(t), x(t), and y(t) were obtained by using the consistent and convergent formulae below, derived from equations (4-1) and (4-2).

$$u(t+\Delta t) = u(t)\left[1 + R\Delta t\right] - f\,v(t)\Delta t + Q_1\Delta t$$

$$v(t+\Delta t) = v(t)\left[1 + R\Delta t\right] + f\,u(t)\Delta t + Q_2\Delta t \qquad (4\text{-}18)$$

Q1, Q2 and at a later stage R, were input hourly. Δ t was allowed to be any fraction of an hour down to a minute. At each step of the solution a discretisation error of $O(\Delta t)$ was incurred.

To check initially for correctness and stability of the model (i.e. that discretisation and rounding errors are not amplified) a theoretical wind input of the same form as was used in the analytical solution was employed. The output, using different Δt values, was checked against the corresponding analytical solutions.

Trial 1

Using a steady 10 knot longshore wind as input and different combinations of t and R it was found that:

1.) if the initial u(t) and v(t) values were equal to the analytical steady state values then u(t) and v(t) remained correct to 2 significant figures at subsequent times regardless of R or Δt.

2.) if the initial u(t) and v(t) were set equal to zero then u(t) and v(t) always approached their steady state values. With 10 tsteps per hour i.e. Δt = 6 minutes, u(t) and v(t) had a discrepancy of less than 10% from their steady state values after about 6-10 hours. However the case with R = -f then overshot its steady solution slightly before settling down. This was not apparent in the R = -2f case. With only 2 tsteps per hour almost a day was necessary to achieve similar accuracy. Thus with 10 tsteps per hour the only significant departure from the analytical solution appears to be due to transient effects and not mathematical complications (c.f. the 5-10 hour "e folding times"mentioned in section 4.5).

Trial 2

A wind input of 5 knots steady longshore, 10 knots diurnal longshore and 15 knots diurnal off-shore/onshore was employed and a comparison was again made between the analytical and stepwise solutions. After transient effects had died down the following results were computed over a 24 hour period.

Table 12: The accuracy of the stepwise solution to the surface layer model

	Analytical	Stepwise
x displacement (n. miles)	-0,92	-0,91
y displacement	1,82	1,83
Total distance	5,79	5,84

Velocity components at any particular time did not vary by more than 0,01 of a knot.

Although the above trials indicate the stepwise model to be accurate and stable, a theoretical examination of stability follows to investigate the conditions for stability.

A forward or Euler scheme was used to obtain solutions to the pair of equations (4-18) which can be combined and expressed as below, where W = u + iv again, and Q is ignored.

$$W^{(n+1)} = W^{(n)}[if + R]\Delta t + W^{(n)} \qquad (4\text{-}19)$$

This equation is a combination of the two equations

$$W^{(n+1)} = W^{(n)} if\Delta t + W^{(n)} \qquad \text{(oscillatory equation)} \qquad (4\text{-}20)$$

$$W^{(n+1)} = W^{(n)} + R\Delta t\, W^{(n)} \qquad \text{(friction equation)} \qquad (4\text{-}21)$$

The Euler scheme is unconditionally unstable for the oscillatory equation but unconditionally stable for the friction equation. That the combined equation is conditionally stable is shown below:

$$W^{(n+1)} = W^{(n)}\left(1 + R\Delta t + if\Delta t\right) \tag{4-22}$$

Define an amplification factor λ such that

$$W^{(n+1)} = \lambda W^{(n)} \tag{4-23}$$

If $|\lambda| \leq 1$ the numerical solution remains bounded as n increases, and as we know the exact solution is bounded the error of the numerical solution is bounded. Then the Euler scheme is stable for equation (4-19).

$$\lambda = \left(1 + R\Delta t + if\Delta t\right) \tag{4-24}$$

$$|\lambda| = \left[1 + 2R\Delta t + (R\Delta t)^2 + (f\Delta t)^2\right]^{1/2} \tag{4-25}$$

For stability $$|\lambda| \leq 1 \Leftrightarrow |\lambda|^2 \leq 1 \tag{4-26}$$

As R is negative

$$-2R\Delta t \geqslant (R\Delta t)^2 + (f\Delta t)^2 \tag{4-27}$$

This condition is easily satisfied for Δt small enough and hence equation (4-19) is conditionally stable. The condition is:

$$\Delta t \leq -2R/(R^2+f^2) \qquad (4\text{-}28)$$

If we take $|R| = 0{,}1f$ (its minimum value in this whole section) and $f = 0{,}2$ hours^{-1}

then Δt must be less than $\frac{0{,}02}{0{,}0004 + 0{,}04} \approx 0{,}5$ (4-29)

Thus if Δt is less than 1/2 an hour (Δt criterion) all solutions discussed are stable, seeing the minimum value for $|R|$ used is $|-0{,}1f|$. Δt was usually set equal to 1/10 hour, a value easily satisfying the stability criterion above. The rounding and discretisation errors for a particular step will diminish in influence in succeeding steps by a step factor of at least $\Delta t/\Delta t$ criterion = 1/5, more generally 1/50 when $R = -f$.

4.9 Simulation of inertial effects (Simulation 1)

An attempt was made to model inertial conditions in this simulation the results of which are shown in Figure 19. A 10 knot y wind component and a 5 knot x wind component were allowed to blow for 12 hours and were then "shut off". Frictional values used were -0,2 f and -f.

SIMULATION OF INERTIAL EFFECTS FIG. 19

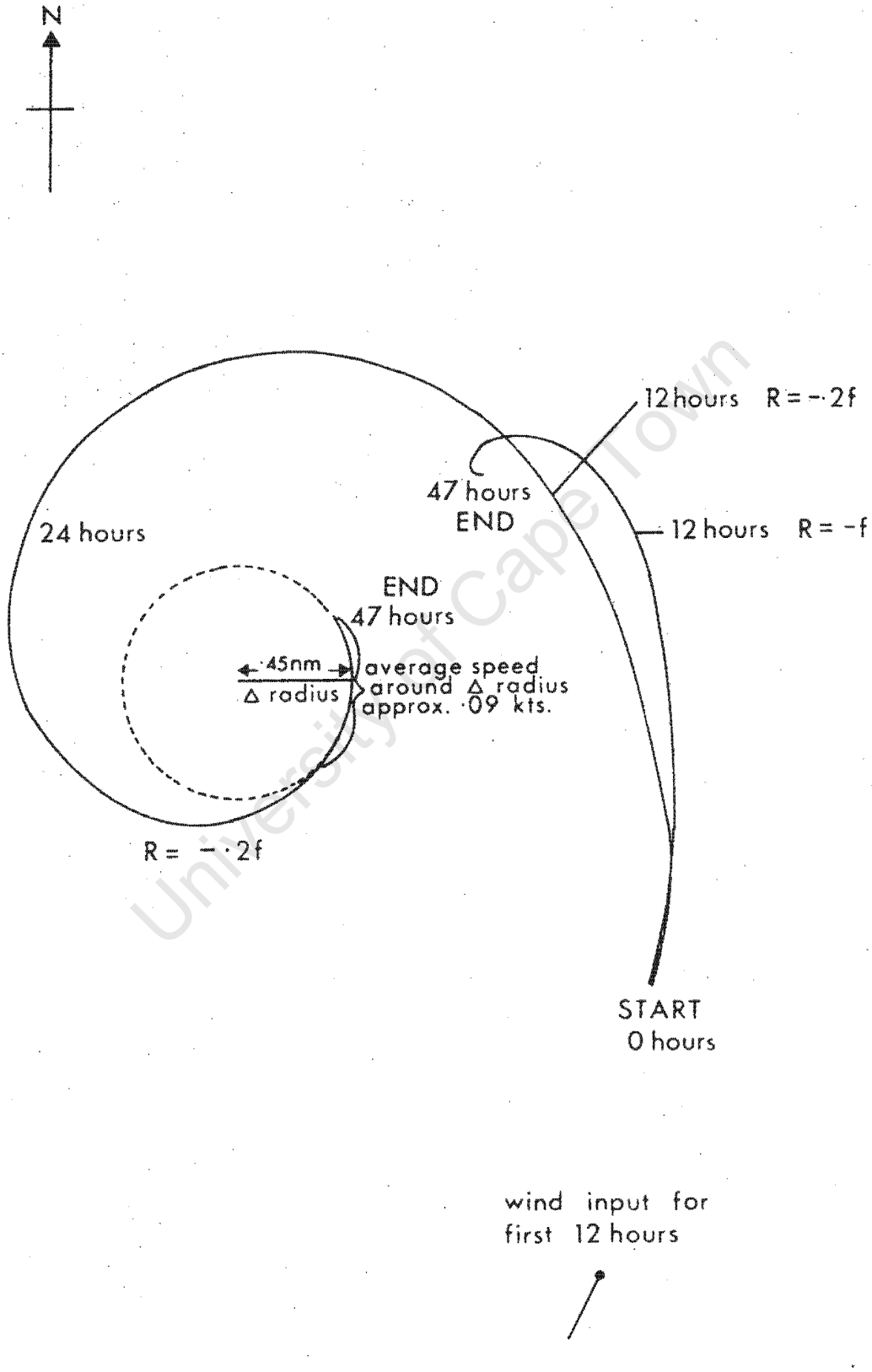

With R = -f a steady current seemed to be reached after 12 hours. The current speed was reduced to $\frac{1}{e}$ of its value 7 hours after the wind stopped (cf. the 10 hour e-folding time of the analytical solution) and was virtually zero (i.e. 0,01 knots) after another 10 hours.

When R was set = -0,2f current speeds were not markedly different under wind forcing (because of renormalisation of tc) but after forcing stopped the current speed was only halved after a full day. The "inertial" part of the trajectory would appear circular if observed over about half a day or less. Graphical estimation of the radius of the latter part of the trajectory using the method of inertial circles as was done in the experimental sections 3.1 gave a Δ radius of 0,45 n. miles. The average speed around this Δ radius was approximately 0,09 kts. One should be able to estimate the value of f from this using f = current speed/radius. This gave a value of 0,20 $\pm$ .01, which is practically the same as 0,196 used in the model.

These results are noteworthy in that they imply that for observed inertial motion to take place in practice R should not be much greater than $|-0,2f|$. This suggests that R could be made a function of windspeed, with a suitable minimum value to allow calm conditions to be realistically simulated.

4.10 Simulation using real diurnal winddata (Simulations 2 and 3)

Two sets of "real" wind data, firstly that recorded during occasions 8 and 9 and secondly a digitisation of "average conditions" at Pelican Point (Table 13) as described by Stander (1964), were used. R was set = -f. The results are shown in Figure 20.

Table 13: A typical daily wind sequence at Pelican Point

(adapted from Stander (1964))

Time	Wind dir.	Speed (kts)	Time	Wind dir.	Speed (kts)
01h00	180	6	13h00	225	12
02h00	180	6	14h00	225	12
03h00	180	6	15h00	225	12
04h00	180	6	16h00	202	14
05h00	180	6	17h00	202	14
06h00	90	4	18h00	202	14
07h00	90	4	19h00	202	14
08h00	90	4	20h00	180	8
09h00	90	4	21h00	180	8
10h00	90	10	22h00	160	6
11h00	90	10	23h00	160	6
12h00	225	12	24h00	180	6

SIMULATED TRAJECTORIES USING REAL AND TYPICAL WINDS FIG. 20

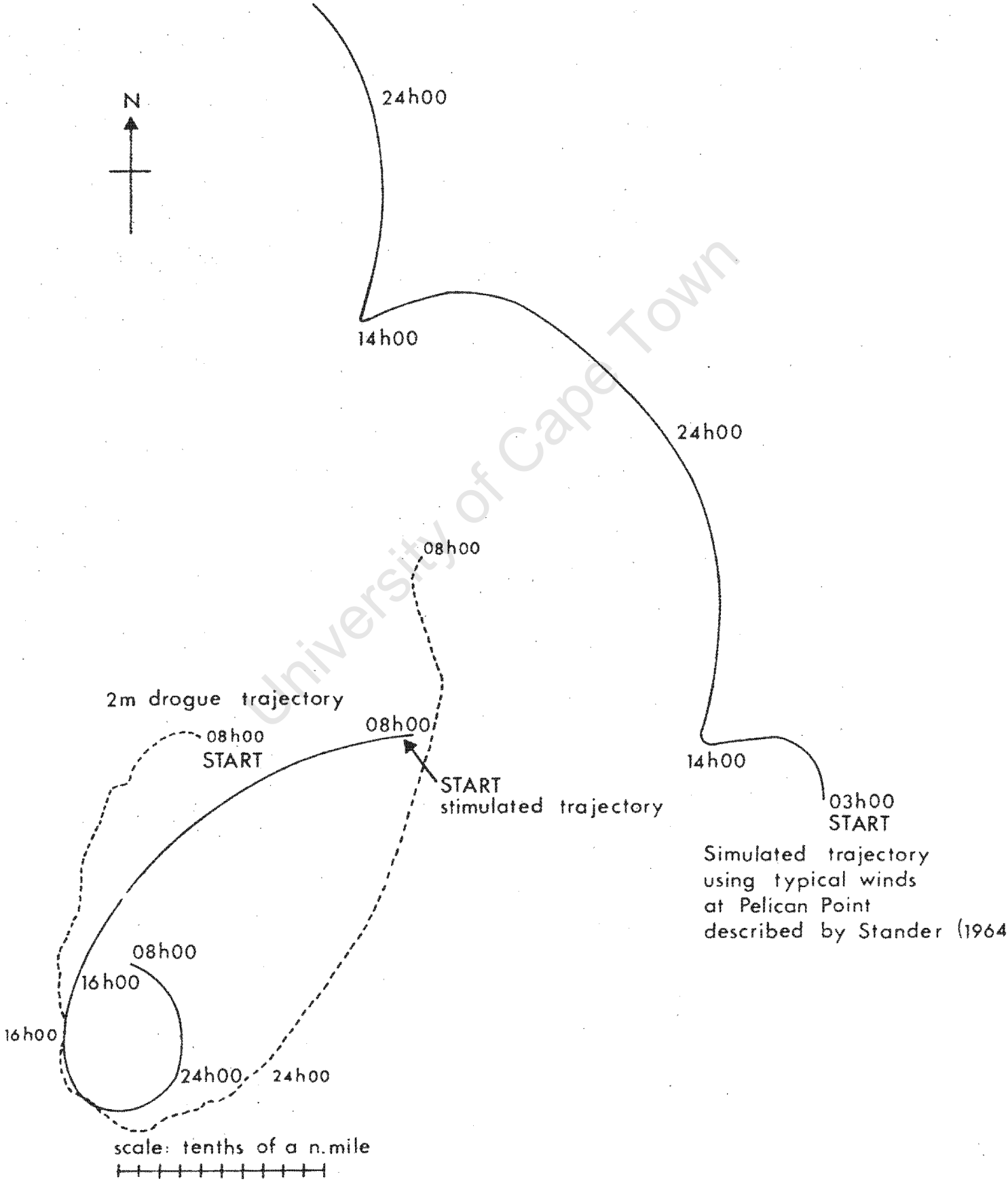

The trajectories for occasions 8 and 9 only resemble reality for the period 08h00 to 16h00. The weaker southerly winds and calms recorded during the night did not give the slab the necessary northward displacement. To do this two options came to mind:

1.) R could be set proportional to windspeed (after renormalisation) in order to speed up currents in low wind speed conditions and reduce them in high windspeed conditions.

2.) A steady longshore velocity could be added to the solution at every step, thereby acknowledging the presence of an apparent residual current of up to 0,1 knot in this case.

The first option will be used in simulation 4, and both are employed simultaneously in simulation 5. These simulations are described in the next section.

The trajectory based on Stander's (1964) winds, showed a definite daily northward displacement over 24 hours, although slight southward movement did occur around midday. The more "apparently realistic" trajectory that occurred with this wind input could be ascribed to the fact that no calms were included. This is where the fixed R assumption seems to break down.

No current trajectories were available for comparison with the above simulation, but comparison of average northward speed of the slab (about 0,12 knots) with the average northward current recorded during June/July 1978 further north off Henties Bay (0,08 knots) is evidence that both

the experimental and theoretical sections of this report have attained a measure of consistency defining typical coastal Benguela current velocities, particularly when the wind differences between Walvis Bay and the research ship (discussed at the end of chapter 3) are borne in mind.

4.11 Simulated trajectories with variable friction and a longshore current

In simulation 4 option 1.) mentioned previously was explored, and R and tc were formulated as below:

$$R = -0{,}05 \cdot f \cdot |\text{Windspeed}| \quad \text{if } |\text{Windspeed}| > 1 \text{ knot}$$

$$R = -0{,}1f \quad \text{otherwise} \qquad (4\text{-}30)$$

$tc = 0{,}017 \cdot \sqrt{2} \cdot f$ i.e. tc is constant now and has a value appropriate to the old R = -f formulation.

As regards simulating the trajectories of occasions 8 and 9 this formulation was only a partial success, the slab stil did not have sufficient northward displacement, and so option 2.) was incorporated as well.

Positive x and y wind components of 3.5 knots were used in order to get a longshore current of the correct magnitude. These were added to the real wind components and R was kept the same as in simulation 4.

Figure 21 shows that at last the model has reproduced all the basic features of the drogue trajectory, but interestingly enough only slightly better than was done by the simple analytic model.

It is unfortunate that, besides occasions 8 and 9, the only other long records of currents were obtained during calm conditions and therefore could only be used to test the model in a limited sense as was done in simulation 1. Still it is felt that this investigation has achieved its primary objective, namely it has revealed both problems and procedures with regard to the prediction of surface layer movement on a timescale of hours from wind data. The contributions of inertial and residual currents have also been identified and included.

The results of the slab model and the experimental work will now be compared to the results of a more sophisticated model (O'Brien et. al., 1977) which also employed diurnal wind input. The hydrological effects of an "independently moving surface layer" will be fully discussed in the next chapter.

FIG. 21 DROGUE TRAJECTORY AND SIMULATED TRAJECTORY WITH VARIABLE FRICTION AND LONGSHORE CURRENT

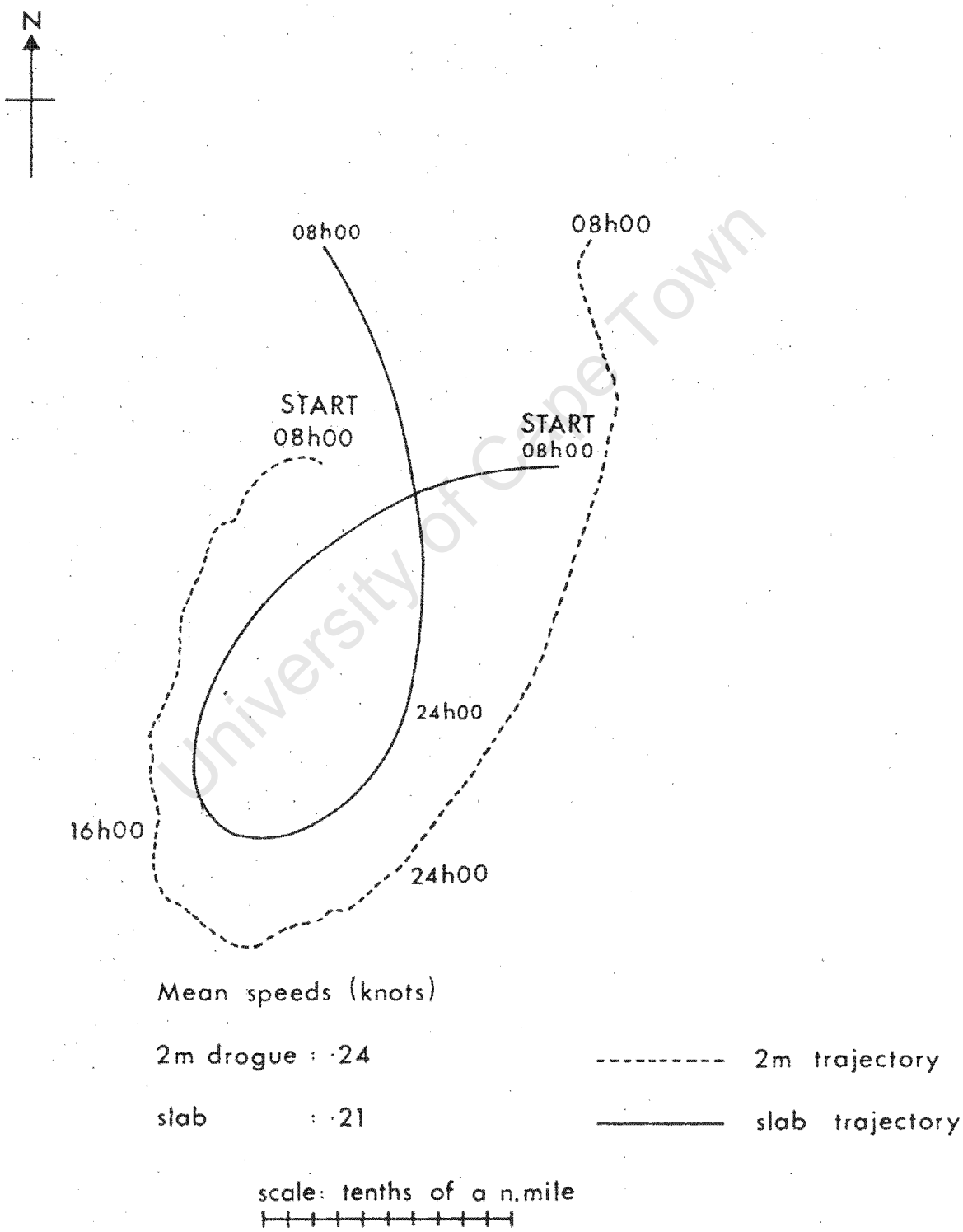

4.12 Comparison with a more sophisticated model

O'Brien et al (1977) presented a coupled ocean-atmospheric model with a primary intention of examining "the oceanic response to sea breeze forcing" and its "role in coastal upwelling".

Some of their results are stated below and compared with those from both the experimental and modelling sections of this work.

1.) "The sea breeze forces a clockwise, rotating, diurnal oscillation in the upper layer of the ocean near the coast which is superimposed on a slowly evolving motion field...".

The slab model and the experimental section have displayed this rotating (anticlockwise in the southern hemisphere) diurnal oscillation quite clearly. Below the thermocline currents at 20 and 30m are more sluggish with a mean speed of just over half of that of the upper layer. The current at 20m is the most consistent, with the highest average velocity : average speed ratio (Table 6) implying a smoothed response to surface slab movement on the diurnal scale.

2.) "Near the coast the velocity perturbation is about 10-15cm $sec.^{-1}$." This is equivalent to the 0,2 - 0,3 knots found both experimentally and in the slab model due to diurnal winds.

As the slab model defines no variation in the depth of the upper layer, discussion of layer depth changes is based on results from the experimental section.

3.) The model of O'Brien et al (1977) showed a diurnal fluctuation in the depth of the upper layer of about 3m, at the coast reducing to zero about 12km from the shore, which they ascribed to the oscillation of the currents and their kinematic coastal boundary condition. A corresponding variation of magnitude of about 3m can be seen in Figure 22 for the periods around the 21st and 26 June, the latter period being that during which drogue tracking occasions 8 and 9 showed oscillatory currents. Although the research site was about 10km from the coast the shallowness of the water (Figure 2) nearer the coast would revise distances in comparison with O'Brien et. al's model.

4.) The two layer model showed a diurnal sea surface temperature fluctuation of the order of 1°C at a point in the upwelling frontal region. Figure 22 shows a similar fluctuation for the two periods mentioned above, the higher temperatures being measured at 20h00, the lower ones at 08h00.

5.) "The sea breeze forcing causes a weak poleward surface counter current to form diurnally within 10km of the shore....". This phenomenon was fully witnessed during occasions 8 and 9, and over shorter periods during other occasions, eg. 4 and 5, 7. (See appendix A).

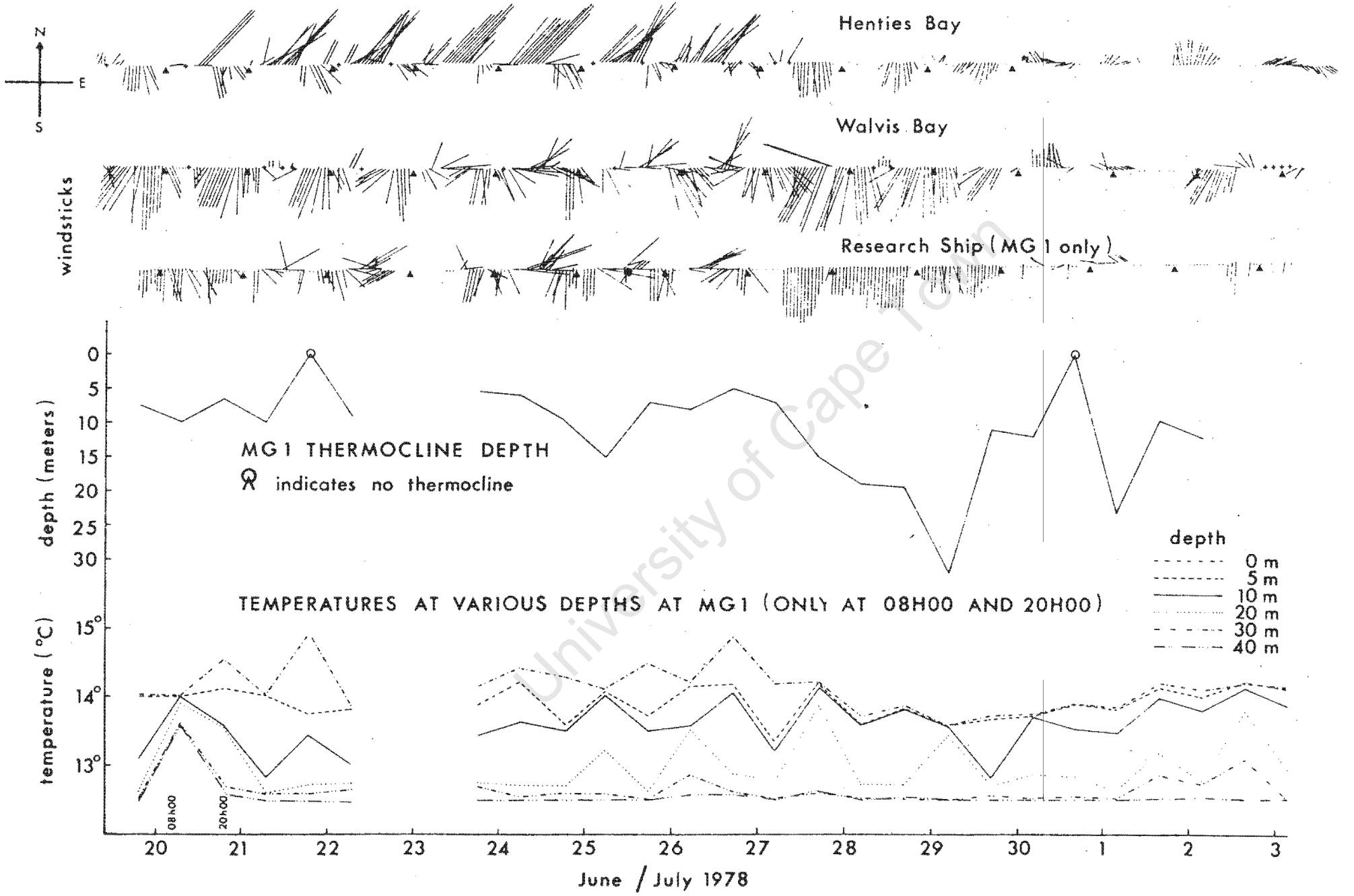

FIG. 22 TIME SERIES OF WINDS, THERMOCLINE DEPTH AND TEMPERATURES AT MG1

Thus the experimental section has not only served as a basis for the slab model described here, but has in addition supplied evidence to help confirm trends of the coupled model presented by O'Brien, et. al. (1977). Also, within the obvious limitations of the slab model, there is no disagreement concerning typical surface current speeds and directions. Unfortunately the magnitude of the sea breeze used in the coupled model is not mentioned, neither is the value assumed for the coriolis parametor f. They did however state: "since the angular frequency of forcing is less than f, the (diurnal) oscillation does not take the form of a propagating wave." They have thus restricted their model to latitudes polewards of 30 degrees.

At 22°S the diurnal frequency of forcing is greater than f, but the slab model cannot simulate propagating waves due to the assumptions of uniform density within the slab and its fixed top and bottom. If one no longer assumed a slab with a fixed top, and ignored at this stage density differences with depth, the equations of motion would be:

$$\frac{\partial u}{\partial t} + fv - Ru = g\frac{\partial \eta}{\partial x} + Q_1 \qquad (4\text{-}31)$$

$$\frac{\partial v}{\partial t} - fu - Rv = g\frac{\partial \eta}{\partial y} + Q_2 \qquad (4\text{-}32)$$

where η is the displacement of the sea surface from a level surface.

It can be seen by adopting scales of 0.1 m/s for Δu and Δv, 6 hours for Δt and a diurnally forced sea surface slope of the order of 10^{-6} that the previously omitted terms $g\frac{\partial \eta}{\partial x}$ and $g\frac{\partial \eta}{\partial y}$ approach same order of magnitude as the others.

The magnitude of the slope was estimated by using the difference in dynamic height between occupations of station MG1 at 08h00 and 20h00 on the 26th of June and a space scale 4km. (This method runs against the assumption of uniform density, but is the only approach open to the author.)

$$\text{The dynamic height difference} = 10\left[0{,}0597 - 0{,}0588\right] / \ 4000$$
$$= 2 \times 10^{-6} \text{ dynamic metres}$$

This comparable to the magnitude of the $\frac{\Delta v}{\Delta t}$ term which equals 5×10^{-6}.

Thus gravity effects will play a role, albeit not the dominant one in the research area. No comment will be made on the propagation of internal waves under the above assumptions, but in the next chapter which discusses the hydrology of the research area the propagation of internal waves in a stratified ocean will be considered.

4.13 Summary of Chapter 4

(The results of each section are stated under the appropriate section number).

1.) The upper layer of the sea to about 8m depth was modelled as a slab. This was done on basis of evidence given in chapter 3 regarding the regular existence of a surface layer, whose movement was basically uni-directional, and which was detached from the lower layers by shear flow. The forces considered acting on this slab were: the coriolis force, friction and time dependent winds. Continuity considerations and topographic influences were excluded.

2.) The basic equations are the same as those used by Pollard and Millard (1970):

$$\frac{du}{dt} + fv = Ru + Q1 \qquad \frac{dv}{dt} - fu = Rv + Q2$$

where f is positive, R is a negative frictional term, and Q1 and Q2 are wind formulations.

3.) A solution to the above equations considering a constant southerly wind was obtained. This was used in conjunction with the result obtained in section 3.8 ($\frac{|\text{"surface" current velocity}|}{|\text{"steady" wind velocity}|} = 0{,}017$) to formulate the slab speed that would be produced by particular winds. Two test values for the angle between current and wind of 45° and 26 1/2° were assummed.

4.) Analytical solutions for velocity and displacement of the slab due to diurnal and steady winds were obtained with the help of complex algebra. The diurnal winds gave the slab no net displacement over a 24 hour period.

5.) Transient effects were reduced to 1/e of their initial value after 5 to 10 hours, using values of R equivalent to $-2f$ and $-f$, (those appropriate to the two "test" angles mentioned in 3.).)

6.) The variable effect of the friction to coriolis ratio at different latitudes for 3 diurnal wind types was discussed in detail.

7.) Characteristic features of the model at 22°S were further examined. Simple theoretical formulations of diurnal and longshore wind enabled trajectories recorded during occasions 8 and 9 to be fairly realistically simulated.

8.) A stepwise model was presented and tested practically and theoretically for stability. The conditional stability criterion was easily satisfied. Transient effects were examined.

9.) An order of magnitude reduction of the frictional term enabled inertial effects to be simulated.

10.) Two sets of real diurnal wind data were used, firstly to simulate the trajectory recorded during occasions 8 and 9 and secondly to assess the effect that the "typical" wind as described by Stander (1964) would have on the slab. The first mentioned simulation was not very successful, due to the failure of the model to reproduce experimental results from calm and low windspeed conditions. In further simulations it was decided to consider friction a function of windspeed.

11.) After friction had been made a function of windspeed and a residual current was included in the model, the drogue trajectories recorded during occasions 8 and 9 were successfully simulated.

12.) Comparison of both the experimental and slab model results of this study with the near-coast results of the coupled ocean-atmosphere model presented by O'Brien et. al. (1977) showed similar features and scales.

To sum up, the simple analytical model proved acceptable under conditions without calms. If a stepwise model is to be employed with real wind input, some of the basic developments necessary to simulate conditions realistically are that friction be made a function of windspeed, and that an allowance be made for a residual current in the absence of gravity terms in the equations.

5. HYDROLOGY.

5.1 Introduction.

It is not the primary objective of this chapter to describe the hydrology of the research area per se, but rather to investigate the hydrological changes and circulation patterns that were brought about by the action of the wind on different time scales. However, the intensive nature of this study also enabled a better picture to be obtained of the underlying hydrology of the area in winter than has been possible to date.

Currents between the surface and 30m depth, the temperature fluctuations and the thermocline depth changes shown in Figure 23 have already been discussed and related to the wind record. This information will now be related to the various hydrological distributions, mainly in the form of vertical sections, after certain preliminary investigations have been carried out. These investigations will serve as further introduction to understanding causal processes in time and space and include assessing the following:

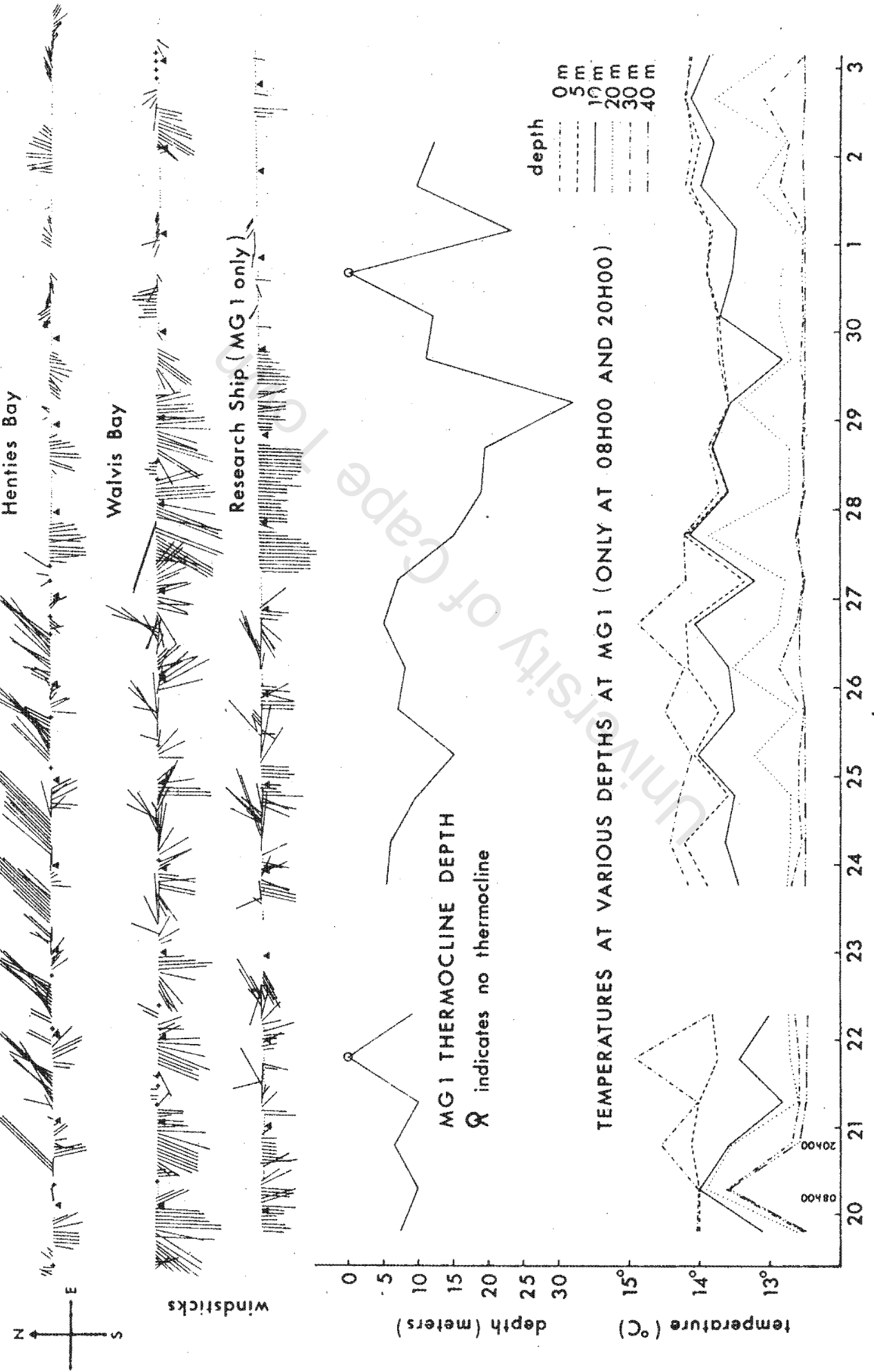

FIG. 23 TIME SERIES OF WINDS, THERMOCLINE DEPTH AND TEMPERATURES AT MG1

a.) the role of entrainment in the hydrological changes at MG1

b.) the importance of internal waves in the research area

c.) the spatial and temporal distribution of thermoclines and temperatures over the research area

d.) the effect of the thermocline on the oxygen and nitrate distributions at station MG1.

Figure 24 shows the results of the brief larger scale survey done before the intensive work began. The low oxygen values at 20m between Walvis Bay and Cape Cross, and 1° to 2°C temperature drop in the top 20m are consistent with results from previous work mentioned in section 1.3. This figure will be referred to again in section 5.9 but is presented here to "set the scene" for the discussion of the intensive area hydrology.

5.2 Turbulence, Mixed layer deepening and entrainment.

A deliberately simple (but in this author's opinion correct) description of the basic hydrological changes that occurred at station MG1 during the programme and the processes responsible is given below. Two time scales are discernible, firstly diurnal and secondly of the order of a few days.

Figure 23 shows that apart from 2 occasions a thermocline existed between 5 and 30m depth. During the diurnal wind regime which prevailed until 27 June, two periods around 21 and 26 June showed

FIG. 24 HYDROLOGICAL CONDITIONS — 15/16 JUNE 1978

SURFACE TEMPERATURE

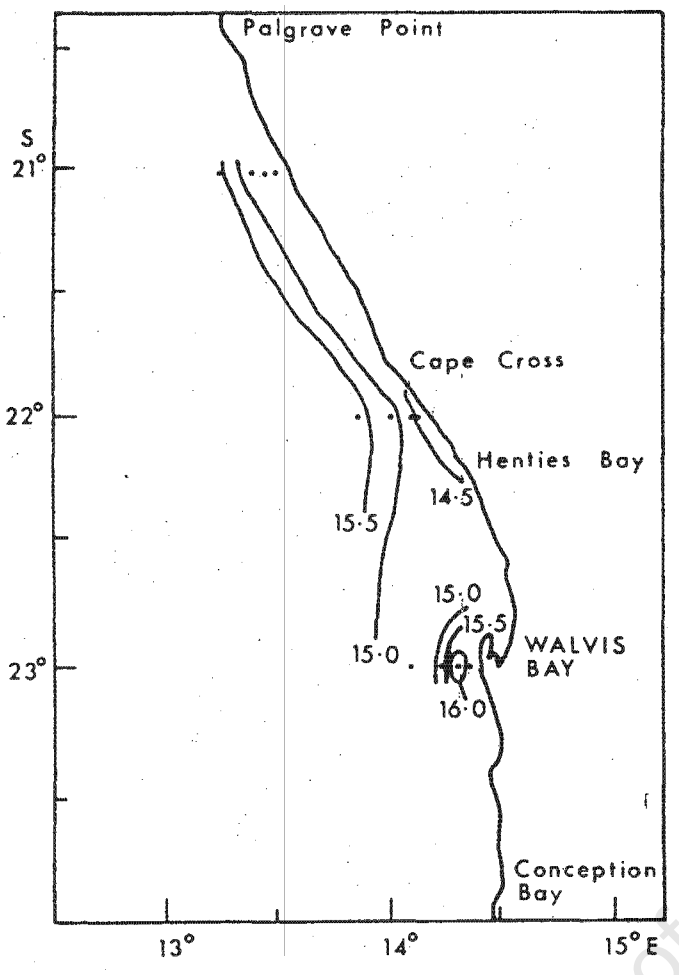

TEMPERATURE AT 20m

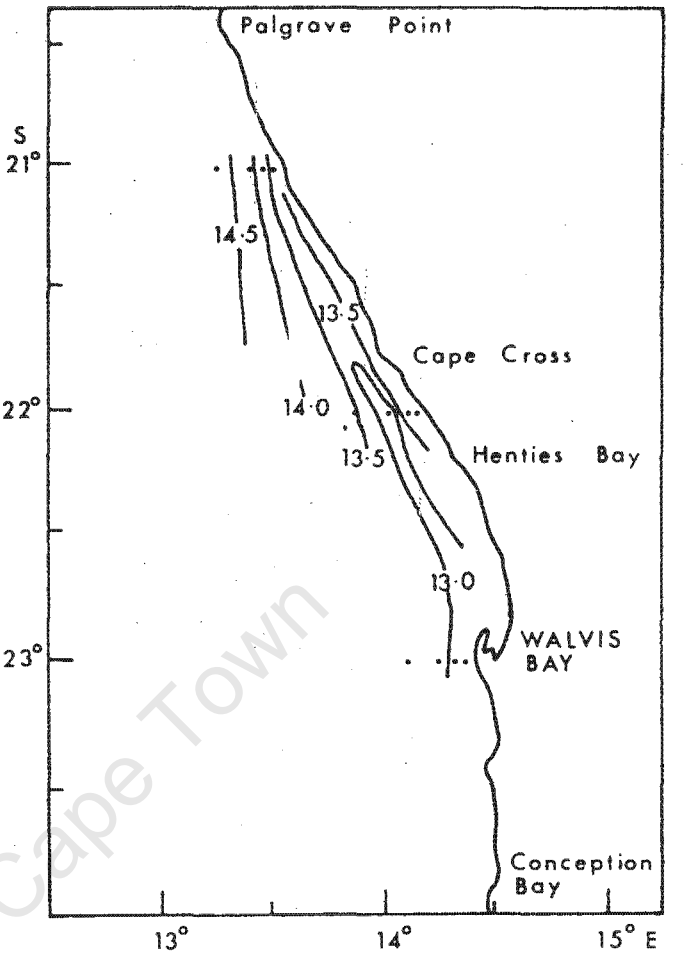

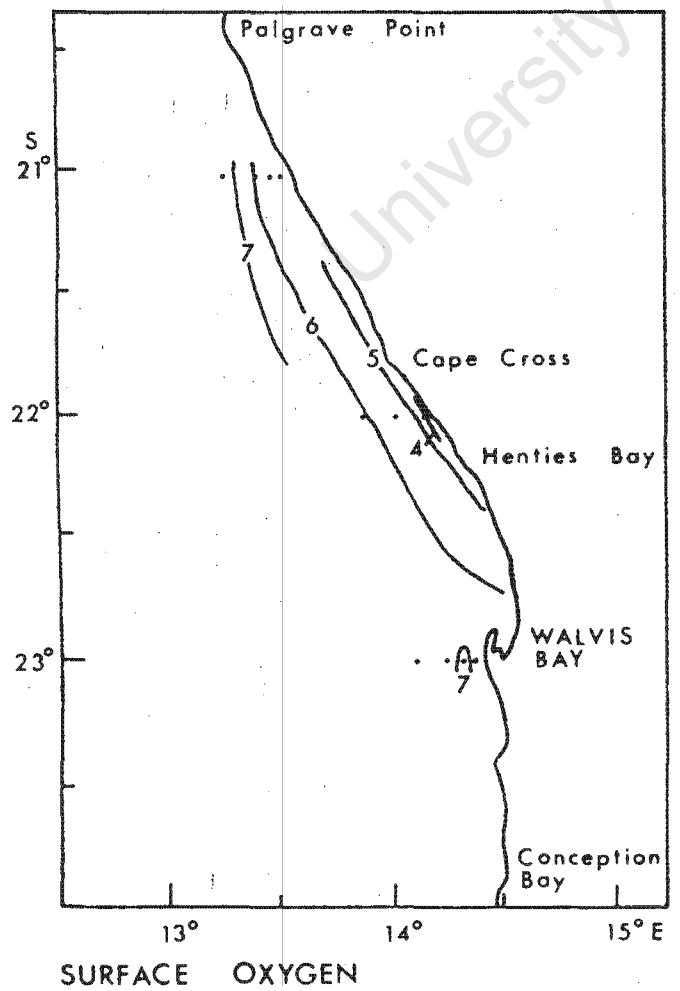

SURFACE OXYGEN

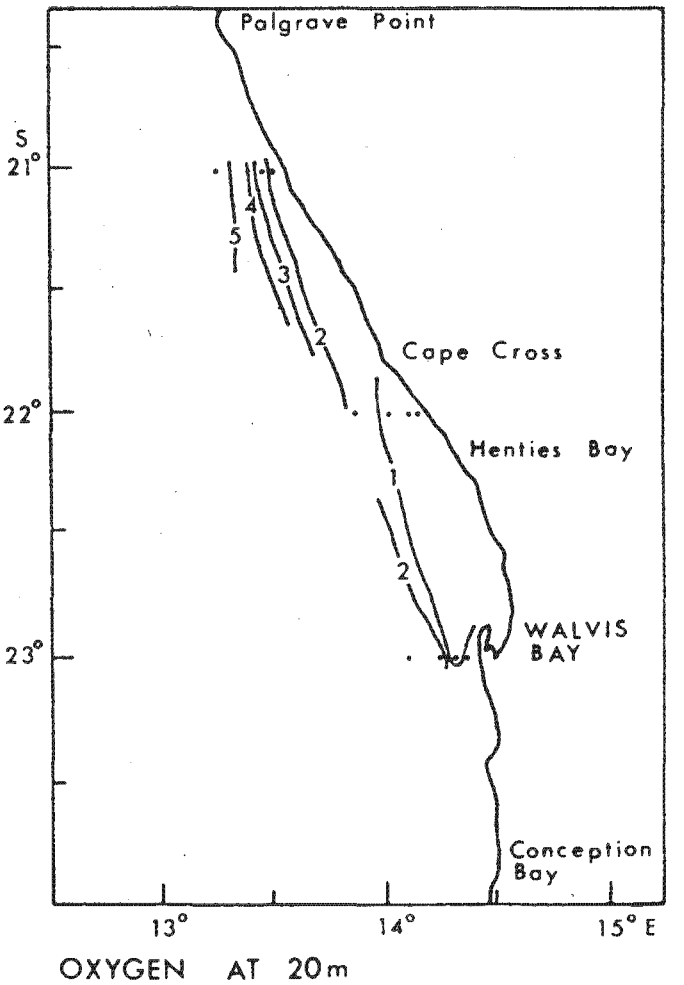

OXYGEN AT 20m

diurnal oscillation of the thermocline with an amplitude of approximately 3m at around 8m depth. When these winds were replaced by a more consistent southerly regime from 27 to 29 June, the thermocline deepened rapidly to below 20m and surface layer temperatures dropped markedly. After 29 June, the temperature of the upper layers rose gradually during calm conditions, although the upper thermocline depth fluctuated markedly largely due to the thermocline's poor definition.

The process that operated during both time scales of thermocline deepening is as follows: Wind energy is transferred downwards from the surface and is distributed throughout the layer above the thermo= cline. This turbulent energy then entrains the top part of the assumed non-turbulent water below the thermocline and mixes it through= out the upper layer. Theoretically only the upper layer would become diluted with the lower layer and the upper layer thus increases in depth and has lower layer properties, such as nutrients, transferred into it. No transfer occurs in the opposite direction.

Some of the energy associated with this deepening may have been propagated out of the area in the form of internal waves if the deepening occurred over a suitable time scale. This aspect will be examined in the next section (5.3).

Surface heating can be responsible for "layer rising" and this involves the formation of a new thermocline above the previous one and turbulence is then confined within this layer. Alternatively offshore movement of water near a coast can cause the lower layers to rise by continuity, and if this process is sustained for a day or more the top layer may be removed offshore and the lower layer will break the surface. However, associated with the offshore movement one will simultaneously have entrainment causing the upper layer to become deeper.

Dominance of one or two of the above processes is primarily determined by the time scales and velocities of the wind, and the intensity of the solar heating which basically follows a seasonal regime but is modified over shorter periods by cloud cover.

For the two periods of small diurnal upper layer oscillations centred around the 21st and 26th June, it can be noted (Figure 23) that the thermocline depth and surface temperatures were highest at 20h00 in the evening and lowest at 08h00. This means that the upper mixed layer decreased in thickness during the day and increased at night.

The rises in the day can be attributed to the east wind (landbreeze) causing offshore surface movement and hence the lower layer rose. (Envisage the effect of moving the upper layer 'wedge' above the 13,5°C isotherm offshore on 21/6/78 (Figure 30).

In the early afternoon the rise in the upper layer during the morning would be augmented by solar heating and limited mixing due to the light winds. Table 10 in Chapter 3 shows clearly the increase in density difference between 0 and 5 metres in the day (of the 26th June).

In the evening, onshore winds increased in strength and tended to become southerly later. This would result in initial onshore movement of the surface layer but coriolis effects would change this to longshore and slightly offshore before morning. The layer deepening during the night can thus primarily be ascribed to entrainment.

The longer time scale of the consistent southerly wind conditions (they prevailed for 48 hours from the 27th of June) caused the surface layer to deepen about 20m at MG1. Surface current speeds were surprisingly low during the three-point drop of occasion 13 on the 28th June and it was mentioned in section 3.3 that it was thought that most of the wind energy was used to deepen the mixed layer.

The gradual warming of the 'surface layer' which extended beyond 10 metres after the 29th June has already been mentioned. The misty prevailing weather would have reduced the solar heating rate in comparison to that applicable to the clear skies of the diurnal wind period, and thus reduced the chances of a new thermocline being formed near the surface.

The above description has related local effects to local causes. The space scale of 'local' effects obviously depends on their time scale, longer time scale effects occurring with somewhat greater uniformity in space as is shown by the wind patterns for the three measuring sites in Figures 14, 15 and 16. Scales will be further mentioned in the next section which deals with internal waves.

5.3 Internal waves.

The possibility of wind energy being transferred to internal wave motions and the propagation of these motions in the vicinity of the research site is examined below.

To avoid complexity, the wave motions considered will be those appropriate to an ocean of limited depth and continuous stratification i.e. a constant buoyancy frequency N. In view of the density difference over the thermocline being small and typically less than half the density change between the top and bottom of the ocean, this representation should be as valid as any in this context. Le Blond and Mysak (1978) give the following formula for the range of frequencies which can propagate in such an ocean.

$$\omega^n = \left[\frac{k^2N^2 + (n\pi/d)^2 f^2}{k^2 + (n\pi/d)^2}\right]^{\frac{1}{2}} \qquad (5\text{-}1)$$

where k is the wave number = $2\pi/\lambda$

n the mode number

d the depth

N the buoyancy frequency (in radians/sec)

These waves will be left bounded in the southern hemisphere and can only receive energy from frequencies between the buoyancy frequencies and f. Further frequency restrictions can be placed upon them depending on the spatial scale one defines.

Let us consider an ocean shelf of 50m depth and the following hydrological values, in line with those recorded at MG1.

Table 13: Typical density data for the area around MG1

	Temperature °C	Salinity	σ_t
Surface	14,5	32,20	26,25
50m	12,5	35,20	26,67

The buoyancy frequency N is given by

$$N \approx (gE)^{\frac{1}{2}} \text{ secs}^{-1} \quad \text{where } E = 10^{-3} \frac{d\sigma_t}{dz} \quad \text{and } g \approx 10 \text{ m/s}^2 \quad (5\text{-}2)$$

$$= 9{,}2 \times 10^{-3} \text{ secs}^{-1} \quad \text{(as a radial frequency)}$$

This corresponds to 5 oscillations per hour.

From (5-1) and using N as above, Table 14 gives the frequencies and periods appropriate to various wavelengths considering only the fundamental mode of propagation.

Table 14: Internal wave time and space scales

Wavelength (km)	Angular frequency ($secs^{-1}$)		Period (hours)
1	9,2	10^{-4}	1,9
2	4,6	10^{-4}	3,8
3	3,1	10^{-4}	5,6
4	2,3	10^{-4}	7,4
5	1,9	10^{-4}	9,1
6	1,6	10^{-4}	11
7	1,4	10^{-4}	12
19	7,3	10^{-5}	24
50	5,7	10^{-5}	31
100	5,5	10^{-5}	32
1000	5,4	10^{-5}	32

Obviously forcing is necessary to give energy to the waves and on the basis of the wind data presented (Figures 14, 15 and 16) the range of wind forced periods would be restricted to between 12 and 24 hours. The 24 hour forcing could be repeated day after day but the 12 hour forcing would have to consist, of say, a single 6 hour easterly followed by relative calm. In sustained calm conditions inertial motion may set up a propagating wave and in this case it would be necessary to restrict λ to about 100km, the longshore distance about the research site over which the depth and width of the shelf and hydrological conditions could be expected to fulfill reasonably the criteria assumed. It is noted though, that the inertial currents observed on 1/7/78 (Figure 6) did not seem to show significant energy gain or loss. Unforced waves will not be specifically considered further. With regard to the propagation of internal waves, the complex topography around Cape Cross (relative to most of the coastal area) would serve to obstruct waves entering the research area from the north. Propagation southwards would be favoured by the uniform topography. A problem arises however, in that the typical forcing wind from the east to north-east probably has a longshore spatial scale much greater than the 7 - 19 km wavelength appropriate to its probable time scale of 12 - 24 hours. Thus these waves will be out of phase with their forcing as they propagate southwards.

It can be noted from Figures 14 and 15 that the strong sustained easterlies recorded at Henties Bay did not occur at Walvis Bay during this research programme. Hence one may be able to define a place between these two localities at which a sudden reduction in wind forcing occurs, and waves may well be able to propagate unhindered from such a spot southwards. The velocity of the 19km wave with a 24 hour period is obviously 19km per day, and this defines the maximum space scale over which a significant reduction in the forcing must take place. Such a sharp wind gradient would not seem likely on account of the uniform nature of the topography of the area. However this author can remember seeing on an occasion during the programme an easterly wind generate a dust cloud stretching several miles out to sea about 10 miles to the south, whilst no such cloud occurred inshore of the research ship. Thus if the easterly wind can have a marked northern boundary a similar feature may occur further south. Satellite photography could help in this regard.

A fluctuating hourly temperature record giving evidence of a propagating internal wave (local conditions could not be held responsible for the fluctuations) was described by Stander (1963). Interestingly it was recorded at a station of 55m depth west of Walvis Bay. However the season was summer and temperature gradients in the upper 20m were pronounced and regrettably the period of the wave could not be established.

So whilst a few ideas have been advanced, this present investigation has given little additional information about the role of diurnally forced waves of South West Africa. What is suspected though, is that much wind energy is initially transferred to waves but that most of it is subsequently dissipated through interference between wind and wave forcing. Propagation at greater depths along the coast due to a single forcing event is another matter, but one which lies beyond the scope of this study with its emphasis on local events.

On the other side of the spectrum, short oscillations with frequencies close to the buoyancy frequency were observed associated with slicks resulting from localised downwelling. These slicks generally occurred between midday and midnight and were most pronounced in the late afternoon/early evening if low wind speed conditions prevailed. A thermograph record of the temperature at about 2m depth taken whilst the ship was at anchor at MG1 is shown in Figure 25. The amplitude of the temperature variation is of the order of a degree celsius indicating a physical wave amplitude of about 5 to 10 metres. (See the temperature time series for MG1 at 20h00 on the 26th June in Figure 23).

These slicks are due to an accumulation of oily biological matter reducing the visible effect of windage on the surface in the downwelling zone, and they thus appear glassy in comparison to the typically slightly choppy appearance of the water on either side of them. They seem to align themselves parallel to the coast, but not necessarily parallel to the wind, and advance onshore. Spacing between individual slicks appeared to be of the order of a couple

WIND AND THERMOGRAPH RECORDS FOR 26/6/78 AT STATION MG1 FIG. 25

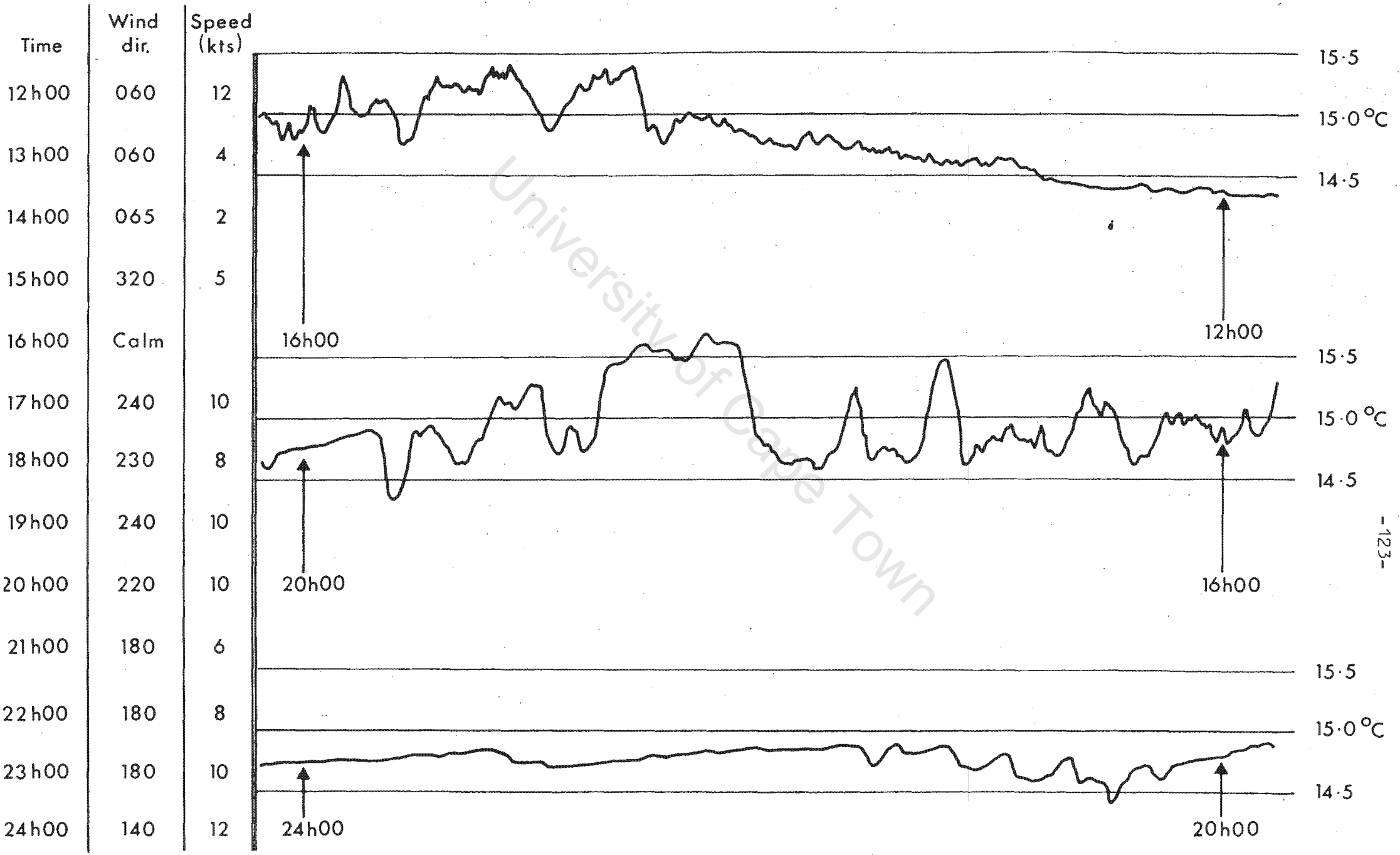

of hundred metres, but between 'major' slicks, detectable on an ART record as spikes, a spacing of several kilometres has been observed (J.J. Agenbag, pers. com.)

The energy source for these Langmuir circulations is still unproved (Pollard, 1977), but he favoured the theory of Garret (1976) who suggested interaction between surface wave and surface current fields to be the source. This investigation supports this theory in that thermograph fluctuations were encountered in calm as well as low wind speed conditions.

These slicks are deserving of further research in view of their widespread and regular occurrence off the South West African coast. Their study would be aided by the fact that they modify the planktonic acoustic scattering layer and hence they can be recorded in 2 dimensions on scientific echo sounders.

5.4 Thermoclines and temperatures over the research area

The various changes in depth and definition of the thermocline at MG1 in response to winds and currents have been discussed already in many contexts. Throughout these changes though, some properties (particularly oxygen and temperature) seemed to maintain remarkably uniform distributions above and below the thermocline. It is thus logical to examine the spatial occurrence of thermoclines over the research area before examining the distributions of other parameters. This will both enable these distributions to be

discussed with greater insight as well as giving an indication of how valid certain quantitative relationships that will be derived at MG1 are over the whole survey area.

The horizontal sections of thermocline depths and surface temperatures over the research area came from the 5 stations and 4 BT stations done every second day. The grid and thermocline depths are shown in Figures 26 and 27, and surface temperatures in Figures 28 and 29. The usual times of station occupation are given below:

MG1	08h00
MG2	09h30
MG3	11h20
MG4	12h20
MG5	14h00
MG1	20h00

In the horizontal sections the 08h00 MG1 stations were used except for the 19th and 23rd of June when they were not done. In the vertical sections the MG3, MG5 and 20h00 MG1 stations were used. The only effect of this non-synopticity on the vertical distributions would be a fractionally higher surface temperature and thermocline depth being recorded at MG1 than if all the 'vertical section stations' had been done around midday. It is also mentioned that the westward direction along 22°S will be considered to be offshore

HORIZONTAL DISTRIBUTION: THERMOCLINE DEPTHS (METRES) FIG. 26

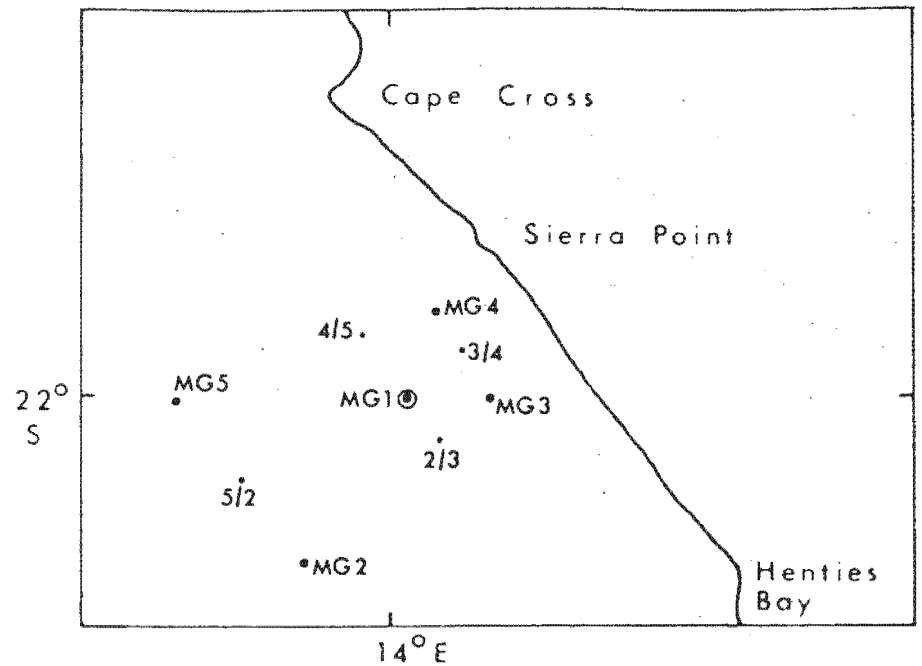

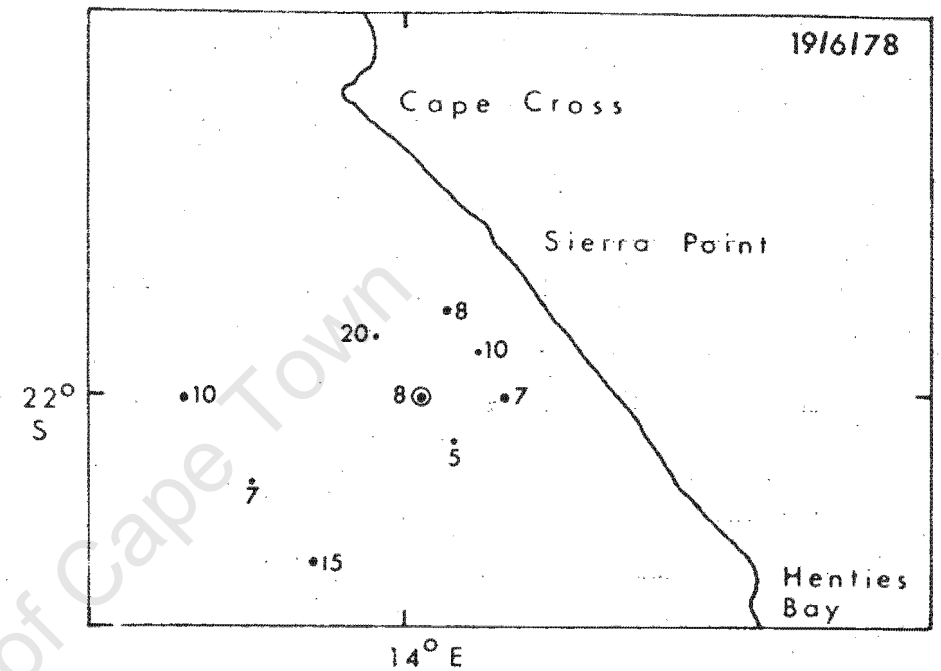

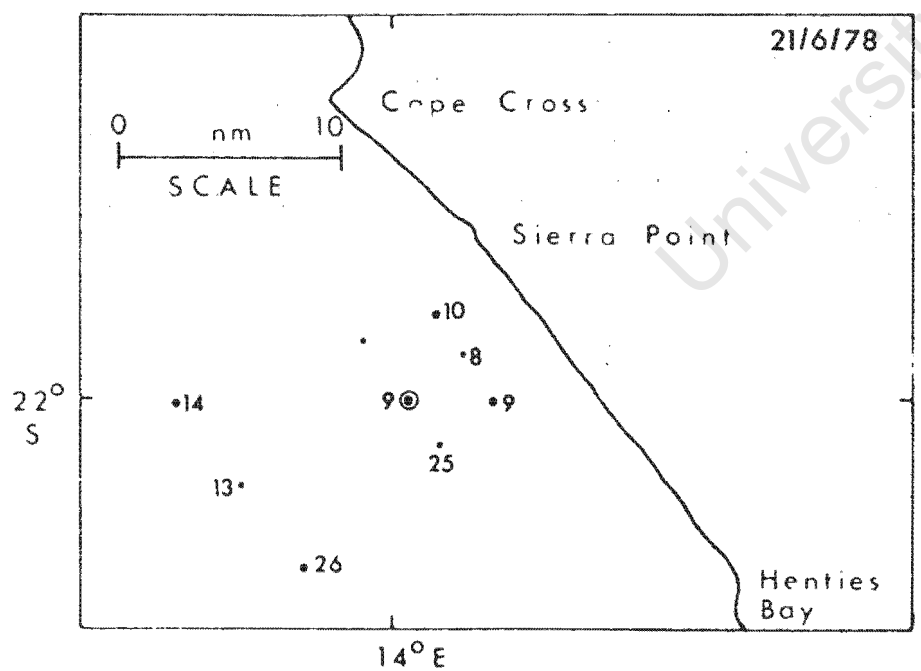

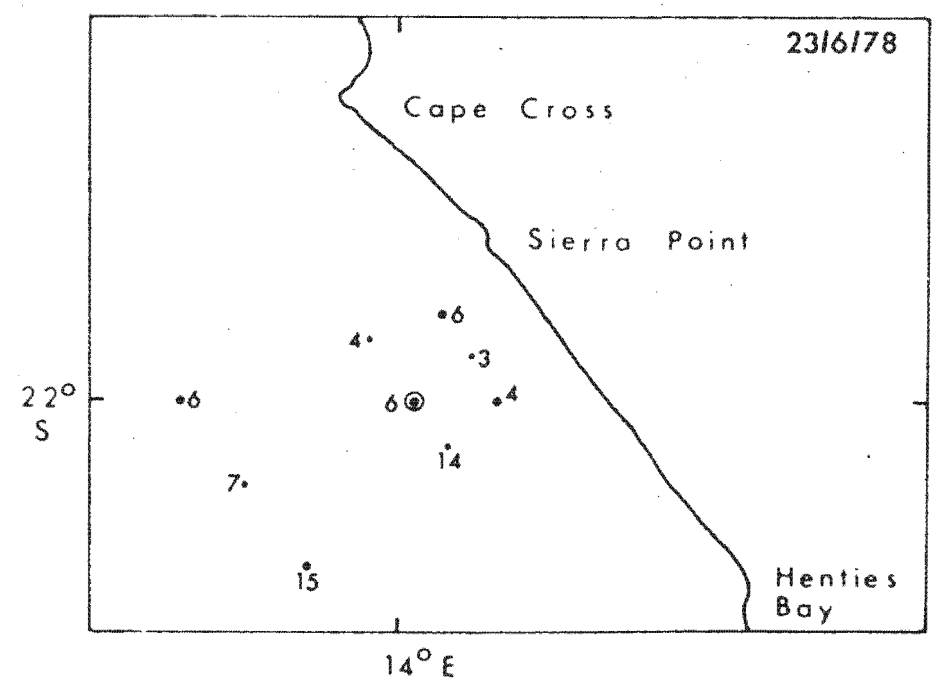

HORIZONTAL DISTRIBUTION: THERMOCLINE DEPTHS (METRES) FIG. 27

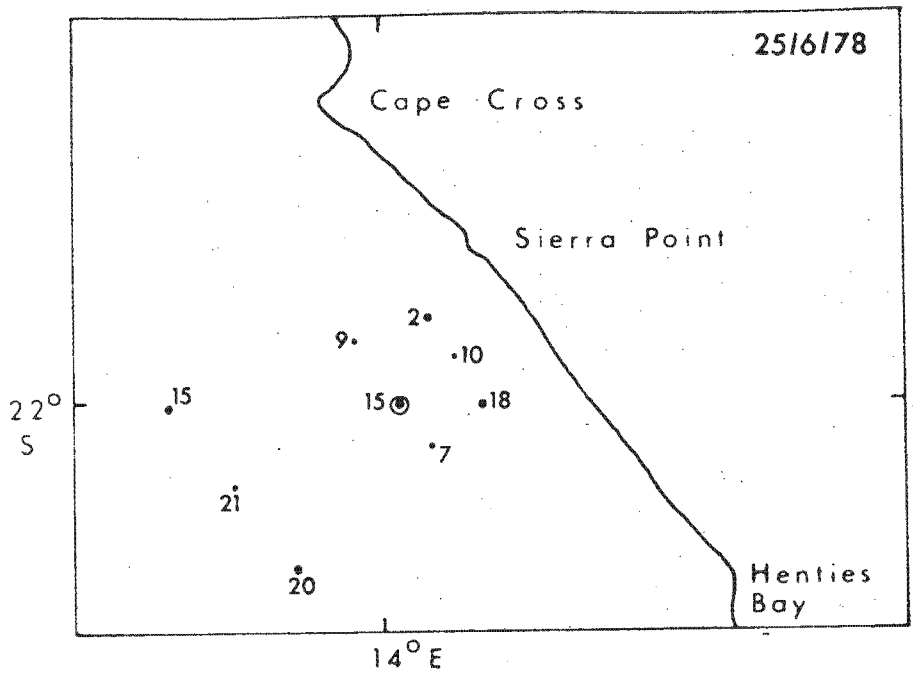

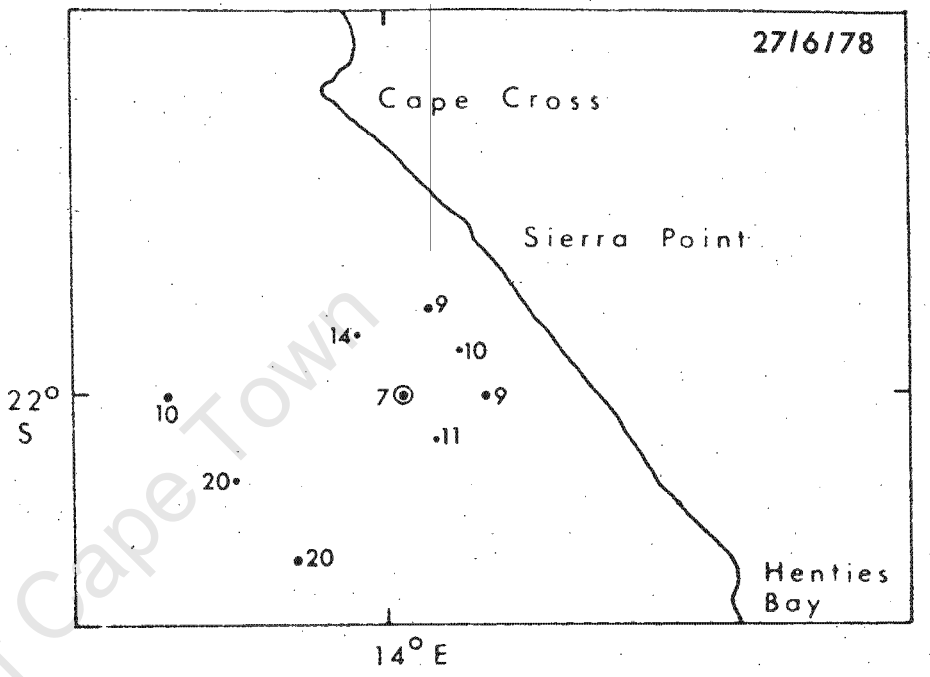

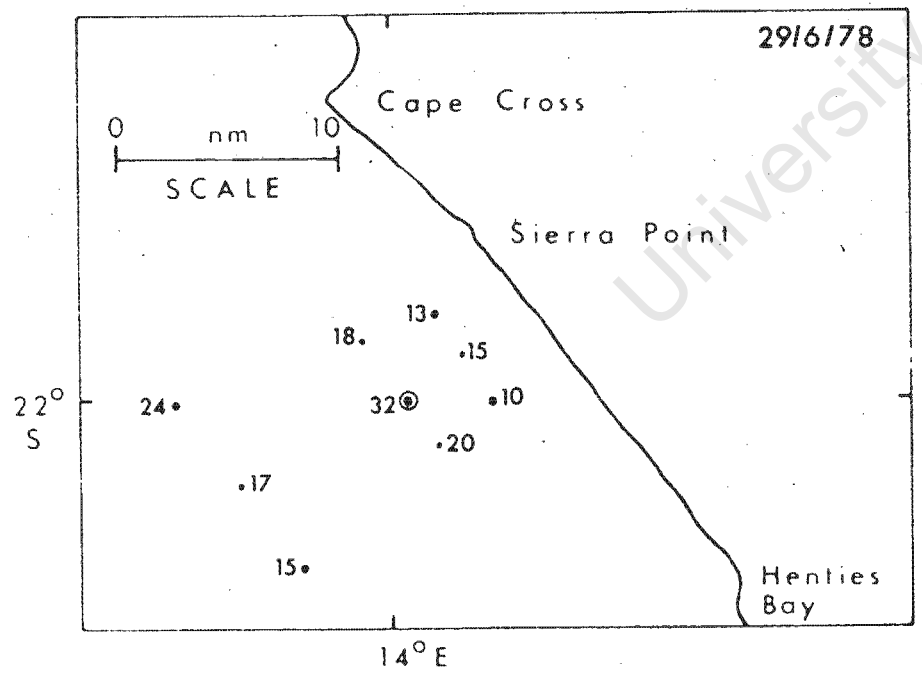

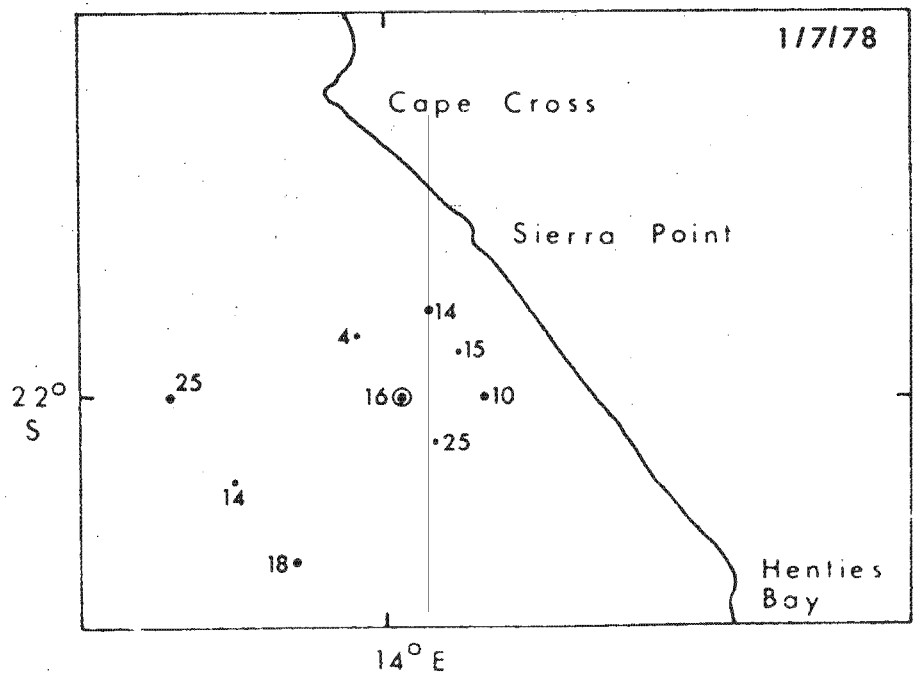

HORIZONTAL DISTRIBUTION: SURFACE T°C FIG. 29

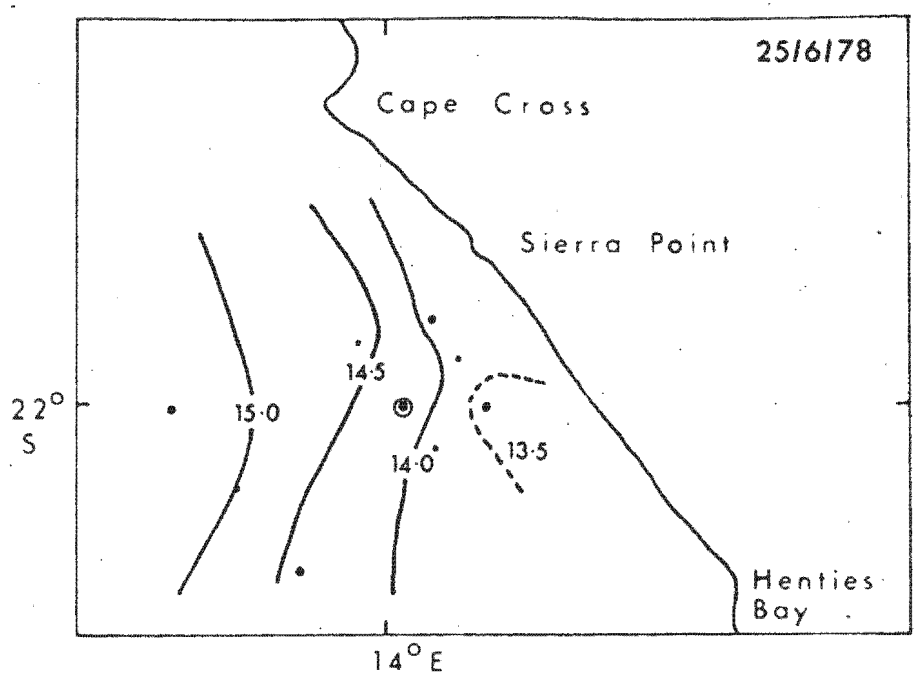

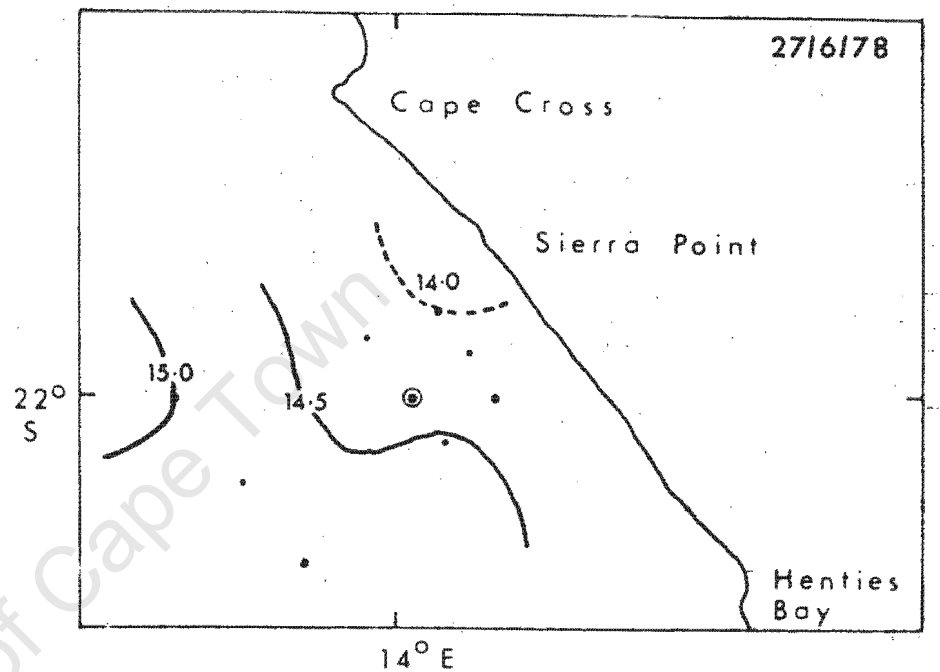

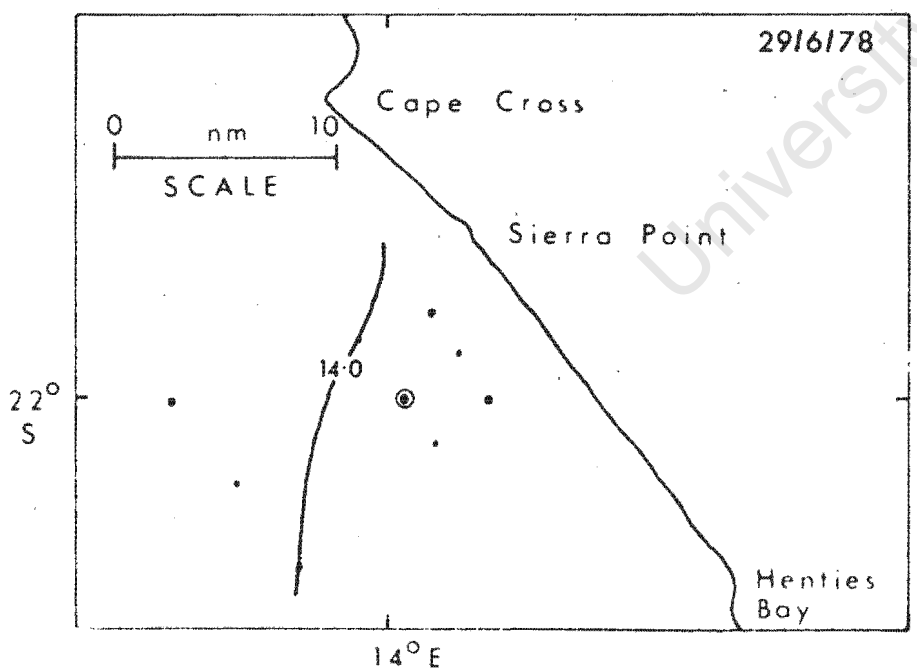

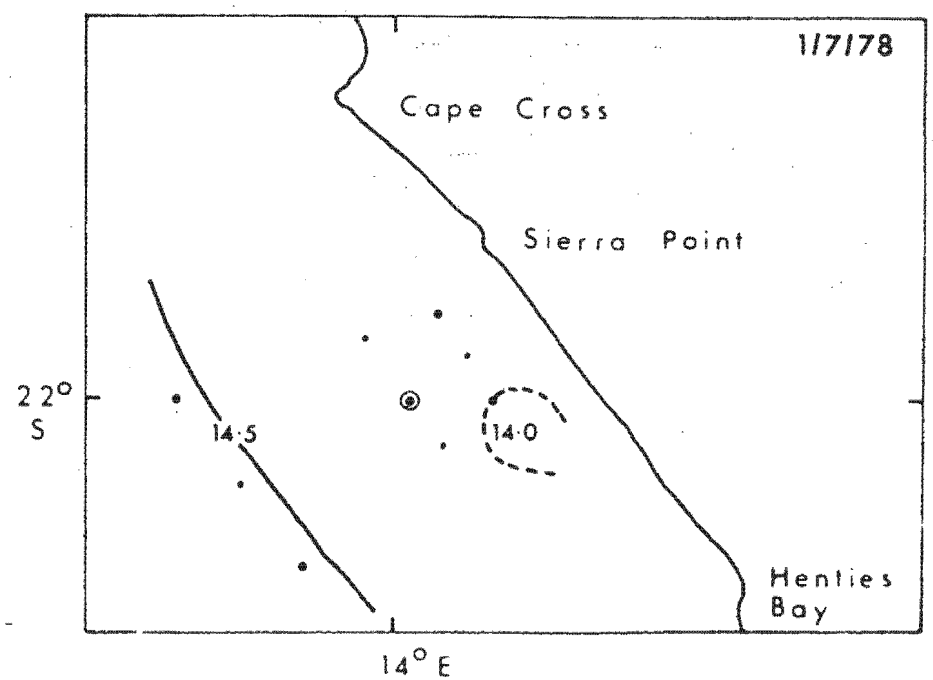

in the following discussions. As can be seen from Figure 1, this is not the case,but this convention is in keeping with previous work off South West Africa.

The thermocline depths seem to vary almost as greatly between successive occupations of the same station as they do amongst different stations, possibly due to the internal waves discussed earlier. Two general features are discernable however. Firstly the thermocline depth was generally greater further offshore, and secondly the layer deepening caused by the two days of southerly winds, although most marked at MG1, resulted in a generally deeper surface layer over the entire area. This can be seen in the horizontal thermocline distribution for 29/6/78 (Figure 27). The wind similarly affected surface temperatures over the grid, the higher temperatures being reduced so that the distribution became more uniform in space. (Figure 29).

The vertical sections in Figure 30 show the same trends as regards thermocline depths. In addition it can be seen that the temperature at the top of the thermocline increased in an offshore direction. Another interesting feature is shown in the section for 16/6/78, done before to intensive survey started. It is that a stratified layer can exist very close to the surface for a substantial distance offshore. Du Plessis (1967) mentioned this fact about the area although with particular reference to stratification in summer. Nevertheless one of his routine stations, that closest to the present research area, still showed 43% occurrence of 'strictly defined'

VERTICAL DISTRIBUTION: T °C AT 22° S FIG. 30

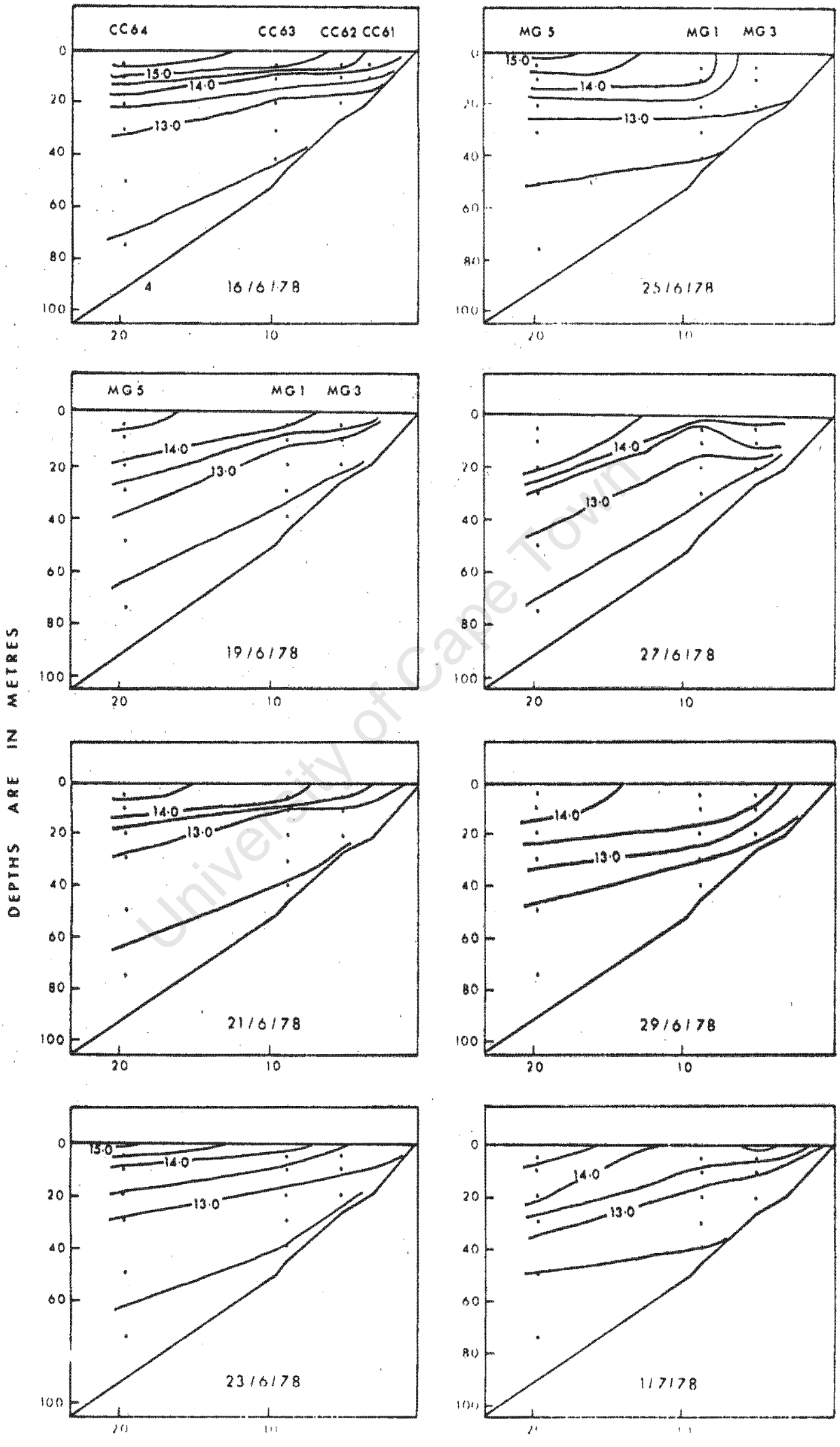

thermoclines in winter, by far and away the highest winter occurrence in his research area (21 - 24°S).

From the above it has been seen that the whole research area was subject to thermoclines during the June/July 1978 programme, and that these conditions are fairly typical. It is in this light that the vertical sections will be discussed and relationships between parameters at MG1 examined.

5.5 Dissolved oxygen, nitrates and temperature at MG1

Figure 31 shows dissolved oxygen and thermocline depth time series at MG1. From this figure can be seen that the surface layer was reasonably oxygenated whilst the bottom layer was practically anoxic. Specifically the surface and 5 metre depths had oxygen values mainly between 3 and 6 ml O_2/1, whilst at 30 and 40 metres oxygen was always below 0,5 ml O_2/1. At 20m oxygen was generally low but increases occurred at more frequent intervals. The oxygen at 10m depth had a range of values from less than 0,5 to greater than 6. Similarly Figure 23 shows that the 10m temperature was sometimes allied with surface layer temperatures, sometimes with lower layer temperatures and on some occasions had intermediate values.

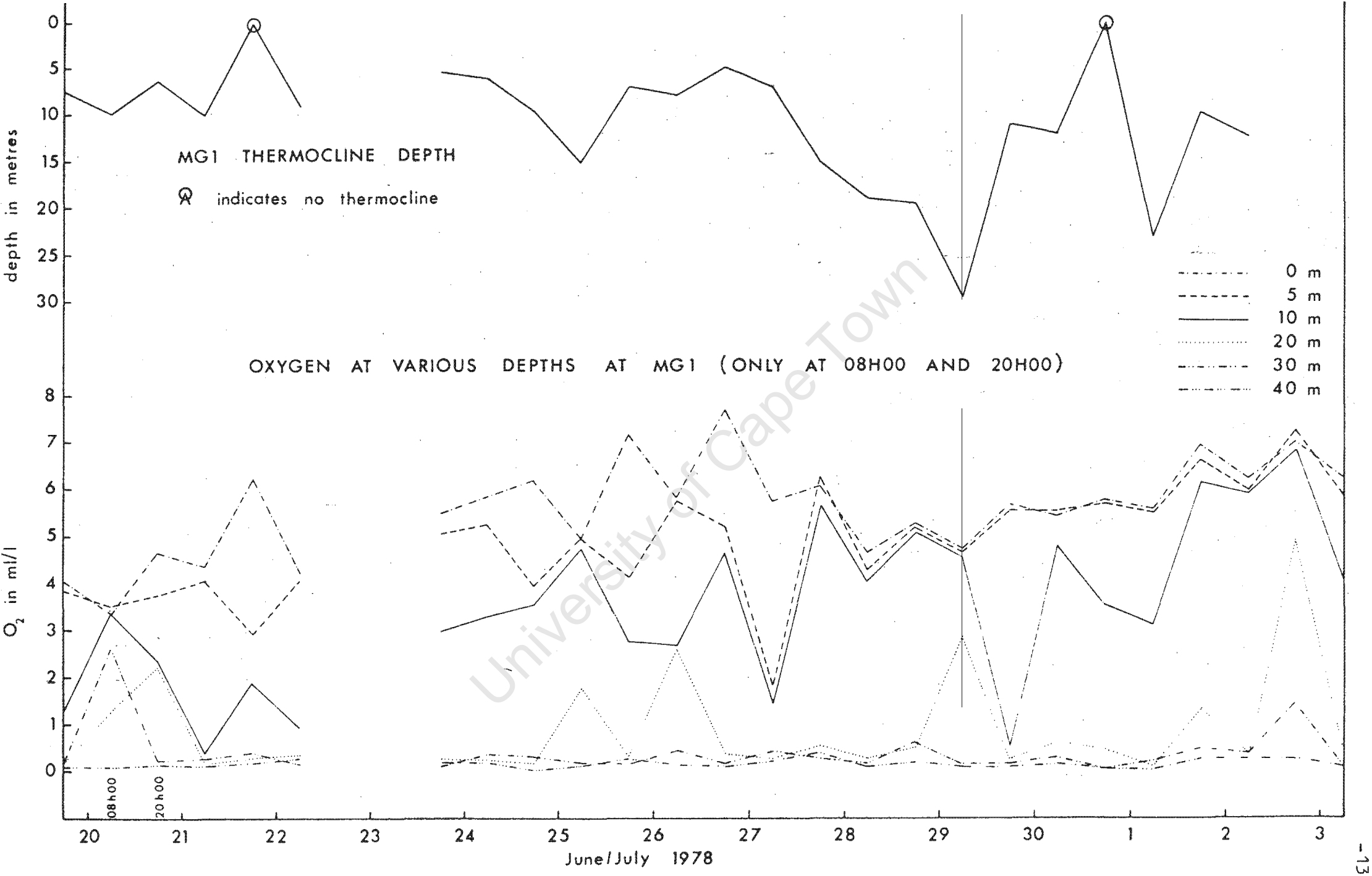

FIG 31 AN OXYGEN AND THERMOCLINE TIME SERIES AT STATION MG 1

It can be concluded the water samples taken at 10m were reasonably equally distributed above, below and in the thermocline. Thus these water samples can be usbd to correlate temperature, oxygen (and nitrates) with one another to study changes over the thermocline at MG1.

Figure 32 plots oxygen (and nitrate) against temperature at 10 metres depth. From this figure it can be seen that when the temperature was greater than 13,7°C the oxygen was greater than 3, whilst at temperatures less than 13,3°C the oxygen was less than 1,5. But the 13,3 and 13,7 range was very much allied with the thermocline (Figure 23) and thus the separation of oxygen values above and below these limits has served both to delineate accurately the temperature range of the thermocline at MG1, and show the effects of thermocline placement on oxygen values, namely keeping the lower layer deprived of oxygen.

This simple division of high oxygen above the thermocline, and very low oxygen below it will be seen to have occurred at all the intensive stations, and will facilitate later discussion of parameters with more complex distributions.

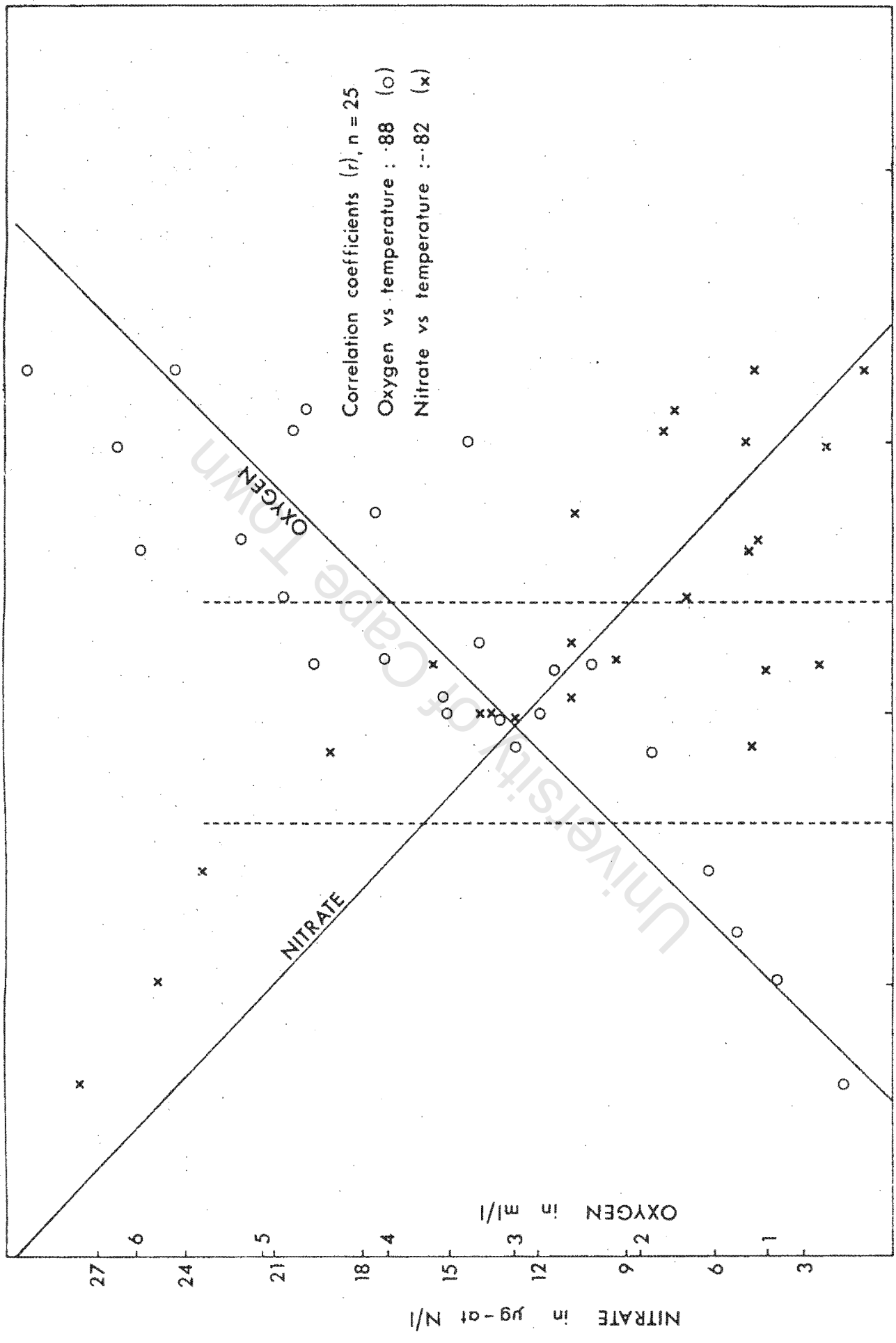

OXYGEN AND NITRATE VS TEMPERATURE AT 10m AT STATION MG1 FIG. 32

Vertical Sections.

5.6 Dissolved oxygen and temperature

A comparison of the vertical dissolved oxygen and temperature sections shown in Figures 30 and 33 respectively, reveals the same division that was found at station MG1: namely high oxygen values above the thermocline and low values below it. However, although gradual temperature changes occurred both above and below the thermocline, this was not the case as regards dissolved oxygen where usually all of the 1 ml O_2/l apart isolines were 'compressed' about the narrow vertical region of the thermocline, with only small variation above it and minimal variation below it. Thus the 8 vertical sections for dissolved oxygen can help to substantiate the description that has been given of thermoclines over the research area.

One can see from Figures 30 and 33 that the temperature and oxygen sections reflect very similarly the effects of wind energy input, particularly when a deviation from the uniformly-deepening-off-shore picture of the thermocline occurred. Examples for comparison are: uplift of lower layer water near the coast on 25/6/78, uplift centered at MG1 on 27/6/78, and the stratified sections of 16/6/78.

VERTICAL DISTRIBUTION: O_2 AT 22° S FIG. 33

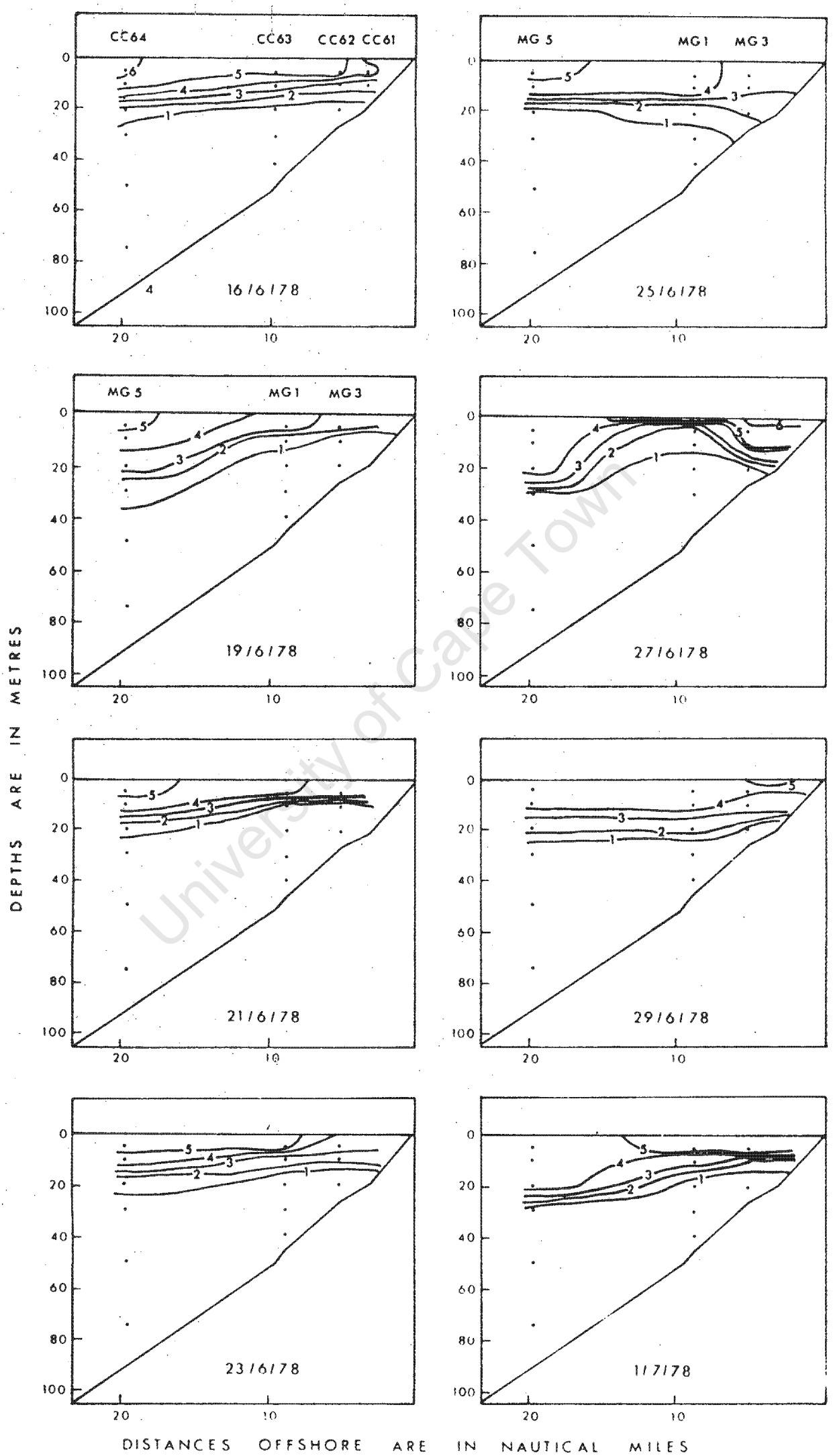

From the oxygen sections in Figure 33 alone, it is immediately clear that during this survey the bulk of the water column could be considered uninhabitable for higher organisms. However, as is the case in many natural environments, this 'hostile area' provides a reservoir in which exploitation does not take place and from which a continuity of essential input, in this case nutrients, is supplied to the productive areas. In fact patterns in this anoxic region, which will be presented later in the vertical sections for nitrates and silicates, will enable this study to document an aspect which has not been fully observed thus far here, namely the continuity of the fundamental circulation of the area.

Before the above mentioned two parameter distributions are discussed however, the salinity and phosphate distributions will be dealt with briefly.

5.7 Salinity and phosphate

Figure 34 shows that the salinity distribution was featureless in the extreme and no general trends are discernible other than that salinities were fractionally higher over the whole area between the 23rd and 27th of June than during the rest of the survey.

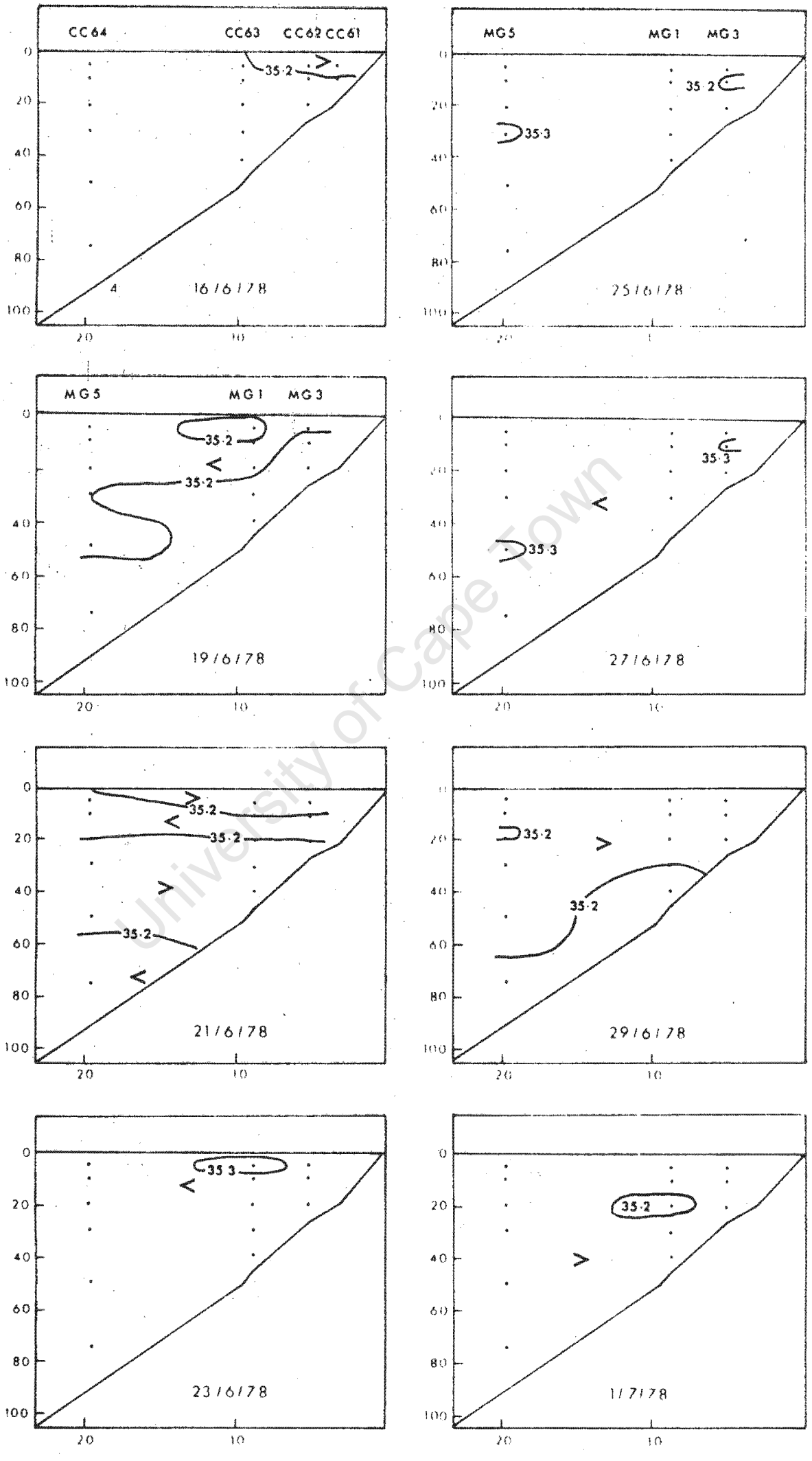

The phosphate distribution (Figure 35) also appears fairly simple and only two points will be mentioned. Firstly, phosphate values were generally high: concentrations were similar to or greater than those found off Walvis Bay by Hart and Currie (1960) and higher than those found off Cape Cross by Calvert and Price (1971). Thus there is no indication of phosphate availability limiting the productivity of the area. Secondly, extremely high concentrations (greater than 5 ug at P/1) were found near the bottom from the 27th June onwards. These can be attributed to the uplift of water at station MG1 on that date, a feature visible on vertical sections for all discussed parameters with the exception of salinity. According to Bailey (1979) these higher concentrations would probably be due to the bottom sediment having been disturbed when the uplift of the water took place. (Appropriate reactions and chemical forms will not be discussed; the reader is referred to Bailey (op. cit.)).

5.8 Nitrates and silicates

Both these nutrients occurred in concentrations ranging from very high to practically zero, and thus they could both serve to limit primary production in the intensive research area. Their distributions (shown in Figure 36 and 38) also show response to thermocline changes as well as reflecting their own supply and recycling processes. The nitrate sections can be described well within the hydrological framework deduced from previously discussed parameters, the silicate sections less easily. Thus a description of the nitrate distribution shown in Figure 36 is given first.

VERTICAL DISTRIBUTION: PO_4-P AT 22° S FIG. 35

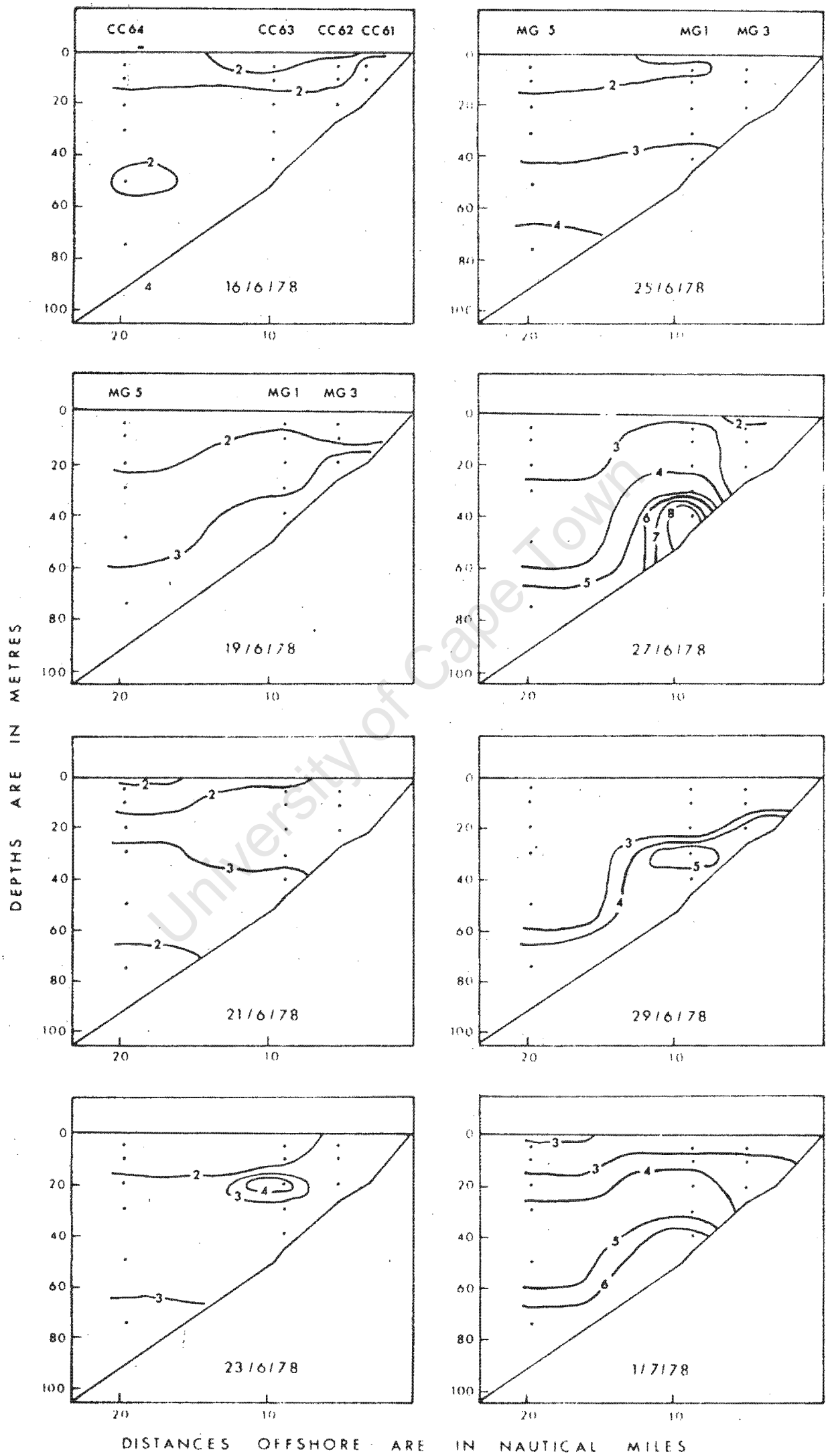

As would be expected from the extremely anoxic conditions near the bottom, nitrate values there are low, as nitrogen would tend to occur as nitrite (Calvert and Price (1971)). Concentrations increase towards middle depths and then abruptly decrease again above the thermocline in the well oxygenated layer, presumably due to biological uptake exceeding supply. (Figure 32 shows the inverse relationship between nitrate and oxygen in the region of the thermocline at MG1.) The upper boundary of the nitrate rich water was clearly effected by thermocline movement and displays the same spatial features already mentioned in the description of temperature and oxygen sections. An explanation of the underlying circulation patterns from the nitrate distribution is attempted below.

Nitrate rich water moves slowly towards the coast and upwards from depths of between about 20 and 70m (at 20nm offshore) rising to 10 - 35m depth at MG1. This is in line with the results of section 3 which showed an average onshore oc 0,07 knots at 20m at this station.

Considering the tongue of water with concentrations greater than 20 ug-at nitrate/l, which is drawn in thicker in Figure 36, one can see that this tongue remains below the thermocline. Thus its movement would be almost entirely in response to continuity considera= tions. Such considerations are now outlined for a diurnal wind regime.

VERTICAL DISTRIBUTION: NO_3 AT 22° S FIG. 36

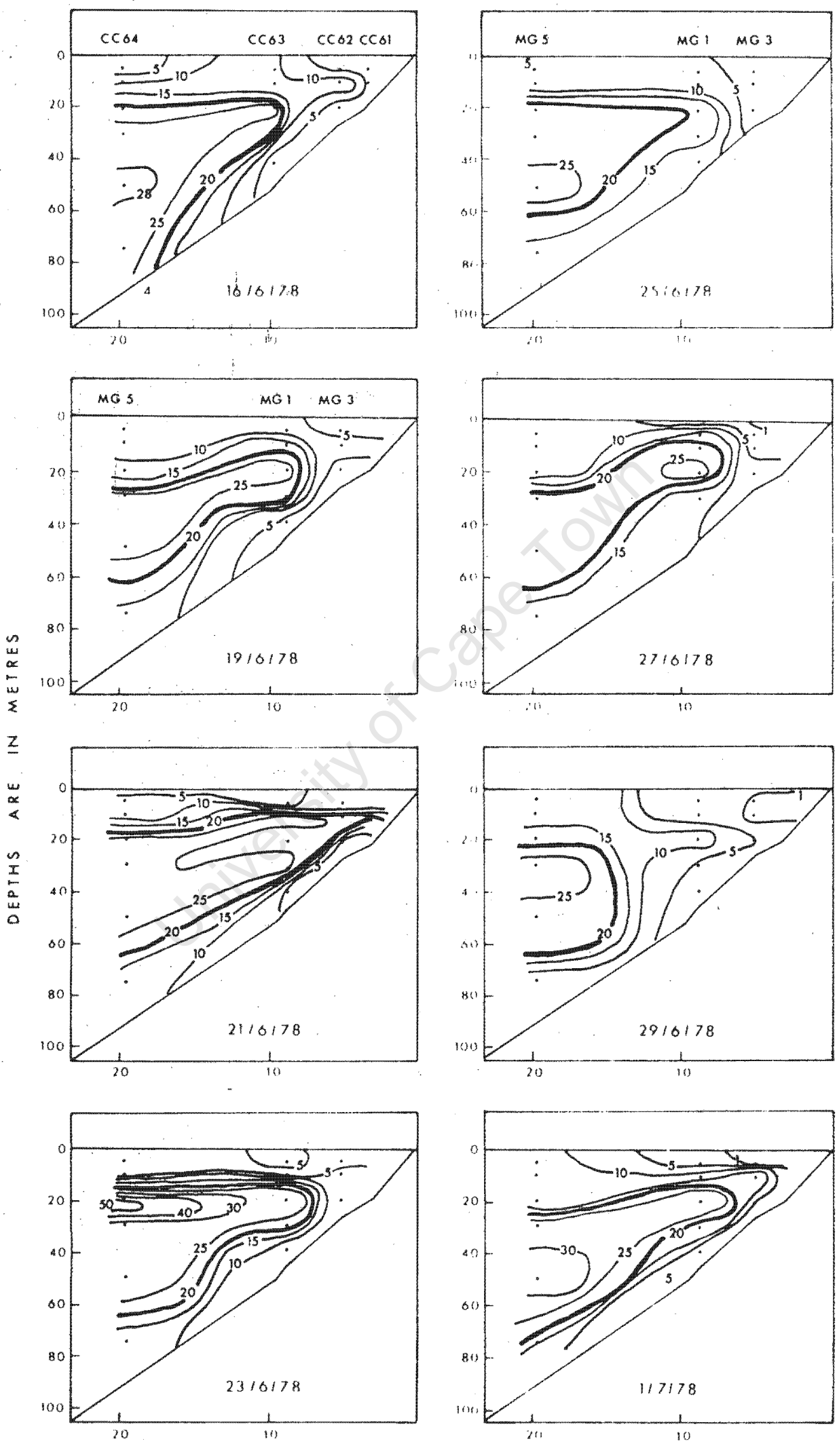

The daily movement of, and turbulence in, the surface layer causes a fair amount of this nitrate rich water to be entrained upwards into this layer whilst at the same time the density interface is not destroyed and no well oxygenated water is transported downwards. Thus there is a daily loss of water to the surface layer which is assumed to be compensated for by offshore movement of this layer. This would lead to the average onshore current measured at 'middle' depths. Scales of this process during a diurnal wind regime are calculated from the schematic representation in Figure 37. Only one experimental result was used, namely that the thermocline depth oscillated with an amplitude of 3m over a 24 hour period of MG1. Very near the coast the schematic model is not accurate but otherwise accuracy should be fair in relation to the speculative nature of the model. Northerly and southerly velocity components which are normal to the section were not considered.

With reference to Figure 37: (times were chosen arbitrarily, but are in keeping with the typical diurnal winds measured at MG1.)

a). At 18h00 a surface layer exists as shown in (A).

b). By 06h00 the surface layer has deepened and entrained 3m of lower layer water. (B).

c). From 06h00 onwards the surface layer is forced offshore by the easterly wind and the lower layer moves inshore until a position such as existed 24 hours ago (at 18h00) is reached (C). The previously entrained water is now, and was since 06h00, fully part and parcel of the upper layer and the process can start again.

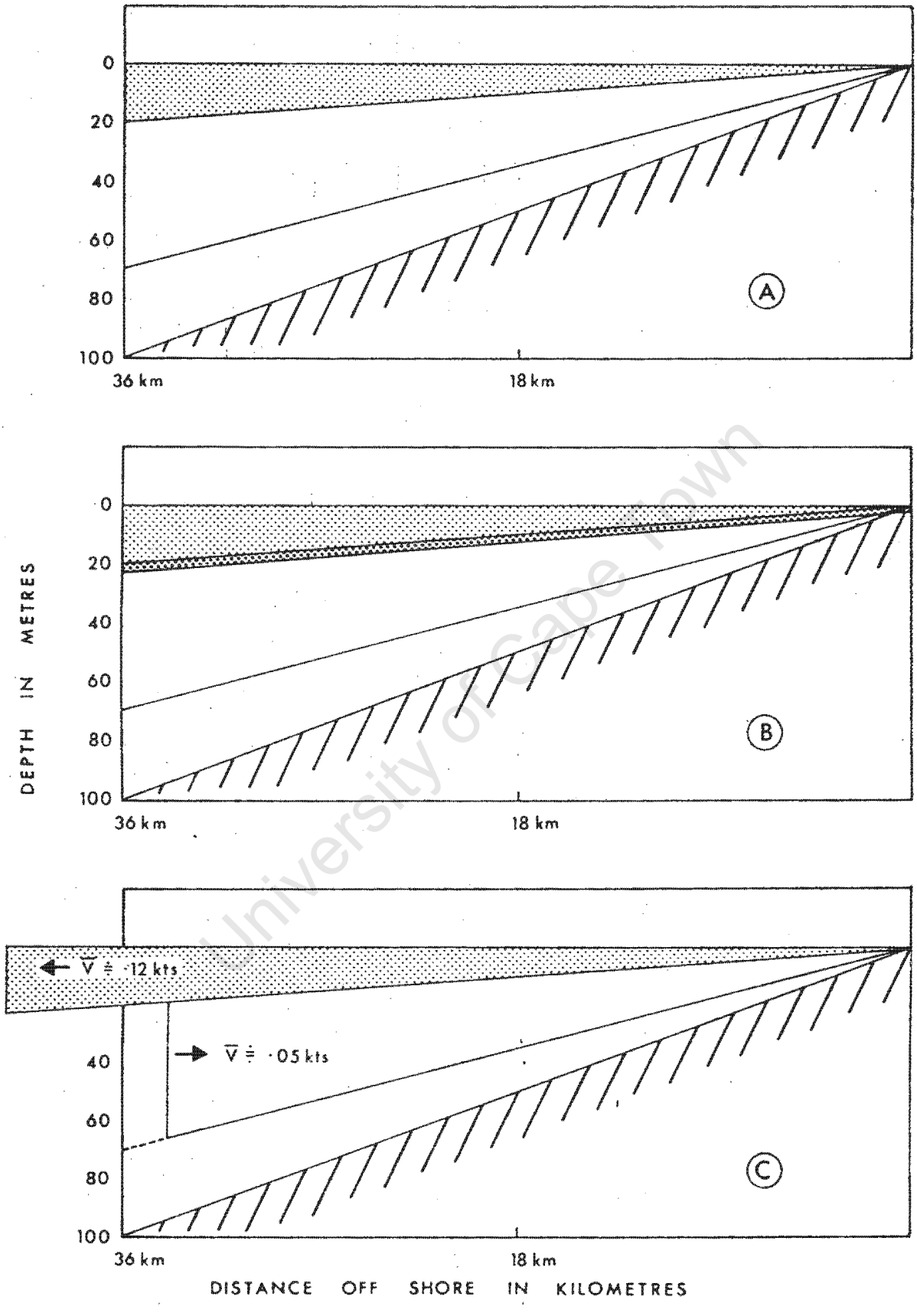

FIG. 37 SCHEMATIC REPRESENTION OF ENTRAINMENT AND "LOWER" AND UPPER LAYER MOVEMENT

The 'vertical' area of water lost by entrainment from the lower layer in 24 hours is 3 x 36000 m. This must be regained in onshore flow. Considering a middle layer depth of 50m at 36km offshore, the average onshore velocity of the wedge over 24 hours will be:

$$\frac{3 \times 36000}{50} \times \frac{1}{86400} = 0{,}025 \text{ m/s}$$

which is equal to 0,05 kts, a result very comparable to the average 0,07 knot onshore current velocity average at MG1, probably in the 'core' of the middle layer. Unfortunately the mandatory off-shore surface current velocity of the model does not agree with the average currents recorded experimentally. This is attributed largely to sampling bias, which has been discussed in sections 2.1, 3.4 and 3.6. However the model trajectories in Chapter 4 did show a definite offshore transport of the upper layer 'slab'.

The above description of the nitrate distribution and its supply and removal processes agrees well with the picture thus far given of processes in the research area. It is within this framework that an explanation of the silicate distribution will be attempted.

Like phosphate but unlike nitrate, silicate does not undergo reactions to other forms in the presence of very low oxygen such as occurred near the bottom during the whole programme. Indeed uplift of water from the bottom, as has been witnessed already in the phosphate and oxygen sections for the 27th of June, shows silicate apparently being released from the bottom sediments in the vicinity of MG1 and trans= ported upwards (Figure 38), but interestingly this occurred two days later on the 29th of June. Values inshore near the bottom ranged

VERTICAL DISTRIBUTION : SiO_3 AT 22° S FIG. 38

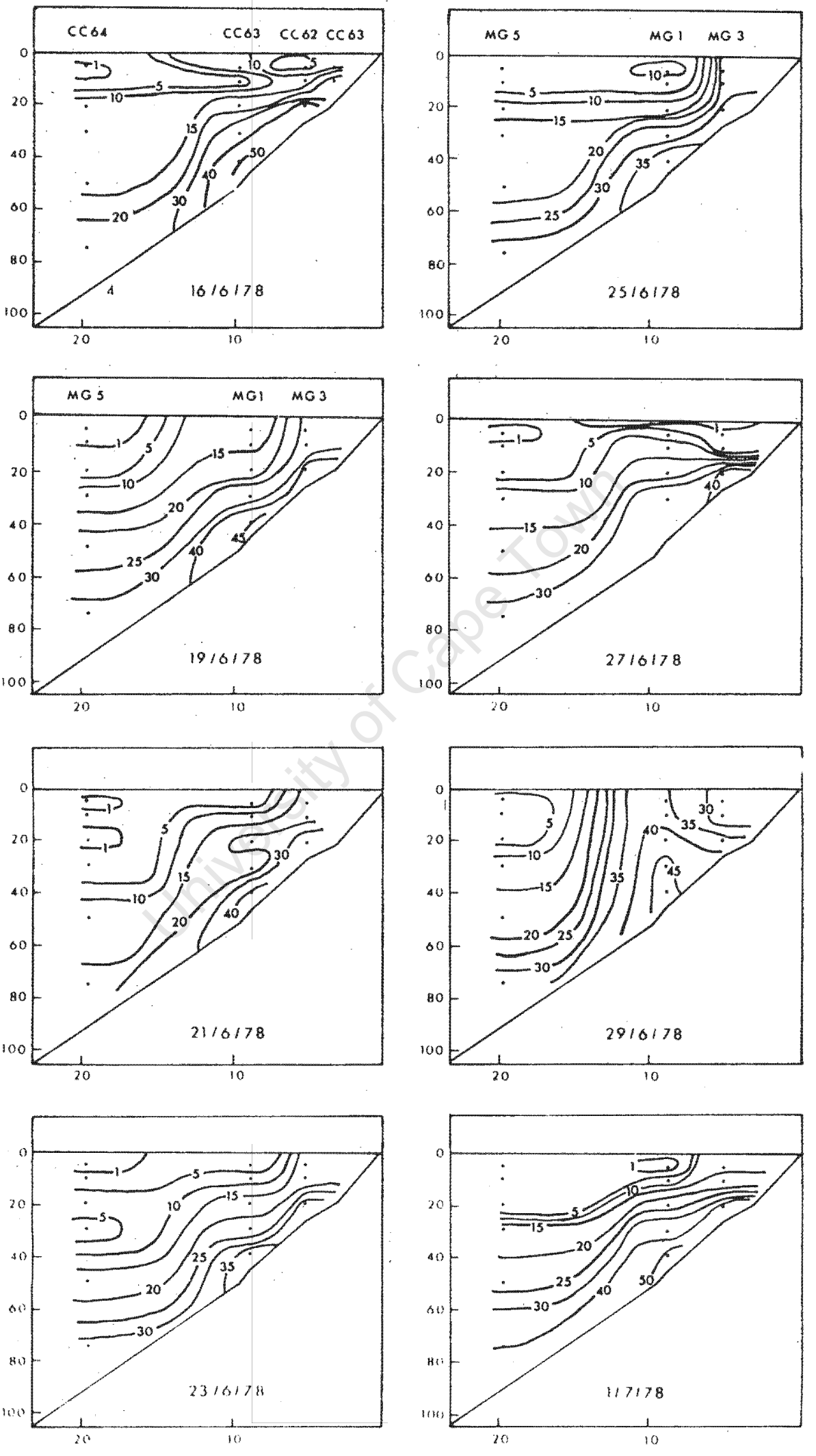

from 30 to 50 ug-at s/l, concentrations comparable to those observed off Cape Cross by Calvert and Price (1971).

The boundary formed by the 20 and 25 ug-at /l lower isolines in the vertical sections are compatible with the definition of the bottom of the tongue of coastward flowing water interpreted from the nitrate distribution. However the silicate isolines can be seen to cut directly across the thermocline on about half the sections in Figure 38, in direct contrast to all other parameter distributions with sharp gradients, whose isolines run largely parallel to the thermocline.

There must be some differential factor operating for silicates with regard to other nutrients to cause this gradient in the surface layer; silicate dropping in concentration from the high values at the coast to depleted values offshore. An explanation is offered based on the following two facts:

Firstly, in the surface layer, nitrate tended to be depleted near the coast and silicate offshore, and secondly the concentration of nitrate is reduced in the presence of low oxygen. This means that at the coast phytoplankton growth would be nitrate limited purely due to the second fact whilst silicate supply "up the shelf" would still be good. (In addition the possibility that the sand blown into the sea may enrich silicate concentrations near the coast, as discussed by Bailey (1979), may have some applicability here, but this idea will not be taken further).

At a greater distance offshore the nitrate supply from lower layers was much greater although nitrate values were low and silicate becomes the limiting nutrient. The silicate concentration offshore may also be less there due to the density of the particulate matter involved with silicate, causing rapid sinking.)

Thus on the occasions when silicate supply at the coast was high and depletion existed offshore a gradient normal to the thermocline can be observed. However the isolines which rise and cut the thermocline position and the surface in no way imply direct water transport paths, although at a first glance a researcher well acquainted with more vigorous upwelling areas, would think this to be the case. It is felt that more than sufficient evidence has been given to show that this is not the case, and that the "thermocline dominated" picture presented of the hydrology is the correct one.

5.9 The extent of the validity of the given hydrological description

The term "research area" has thus far in this thesis implied the intensive research area shown in Figure 1, but it is obviously of importance to know over what larger geographic area off South West Africa the results of this study are applicable. This can be best assessed by relating the extent of the characteristic conditions determined by previous hydrological research and noted in section 1.3, to the present results.

The following 4 points will be made in this regard:

1.) The area between Walvis Bay (23°S) and Cape Cross (21°45'S) has a wide-shelf bottom topography (Figure 1).

2.) Du Plessis 1967 found the area from 22°30' to 21°30 more susceptible to thermocline occurrence in all seasons than areas further north or south.

3.) Low oxygen conditions in the lower layers are found extensively along the South West African coast. Figure 24 indicates that just prior to the intensive survey of June/July 1978, at 20m depth, the low oxygen phenomenon was most pronounced from Walvis Bay to Cape Cross and within 15 miles of the coast.

4.) The wind records from Walvis Bay, Henties Bay and the research ship show marked differences in wind velocity amongst these 3 sites. Hence consequent differences could be expected in surface current velocities and the scales of the upwelling process.

On the basis of the above 4 points it is concluded that the processes operating at the research site can be considered representative of those occurring from just north of Walvis Bay to just north of Cape Cross. However in late spring, summer and autumn, when thermoclines are more prevalent, these processes could be expected to occur over a larger area, determined in the main by the bottom topography and the wind patterns.

5.10 Summary of Chapter 5

(The results of each section are stated under the appropriate section number.)

1.) The approach and scope of this chapter are outlined.
The approach is to relate the hydrology to thermocline and current information, thus completing the triad: winds, currents and hydrology.

The scope of the chapter is by design broader than that of the previous two. Topics such as internal wave and entrainment which have been mentioned previously, are discussed as further introduction to the "mainstream" hydrology.

2.) A simple interpretation of the hydrological changes that occurred at MG1 during the programme is given. Two time scales, daily, and "of several days" are identified and treated separately. Entrainment is proposed as the mechanism responsible for the transfer of lower layer water properties into the upper layer during both time scales.

3.) The possibilities and characteristics of internal waves propagating into or from the research area are investigated under the simplifying assumption of a limited depth, continuously stratified ocean. It is considered likely that forced waves will soon become out of phase with their forcing as they propagate southwards from the research area, and hence their energy will soon be disipated.

Slicks, which are evidence of Langmuir circulation were observed during the programme. As they occurred in calm as well as low windspeed conditions, it was concluded that they were caused by current field-wave field interactions as proposed by Garret (1976).

4.) Thermoclines existed over the whole research area during the programme but large temporal and spatial changes in thermocline depth occurred. It is largely in the light of these two facts that other hydrological data will be discussed.

5.) Disolved oxygen was found to be depleted (less than 1 ml O_2/l) below the thermocline at MG1. The transition to higher values in and above the thermocline was very abrupt. It is concluded that the thermocline prevented downward mixing of water properties. Nitrates were inversely related to oxygen in the region of the thermocline.

6.) Vertical sections for dissolved oxygen and temperature show that the trends, noted in section 5.5 are valid between the coast and a distance of at least 20 miles offshore. This means by far the larger proportion of the water column in this area has oxygen values below 1 ml O_2/l.

7.) The salinity sections showed nothing. The phosphate sections showed phosphates were generally high and that during a period of more vigorous mixing phosphate seemed to be released from the shelf sediments.

8.) Vertical sections for nitrates and silicates showed both these nutrients occurring in concentrations ranging from very high to depletion. Silicates had their highest concentration near the bottom and inshore, concentrations decreasing towards the surface and offshore.

Nitrates, on the other hand, showed their greatest concentrations off shore and at middle depths. The lower values near the bottom are attributed to nitrogen occurring mainly in forms other than nitrate due to the anoxic conditions. Low concentrations at the surface are thought due to biological uptake, and low values inshore due to poor supply. The supply and removal of nitrate in the research area was modelled using results concerning thermocline fluctuation and entrainment, and the inferred onshore water transport rate of the model at middle depths agrees with that found experimentally. It is proposed that no direct nutrient supply occurs to the upper layer; supply occurs by transfer across the thermocline and thus the supply rate is limited.

9.) The area of applicability of the hydrological processes found at the research site is concluded to be from just north of Walvis Bay to just north of Cape Cross, but with likely extensions north and south as the area subject to subject to persistent thermoclines increases in late spring, summer and autumn.

10.) In summary it can be said that the research site can be considered an anomalous upwelling area, firstly because of the manner in which nutrient supply to the upper layer takes place, and secondly because the bulk of the water column below the thermocline consists of an anoxic nutrient reservoir, unsuitable for many higher forms of marine life such as pelagic fish.

The following chapter will not repeat the results and conclusions of this study: these can be found at the end of Chapters 3,4 and 5 and in the abstract. Instead it will present some of the author's views with regard to physical research in the Benguela Upwelling System.

6. THE DIRECTION OF FUTURE PHYSICAL RESEARCH IN THE BENGUELA UPWELLING SYSTEM: A SUBJECTIVE VIEW.

The Benguela Upwelling System, which extends along the west coast of southern Africa from Cape Point (34°30'S) to north of the Cunene River (17°40'S) has been subjected to an increase in intensive physical research during the past few years. Because of its nature, this research has been limited to a few selected localities no more than 200 miles in extent along the coast. The work of Bailey (1979), Jury (1980) and the present study will now be considered briefly as an introduction to a discussion of the direction of physical research in the Benguela Upwelling System in general.

The upwelling off the Cape Peninsula region is known to be controlled by the characteristics of definable upwelling wind events of a few days' duration and it was these events and their effects on the upper layer of the sea that were measured (on appropriate scales) and described by Jury (1980). In addition Jury (op. cit.) showed the influence of orography on these winds.

Further north in the Lüderitz area (26°S), upwelling is persistent for the larger part of the year because of the more regular nature of the southerly winds. The time-scale of the dominant hydrological changes is seasonal, and Bailey (1979) was therefore able to describe the hydrological features of the area on the basis of seasonal occupation of a closely spaced grid of stations.

In contrast to the two areas mentioned above which have been shown capable of supporting active upwelling under suitable wind conditions, the region between Walvis Bay and Cape Cross, with its wide shallow bottom topography, did not seem to be able to respond in a similar manner. In the present study, it was found that two days of sustained southerly winds served to deepen the upper mixed layer (at a distance of six miles off shore) rather than remove it.

Therefore, two factors appear to determine the nature of the upwelling process at these three sites in the Benguela Upwelling System: namely, winds and bottom topography. The bottom topography is known but only recently has it been incorporated in mathematical models of the Benguela Upwelling System with any degree of success (Brundrit and van Foreest, 1981). In coastal areas stratification can complicate the picture further. (This led to the model presented in this thesis being confined to the upper layer above the thermocline.) This study also showed that marked variations occurred in the winds as measured at three sites, all within 60 n. miles of each other in an area where the land topography is comparatively featureless.

Consequently, difficulties are associated with the incorporation of detailed bottom topography in mathematical models, and we lack data on the <u>in situ</u> winds over the greater area of the Upwelling System. This leads the author to conclude that we are still far from obtaining a physical understanding of the Benguela Upwelling System that could be employed in any predictive sense. However, progress in these areas of modelling and wind data collection is both necessary and at present being made.

However, what future rôle is there for quantitative practical research? Additional localities could be intensively studied between the Cape, LÜderitz and Walvis Bay sites; the nature of the hydrological transitions could be assessed from previous works if their inferred currents could be substantiated by direct current measurements. Nevertheless, only around the Cape Peninsula could the practical resources be mustered for what could be called a continuous intensive effort.

For the rest of the Upwelling System, it is felt that physical research should address itself largely to the nature of physical influences on the pelagic fish stocks of South Africa and South West Africa and the localities of major importance in this regard. The physical factors with proven influence on spawning, larval development, survival and transport are temperature and currents. The South West African Pelagic Egg and Larval Survey (S.W.A.P.E.L.S.) allows for extensive temperature measurements along with ichthyoplankton sampling during the pilchard and anchovy spawning seasons, and similar work has been done around the Cape. These surveys have, in addition, revealed the desirability of direct current measurements in ascertaining larval drift, particularly in the localities not yet researched intensively; namely between Cape Columbine and LÜderitz and in the vicinity of Cape Frio. As an example of the potential of such measurements, a single satellite-tracked drogue trajectory presented by Harris and Shannon (1979) not only allowed them to substantiate previously inferred currents in an off-shore region, but also permitted Badenhorst and Boyd (1980) to show the feasibility of anchovy larval transport between the Cape and South West Africa.

Effective coverage is presently being obtained in respect of the temperature conditions in the Benguela Upwelling System. The incorppration of the direct measurement of currents into research programmes would yield some problems, but so far this work has suffered as a result of its low priority. It is hoped that this study (based on just over two weeks of directed ship's time) has shown what can be achieved.

APPENDIX A: DROGUE TRACKING DATA

Windspeed in knots : distances in nautical miles.

OCCASION 1 DATE 200678

TIME	WIND DIR	WIND SP	2M DRG BRG	2M DRG DIST	5M DRG BRG	5M DRG DIST	10M DRG BRG	10M DRG DIST	20M DRG BRG	20M DRG DIST	30M DRG BRG	30M DRG DIST
800	140	8										
830	100	5										
900	100	5										
930	100	2										
1000	CLM	0										
1030	CLM	0										
1100	CLM	0										
1130	150	6										
1200	150	11										
1230	150	11										
1300	155	12	300	0.05	310	0.10	312	0.15	18	0.20	350	0.11
1330	160	13	296	0.14	304	0.17	318	0.19	18	0.35	349	0.24
1400	180	10	301	0.22	307	0.25	318	0.30	16	0.47	345	0.25
1430	180	10	303	0.35	304	0.34	320	0.40	11	0.61	340	0.31
1500	180	10	303	0.47	306	0.44	320	0.51	10	0.72	336	0.39
1530	180	7	302	0.59	304	0.52	319	0.62	5	0.81	332	0.46
1600	180	5	302	0.70	303	0.60	319	0.71	2	0.91	329	0.51
1630	180	7	304	0.82	304	0.70	318	0.85	359	1.01	327	0.60

OCCASION 2 DATE 200678

TIME	WIND DIR	WIND SP	20M DRG BRG	20M DRG DIST
1800	180	5		
1830	180	5		
1900	180	5		
1930	175	5		
2000	170	5		
2030	150	5		
2100	130	5		
2130	130	2	328	0.08
2200	CLM	0	327	0.19
2230	CLM	0	327	0.21
2300	CLM	0	331	0.25
2330	CLM	0	331	0.29
2400	CLM	0	332	0.32
30	CLM	0	335	0.39
100	CLM	0	336	0.41
130	CLM	0	336	0.46
200	170	3	338	0.50

OCCASION 3 DATE 210678

TIME	WIND DIR	WIND SP	2M BRG	2M DIST	10M BRG	10M DIST	20M BRG	20M DIST
1400	CLM	0						
1430	CLM	0						
1500	CLM	0						
1530	CLM	0						
1600	180	5						
1630	185	7						
1700	190	9						
1730	180	8						
1800	180	3	332	0.15	318	0.14		
1830	150	5	330	0.26	314	0.26	311	0.10
1900	CLM	0	336	0.36	328	0.41	308	0.16
1930	CLM	0	327	0.52	322	0.54	305	0.22
2000	CLM	0	330	0.70	326	0.74	307	0.29
2030	CLM	0	332	0.85	326	0.91	312	0.35
2100	CLM	0	334	0.88	327	0.96	312	0.37
2130	CLM	0					312	0.39
2200	160	4						

OCCASION 4 DATE 220678

TIME	WIND DIR	WIND SP	5M BRG	5M DIST	10M BRG	10M DIST	20M BRG	20M DIST	30M BRG	30M DIST
400	160	7								
430	145	8								
500	130	10								
530	115	10								
600	100	10								
630	95	11								
700	90	12								
730	90	18								
800	90	20	278	0.21	278	0.23	288	0.14	295	0.12
830	80	16	274	0.50	277	0.45	291	0.25	294	0.20
900	65	14	268	0.74	273	0.58	289	0.33	294	0.23
930	50	13	266	0.85	270	0.72	287	0.39	294	0.26
1000	50	8	263	1.01	268	0.82	288	0.40	299	0.26
1030	60	18	261	1.10	265	0.88	290	0.41	304	0.26
1100	60	18	258	1.20	264	0.96	292	0.42	308	0.27
1130	60	14					293	0.43	317	0.29
1200	60	9					294	0.44	325	0.30
1230	60	8							333	0.32
1300	30	4							341	0.34
1330	340	12							346	0.36
1400	290	13							351	0.40
1430	260	10							359	0.47
1500	260	5							360	0.55
1530	245	5							360	0.61
1600	240	8								

OCCASION 5 DATE 220678

TIME	WIND DIR	WIND SP	5M DRG BRG	5M DRG DIST	10M DRG BRG	10M DRG DIST	20M DRG BRG	20M DRG DIST	30M DRG BRG	30M DRG DIST
800	90	20								
830	80	16								
900	65	14								
930	50	13								
1000	50	8								
1030	60	18								
1100	60	18								
130	60	14								
1200	60	9								
1230	60	8								
1300	30	4								
1330	340	12								
1400	290	13	172	0.06	154	0.05	115	0.05	351	0.40
1430	260	10	156	0.16	139	0.14	80	0.09	359	0.47
1500	260	5			131	0.21	68	0.15	360	0.55
1530	245	5			130	0.23	62	0.21	360	0.61
1600	240	8								

OCCASION 6 DATE 240678

TIME	WIND DIR	WIND SP	20M DRG BRG	20M DRG DIST	30M DRG BRG	30M DRG DIST
300	CLM	0				
400	150	10				
500	90	10				
600	95	20				
700	90	20				
800	90	20				
830	90	25				
900	70	27				
930	70	27	302	0.32	261	0.24
1000	70	20	295	0.37	256	0.30
1030	70	22				
1100	70	22				
1130	70	20				
1200	70	20				
1230	45	18	292	0.41	234	0.31
1300	30	13	294	0.37	230	0.27
1330	40	10	299	0.34	219	0.24
1400	40	7	306	0.30	209	0.20
1430	40	5	327	0.26	189	0.15
1500	50	7	332	0.25	173	0.12
1530	40	3	348	0.26	138	0.11
1600	40	10	358	0.29	116	0.11
1630	190	10	8	0.39	82	0.17
1700	180	10	10	0.44	68	0.19
1730	200	13	10	0.55	48	0.27
1800	200	10	11	0.61	40	0.30
1830	195	11	12	0.64	31	0.38
1900	190	12	12	0.66	23	0.46
1930	190	10			18	0.54
2000	200	10			9	0.62
2030	190	13			4	0.70
2100	180	15			359	0.77
2130	180	10				

OCCASION 7 DATE 240678

TIME	WIND DIR	WIND SP	2M DRG BRG	2M DRG DIST	5M DRG BRG	5M DRG DIST	10M DRG BRG	10M DRG DIST	20M DRG BRG	20M DRG DIST	30M DRG BRG	30M DRG DIST
1200	50	20										
1230	45	18										
1300	30	13										
1330	40	10										
1400	40	7										
1430	40	5										
1500	50	7										
1530	40	3										
1600	40	10										
1630	190	10	182	0.16	178	0.16	70	0.01	8	0.39	82	0.17
1700	180	10	184	0.23	180	0.29			10	0.44	68	0.19
1730	200	13	177	0.37	180	0.46			10	0.55	48	0.27
1800	200	10	177	0.40	178	0.48			11	0.61	40	0.30
1830	195	11	174	0.50	176	0.47			12	0.64	31	0.38
1900	190	12	171	0.60	172	0.46			12	0.66	23	0.46
1930	190	10					70	0.10			18	0.54
2000	200	10					55	0.11			9	0.62
2030	180	13					56	0.15			4	0.70
2100	180	15					56	0.19			359	0.77
2130	180	10					52	0.20				

OCCASION 8 DATE 260678

TIME	WIND DIR	WIND SP	2M DRG BRG	2M DRG DIST	5M DRG BRG	5M DRG DIST	10M DRG BRG	10M DRG DIST	20M DRG BRG	20M DRG DIST	30M DRG BRG	30M DRG DIST
400	CLM	0										
500	CLM	0										
600	100	8										
700	90	10										
800	90	17										
830	70	18	261	0.11	288	0.05	34	0.03	219	0.10	206	0.05
900	70	20	260	0.32	280	0.20	323	0.05	199	0.07	220	0.15
930	70	18	256	0.43	274	0.21	281	0.08	206	0.11	222	0.24
1000	70	17	244	0.52	260	0.39	263	0.12	207	0.12	215	0.27
1030	60	18	244	0.70	258	0.50	259	0.12	207	0.14	211	0.36
1100	60	15	245	0.84	253	0.62	253	0.30	207	0.19	206	0.41
1130	60	13	238	1.00	249	0.75	248	0.40	207	0.24	204	0.49
1200	60	12	236	1.15	246	0.82	245	0.47	206	0.27	200	0.55
1230	60	10	232	1.30	241	0.94	240	0.51	202	0.32	205	0.61
1300	60	4	229	1.39	237	1.07	236	0.62	199	0.35	190	0.67
1330	65	3	227	1.47	232	1.04	231	0.70	194	0.39	185	0.76
1400	65	2	225	1.59	230	1.09	217	0.75	186	0.39	180	0.81
1430	CLM	0			226	1.16	218	0.79	180	0.40	177	0.87
1500	320	5	223	1.76	226	1.25	219	0.86	174	0.41	175	0.92
1530	280	8	219	1.82	222	1.32	216	0.90	166	0.45	169	1.01

OCCASION 9 DATE 260678

TIME	WIND DIR	WIND SP	2M DRG BRG	2M DRG DIST	5M DRG BRG	5M DRG DIST	10M DRG BRG	10M DRG DIST	20M DRG BRG	20M DRG DIST	30M DRG BRG	30M DRG DIST
1600	CLM	0					214	0.97	160	0.45	165	1.04
1630	260	10	176	0.19	165	0.11	210	1.04	150	0.51	160	1.10
1700	240	10	172	0.24	168	0.16	205	1.06	140	0.59	158	1.14
1730	250	10	168	0.34	164	0.19	196	1.01	134	0.62	151	1.21
1800	230	8	167	0.41	165	0.27	192	1.12	129	0.71	149	1.25
1830	240	12	157	0.54	160	0.36	188	1.14	126	0.72	145	1.27
1900	240	10	146	0.64	152	0.40	186	1.17	122	0.79	142	1.32
1930	200	10	142	0.72	149	0.49	183	1.22	120	0.85	140	1.32
2000	220	10	136	0.79	143	0.51	177	1.24	117	0.87	137	1.32
2030	200	11	129	0.85	138	0.54	173	1.27	115	0.89	136	1.35
2100	180	6	118	0.91	137	0.59	170	1.31	115	0.91	135	1.39
2130	180	8	113	0.98	121	0.61	165	1.32	112	0.94	133	1.36
2200	180	8	109	0.99	115	0.67	164	1.37	113	0.90	134	1.37
2230	180	10	107	1.02	104	0.77	161	1.40	112	0.87	135	1.36
2300	180	10	100	1.07	91	0.85	158	1.40	112	0.80	134	1.34
2330	170	10	96	1.14	85	0.96	156	1.44	114	0.76	136	1.34
2400	140	12	91	1.20	82	1.05	156	1.44	116	0.72	139	1.31
30	CLM	0	85	1.26	75	1.12	154	1.42	119	0.65	140	1.33
100	CLM	0	80	1.36	71	1.24	153	1.45	123	0.64	142	1.34
130	CLM	0	77	1.49	69	1.42	152	1.49	127	0.69	144	1.39
200	CLM	0	73	1.61	65	1.49	149	1.55	128	0.74	144	1.41
230	CLM	0	70	1.72	64	1.61	149	1.55	130	0.76	144	1.45
300	CLM	0	66	1.86	60	1.74	146	1.60	127	0.84	143	1.52
330	215	3	63	2.00	59	1.85	145	1.60	126	0.87	144	1.60
400	CLM	0	60	2.12	55	1.96	143	1.62	125	0.90	143	1.62
430	CLM	0	56	2.29	52	2.09	144	1.63	121	1.00	142	1.66
500	CLM	0	53	2.46	51	2.26	145	1.74	117	1.03	141	1.76
530	180	8	51	2.59	48	2.40	143	1.75	115	1.14	140	1.84
600	CLM	0	48	2.71	47	2.49	142	1.80	113	1.16	139	1.89
630	CLM	0	47	2.82	45	2.59	142	1.84	113	1.19	137	1.91
700	CLM	0	43	2.91	42	2.75	142	1.87	112	1.25	137	1.96
730	CLM	0			40	2.90	142	1.90	110	1.30	137	1.99
800	CLM	0	38	3.09	38	2.90	141	1.99	107	1.29	136	2.05
830	200	2	38	3.17	38	2.99	143	2.01	110	1.34	140	2.10

OCCASION 10 DATE 300678

TIME	WIND DIR	WIND SP	5M BRG	5M DRG DIST	5M BRG	5M DRG DIST	30M BRG	30M DRG DIST	30M BRG	30M DRG DIST
1500	CLM	0								
1600	CLM	0								
1700	270	5								
1800	250	5								
1830	180	3			70	1.10			116	1.10
1900	180	5	291	1.10	68	1.16	206	0.94	117	1.15
1930	CLM	0								
2000	CLM	0	295	1.11	62	1.36	210	0.92	116	1.19
2030	CLM	0	302	1.05	59	1.46	195	0.92	117	1.27
2100	CLM	0	302	1.06	58	1.56	193	0.99	118	1.37
2130	CLM	0	303	1.06	54	1.66	187	1.00	116	1.42
2200	CLM	0	307	1.04	52	1.75	183	1.01	116	1.46
2230	CLM	0	314	1.05	49	1.84	179	1.04	116	1.54
2300	CLM	0	315	1.05	47	1.89	177	1.05	116	1.57
2330	CLM	0	317	1.06	46	1.94	174	1.07	117	1.60
2400	CLM	0	324	1.12	42	2.02	169	1.12	116	1.61
30	CLM	0	320	1.09	41	2.04	167	1.14	115	1.64
100	CLM	0	321	1.17	40	2.10	165	1.17	115	1.64
130	CLM	0	320	1.16	37	2.11	162	1.22	114	1.66
200	CLM	0	324	1.24	36	2.11	161	1.24	116	1.66
230	280	8	321	1.26	32	2.15	159	1.27	115	1.65
300	280	8	323	1.29	32	2.19	160	1.33	117	1.67
330	280	8	320	1.31	30	2.20	159	1.33	117	1.70
400	280	8	320	1.29	30	2.20	158	1.35	118	1.74
430	270	3	318	1.26	29	2.17	159	1.44	120	1.77
500	270	5	315	1.29	26	2.19	156	1.47	119	1.85
530	270	3	314	1.25	26	2.15	156	1.54	120	1.90
600	270	5	314	1.22	26	2.09	154	1.61	121	1.94
630	270	5	311	1.17	24	2.06	152	1.66	120	2.06
700	270	5	310	1.12	24	2.00	151	1.74	120	2.11
730	270	3	308	1.10	25	1.99	151	1.80	122	2.16
800	310	5	307	1.05	24	1.96	149	1.85	121	2.25
830	310	5	309	1.05	27	1.90	150	1.91	124	2.34

OCCASION 11 DATE 10778

TIME	WIND DIR	WIND SP	2M BRG	2M DRG DIST	5M BRG	5M DRG DIST	10M BRG	10M DRG DIST	20M BRG	20M DRG DIST	30M BRG	30M DRG DIST
1400	270	3										
1500	270	2										
1600	270	4										
1700	270	5										
1800	CLM	0										
1900	CLM	0										
2000	CLM	0										
2030	CLM	0	33	0.17	33	0.16						
2100	CLM	0	32	0.35	34	0.34	39	0.15				
2130	CLM	0	34	0.51	35	0.56	48	0.20	72	0.09		
2200	CLM	0	33	0.71	35	0.74	44	0.35	77	0.14	123	0.10
2230	CLM	0	34	0.89	35	0.90	42	0.45	81	0.20	123	0.17
2300	CLM	0	32	1.02	33	1.05	43	0.56	85	0.27	126	0.25
2330	CLM	0	28	1.20	29	1.21	41	0.60	83	0.34	123	0.30
2400	CLM	0	24	1.32	26	1.34	40	0.60	82	0.37	122	0.34
30	CLM	0	25	1.47	24	1.50	40	0.60	83	0.41	124	0.40
100	CLM	0	22	1.65	23	1.66	39	0.67	81	0.44	125	0.44
130	CLM	0	22	1.81	22	1.81	37	0.81	82	0.50	126	0.50
200	CLM	0	17	1.98	18	1.99	33	0.81	78	0.54	124	0.56
230	CLM	0	14	2.05	15	2.10	29	0.85	75	0.52	124	0.59
300	CLM	0	11	2.16	12	2.20	25	0.86	75	0.54	126	0.59
330	CLM	0	8	2.20	8	2.29	22	0.91	75	0.52	127	0.61
400	CLM	0	5	2.24	4	2.34	20	0.94	72	0.56	126	0.64
430	CLM	0	1	2.46	2	2.34	15	0.95	71	0.57	124	0.65
500	CLM	0	358	2.54	0	2.42	12	0.92	72	0.59	124	0.65
530	CLM	0	356	2.61	359	2.49	14	0.97	71	0.60	127	0.62
600	CLM	0	353	2.67	353	2.50	8	1.00	70	0.62	126	0.61
630	CLM	0	351	2.77	354	2.62	5	1.10	64	0.71	124	0.69
700	CLM	0	348	2.84	351	2.65	2	1.16	60	0.75	121	0.70
730	CLM	0	346	2.94	350	2.69	2	1.16	62	0.77	122	0.72
800	CLM	0	344	2.95	349	2.76	358	1.15	59	0.82	119	0.77
830	CLM	0	343	3.02	347	2.79	356	1.21	59	0.84	118	0.82
900	CLM	0	339	3.11	343	2.92	354	1.22	59	0.92	115	0.90

OCCASION 12 DATE 20778

TIME	WIND DIR	WIND SP	2M BRG	2M DRG DIST	2M BRG	2M DRG DIST	10M BRG	10M DRG DIST	20M BRG	20M DRG DIST	30M BRG	30M DRG DIST
1000	CLM	0	257	0.09	255	0.10	351	1.24	59	1.06	110	0.97
1030	CLM	0	246	0.14	243	0.16	349	1.20	60	1.10	109	1.02
1100	CLM	0	238	0.21	237	0.22	348	1.20	61	1.16	108	1.07
1130	CLM	0	234	0.25	233	0.26	345	1.20	60	1.21	105	1.10
1200	CLM	0	232	0.31	232	0.34	343	1.20	59	1.26	103	1.14
1230	CLM	0	230	0.41	230	0.42	340	1.21	51	1.31	100	1.17
1300	CLM	0	218	0.50	218	0.52	337	1.21	53	1.36	95	1.17
1330	CLM	0	226	0.52	226	0.54	336	1.24	51	1.42	93	1.17
1400	180	2	225	0.57	225	0.59	336	1.25	48	1.49	90	1.20
1430	180	2	226	0.59	226	0.61	335	1.30	46	1.59	86	1.19
1500	180	5	216	0.65	216	0.67	332	1.35	43	1.61	82	1.20
1530	170	7	224	0.64	224	0.66	331	1.37	37	1.66	77	1.20
1600	180	7	225	0.67	225	0.69	329	1.42	36	1.75	72	1.21
1630	180	10					332	1.49	37	1.76	71	1.22
1700	180	12					333	1.54	34	1.86	66	1.20
1730	180	12					333	1.61	33	1.91	63	1.20

OCCASION 13 DATE 280678

TIME	WIND DIR	WIND SP	5M BRG	5M DRG DIST	30M BRG	30M DRG DIST	5M BRG	5M DRG DIST	30M BRG	30M DRG DIST	5M BRG	5M DRG DIST	30M BRG	30M DRG DIST
1150	180	13	270	2.20										
1210	180	12			275	2.10								
1211	180	12					360	0.20						
1224	180	14							360	0.20				
1225	180	14									89	1.90		
1226	180	14											87	1.95
1346	180	15	278	2.10										
1347	180	15			278	2.10								
1405	180	15					330	0.30						
1410	180	15							15	0.65				
1425	180	15											81	1.75
1428	180	15									80	1.87		
1517	180	15	288	2.20										
1543	180	15			282	2.25								
1607	180	15					5	1.20						
1614	180	15							330	0.70				
1632	180	15									73	1.93		
1637	180	15											78	1.95
1730	180	15	295	2.55										
1737	180	15			288	2.20								
1757	180	15					360	1.75						
1808	180	15							360	0.50				
1823	180	15									65	2.10		
1824	180	15											73	1.80

LITERATURE CITED

AGENBAG, J.J. 1980 - General distribution of pelagic fish off South West Africa as deduced from aerial fish spotting (1971-1974 and 1977) and as influenced by hydrology. Fish. Bull. S. Afr. 13: 55-67.

BADENHORST, A. and A.J. BOYD 1980 - Distributional ecology of the larvae and juveniles of the anchovy Engraulis capensis Gilchrist in relation to the hydrological environment off South West Africa, 1978/79. Fish. Bull. S. Afr. 13: 83-106.

BAILEY, G.W. 1979 - Physical and chemical aspects of the Benguela current in the Lüderitz region. MSc thesis, University of Cape Town: 225 pp.

BANG, N.D. 1971 - The southern Benguela current in February 1966. Part II: Bathythermography and air-sea interactions. Deep-Sea Res. 18: 201-224.

BRUNDRIT, G.B. and D. VAN FOREEST 1981 - Benguela Current Modelling Project Reports. Dept. of Oceanography. University of Cape Town.

CALVERT, S.E. and N.B. PRICE 1971 - Upwelling and Nutrient Regeneration in the Benguela Current, October, 1968. Deep-Sea Res. 18: 505-523.

COPENHAGEN, W.J. 1953 - The periodic mortality of fish in the Walvis Bay region: a phenomenon within the Benguela Current. Investl Rep. Div. Fish. Un. S. Afr., 14: 1-35.

DU PLESSIS, E. 1967 - The Pilchard of South West Africa (Sardinops ocellata). Seasonal occurrence of thermoclines off Walvis Bay, South West Africa, 1959-1965. Investl. Rep. mar. Res. Lab. S.W. Afr. 13: 16 pp. + 11 pp. of Charts and 8 pp. of Tables.

EKMAN, V.W. 1905 - On the influence of the earth's rotation on ocean currents. Ark. Math. Astr. Fys. Bd. 11, no. 11.

GARRET, C.J.R. 1976 - Generation of Langmuir circulations by surface waves - a feedback mechanism. J. Mar. Res. 34: 117-130.

HART, T.J. and R.I. CURRIE 1960 - The Benguela Current. Discovery Reports 31: 123-297.

HARRIS, T.F.W. and L.V. SHANNON 1979 - Satellite-tracked drifter in the Benguela Current System. S. Afr. J. Sci. 75(7): 316-317.

JURY, M.R. 1980 - Characteristics of summer wind fields and air-sea interactions over the Cape Peninsula Upwelling Region. MSc thesis, University of Cape Town: 131 pp.

KIRWAN (Jr), A.D., McNALLY, G., CHANG, M.-S., and R. MOLINARI 1975 - The Effect of Wind and Surface Currents on Drifters. J. Phys. Oceanogr. 5: 361-368.

LE BLOND, P.H. and L.A. MYSAK 1978 - Waves in the Ocean. Amsterdam : Elsevier. 602 pp.

MURRAY, S.P. 1975 - Trajectories and Speeds of Wind-Driven Currents Near the Coast. J. Phys. Oceanogr. 5: 347-360.

MOROSHKIN, K.V., BUBNOV, V.A. and R.P. BULATOV 1970 - Water Circulation in the Eastern South Atlantic Ocean. Oceanology 10.1: 27-34.

NEUMANN G. and W.J, PIERSON 1966 - Principles of Physical Oceanography. Prentice-Hall 545 pp.

O'BRIEN, J.J., CLANCY, R.M., CLARKE, A.J., CREPON, M., ELSBERRY, R., GAMMELSRØD, T., MCVEAN, M., ROED, L.P. and J.D. THOMPSON 1977 - Upwelling in the Ocean: Two- the Three-dimensional Models of Upper Ocean Dynamics and Variability. In : Modelling the upper layers of the ocean, E.B. Krauss, editor, Advanced Study Institute - Urbino, NATO, 325 pp.

PIETERSE, F. and D.C. VAN DER POST 1967 - The Pilchard of South West Africa (Sardinops ocellata). Oceanographical conditions associated with red-tides and fish mortalities in the Walvis Bay Region. Investl Rep. mar. Res. lab. S.W. Afr. 14. 125 pp.

PHILLIPS, O.M. 1977 - Entrainment. In: Modelling the upper layers of the ocean, E.B. Krauss, editor, Advanced Study Institute - Urbino, NATO, 325 pp.

POLLARD, R.T. and R.C. MILLARD (Jr) 1970 - Comparison between observed and simulated wind-generated inertial oscillations. Deep-Sea Res., 17, 813-821.

POLLARD, R.T. 1977 - Observations and Models of the Structure of the Upper Ocean. In : Modelling the upper layers of the ocean, E.B. Krauss, editor, Advanced Study Institute - Urbino, NATO, 325 pp.

SCHELL, I.I. 1968 - On the Relation between Winds off Southwest Africa and the Benguela Current and Agulhas Current Penetration in the South Atlantic. Dr. Hydrogr. Z. 21 : 109-117.

STANDER, G.H. 1963 - The Pilchard of South West Africa (Sardinops ocellata). Temperature: Its Annual Cycles and Relation to Wind and Spawning. Investl Rep. mar. Res. Lab. S.W. Afr. 9: 57 pp.

STANDER, G.H. 1964 - The Pilchard of South West Africa (Sardinops ocellata). The Benguela Current off South West Africa. Investl Rep. mar. Res. Lab. S.W. Afr. 12: 43 pp. + Plates 5-81.

STANDER, G.H. and A.H.B. DE DECKER 1969 - Some physical and biological aspects of an oceanographic anomaly off South West Africa in 1963. Investl Rep. Div. Sea Fish. S. Afr. 81 : 1-46.

TAYLOR, G.I. 1931 - Effect of variation in density on the stability of superposed streams of fluid. Proc. Roy. Soc. London, Ser. A. 132. 499-523. (133), (263).